Trinity College Dublin

The University of Dublin

Pre-clinical development of NOX2/ROS blood-based biomarker of TBI

Isabella Dias Filogônio Emediato, MD

MSc. Immunology Thesis

Supervisor: Dr. David Loane

Neurotrauma & Neuroimmunology Lab

School of Biochemistry & Immunology

2022

DECLARATION OF AUTHORSHIP

I declare that this thesis has not been submitted as an exercise for a degree at this or any other university and it is entirely my own work. I agree to deposit this thesis in the University's open access institutional repository or allow the Library to do so on my behalf, subject to Irish Copyright Legislation and Trinity College Library conditions of use and acknowledgement.

I consent to the examiner retaining a copy of the thesis beyond the examining period, should they so wish (EU GDPR May 2018).

Isabella Dias Filogônio Emediato

ABSTRACT

There is an urgent need to develop predictive biomarkers for traumatic brain injury (TBI) to aid clinical diagnosis and treatment of head injury patients. NADPH oxidase 2 (NOX2) activity and oxidized biomarkers are being evaluated as clinical biomarkers of neurodegenerative diseases. DHR123 is a reactive oxygen species (ROS) dye routinely used to diagnose chronic granulomatous disease (CGD), a genetic disorder characterised by defects in NOX2 activity. It can be used to measure ROS release in fresh whole blood using flow cytometry protocols.

Previous studies from our lab used DHR123 to investigate systemic immune function following moderate-to-severe TBI in mice, and they revealed that TBI significantly increases leukocyte-derived ROS levels at day 3 post-injury. There appears to be a biphasic response to TBI because ROS levels in blood decrease below baseline at day 7 post-injury, before rebounding and becoming highly elevated at day 60 post-injury. DHR123 was also used to assess stimulus-induced respiratory burst activity (PMA/ionomycin challenged) in peripheral leukocytes after TBI. Under these conditions there was no change in burst potential in bone marrow-derived myeloid cells at day 3 post-injury. However, stimulus-induced ROS was significantly reduced by >50% in monocytes and neutrophils at day 60 post-injury. These data indicate that, upon stimulation, respiratory burst is impaired in peripheral myeloid cells at chronic time points after TBI. Based on these findings the goal of this project was to combine DHR123 and a NOX2 specific antibody to measure peripheral NOX2/ROS activity in leucocytes in the blood of sham and TBI mice during acute and chronic time points.

We initially developed and optimized the NOX2/ROS assay *in vitro* using a human neutrophil-like cell line (HL-60) and had some successful results. We performed linear regression analyses between MFI DHR123 (ROS probe) and MFI NOX2 ($gp91^{phox}$ antibody) to assess the correlation between these two probes in different conditions (non-stimulated, stimulated, with NOX2 inhibitors) and successfully demonstrated a significant correlation that encouraged us to move forward in our project and apply this assay to experimental TBI studies in mice.

We then examined ROS release and NOX2 activity/expression in baseline and stimulated states of neutrophils and monocytes from the blood of sham and TBI mice at different time points (1,7, and 14 days post-injury). Interestingly, we observed that upon stimulation at 14 days post-injury the peripheral immune system already shows signs of impairment, whereas previously this impairment was observed at 2 months post-injury. Blood neutrophils from injured mice did not respond as expected after PMA/ionomycin stimulation in both outputs: MFI DHR123 and MFI NOX2. Our preliminary results were promising and corroborated our hypothesis that after TBI the peripheral immune response becomes dysfunctional with time. These preliminary experiments demonstrate that the NOX2/DHR123 flow cytometry assay is easy to use and could potentially be translated to the clinical setting as a *functional biomarker*, to aid management and outcome prediction in TBI patients.

ACKNOWLEDGMENTS

Firstly, I would like to thank my supervisor David Loane, for offering me a Research Master's position in his newly created lab at Trinity. He has been kind to me since the first email I sent him from Brazil asking to volunteer in his lab. Thank you for the opportunity to carry out my research with you and for all the guidance throughout.

I would like to thank Janeen for being an amazing lab partner. It was a pleasure to share the bench with you although sometimes you used my space as well (hahahaha!). I miss all the laughs, coffees from Honey Truffle, the walking/running in the middle of the day to get some fresh air. Thank you for all the support in the most difficult moments I had moving to a new country, my dear Irish friend.

My most sincere thanks go to Marie. I would not have completed this without you. Thank you for guiding me in every step of my project and for being so thoughtful. I know you will be a huge success wherever you are! It is difficult to describe how indebted I am to you for all the support given but I have decided to not mention the kidney this time.

To Kyle for answering thousands of my questions daily, even after leaving the lab. Thank you for being so kind and welcoming since my first day. I would like to extend my warmest thanks to all the members of the Mills lab: Caroline, Lisa, Mieszko, Caitlín, Lucy, Charlotte, Pauline and Béré. Thank you for the encouragement and help from the very beginning. I was very lucky and grateful to share the lab with you all. To Barry, my many thanks for all the guidance and patience with my flow experiments.

To my family, despite being miles away, they still managed to be supportive and encouraging. And finally, I would like to thank my lovely husband Fred for agreeing to live this adventure with me, which is life. Thank you for being there for me in all the achievements and failures, I love you immensely.

ABBREVIATIONS

AD	Alzheimer's Disease
ALS	Amyotrophic lateral sclerosis
ANOVA	Analysis of variance
ATP	Adenosine triphosphate
BBB	Blood Brain Barrier
CGD	Chronic granulomatous disease
CNS	Central Nervous System
CSF	Cerebrospinal fluid
CT	Computed Tomography
DAMP	Damage associated molecular patterns
dHL-60	Differentiated HL-60
DHR	Dihydrorhodamine
DMEM	Dulbecco's Modified Eagle's- Medium
DMSO	Dimethyl sulfoxide
DPI	Day Post-Injury
DPI	Diphenyleneiodonium chloride
FAD	Flavin adenine dinucleotide
FBS	Fetal Bovine Serum
FDA	Food and Drug Administration
GCS	Glasgow Coma Scale
GFAP	Glial fibrillary acidic protein
H_2O_2	Hydrogen Peroxide
IL	Interleukin
MFI	Mean Fluorescent Intensity
NADPH	Nicotinamide adenine dinucleotide phosphate
NFL	Neurofilament light
NOX2	NADPH oxidase 2
NSE	Neuron- Specific Enolase
PBS	Phosphate buffered saline
PMA	Phorbol Myristate Acetate
PKC	Protein Kinase C
ROS	Reactive oxygen species
S100B	S100 calcium binding protein B

SOD	Superoxide dismutase
TNFα	Tumour Necrosis Factor alpha
TLR	Toll like receptor
TBI	Traumatic Brain injury
TBS	Tris-buffered saline
TBS-T	Tris buffered saline-Tween 20
UCH- L1	Ubiquitin carboxy-terminal hydrolase- L1
WHO	World Health Organization

TABLE OF CONTENTS

LIST OF FIGURES

LIST OF TABLES

CHAPTER 1: INTRODUCTION

1.1 Epidemiology of Traumatic Brain Injury

Traumatic Brain Injury (TBI) is the main cause of death and disability following injury in the world. Studies estimate that 50 – 60 million new cases of TBI occur per year and that sums up to the total amount of US$400 billion annually to the international economy (GBD Neurology, 2019). According to Acquired Brain Injury Ireland, 10,000 people are hospitalised with TBI annually in Ireland (Figure 1-1).

Epidemiological reports on TBI are limited globally, and the ones that do exist lack consistency. Incidence, prevalence, and mortality rates diverge greatly between countries and for various reasons including variations in data acquisition, data reporting and different definitions of TBI. Even the World Health Organization (WHO)'s definition of TBI, "an acute brain injury resulting from mechanical energy to the head from external forces", is not complete enough, as it excludes manifestations caused by penetrating craniocerebral injuries. A recent systematic review was published with the TBI epidemiology in Europe (Brazinova et al., 2021) and they found that for all ages, all TBI severity studies, the crude incidence rate ranged from 47.3 to 849 per 100,000 population per year; and crude mortality varied between 3.3 to 28.10 per 100,000 population per year. There is an urgent need to standardise the global epidemiological reporting and to publish age-adjusted data which is an inherent requirement for valid comparisons between countries.

TBI is classified as mild, moderate and severe according to the Glasgow Coma Scale (GCS). (Teasdale & Jennett, 1974, 1976) GCS is a widely used tool to objectively assess level of consciousness based upon three criteria: eye-opening, motor, and verbal responses. This assessment yields a score from 3 to 15 (mild: 13-15; moderate: 9-12; severe: 3-8). Most cases reported are classified as mild (Faul & Coronado, 2015), but studies have shown that even in mild TBI, especially after repetitive concussions, patients may present with increased rates of neurodegenerative diseases like Parkinson's and Alzheimer's disease, as well as higher risk of acquiring secondary infections and reduced life expectancy (Sharma et al., 2019). Severe TBI is considered a risk factor for dementia, stroke, and epilepsy, and is known to increase mortality rate (Maas et al., 2017; Taylor et al., 2017).

Despite the scarcity of statistical studies, it is widely accepted that TBI is a major public health issue, increasing continuously worldwide, although at differing rates and causal factors vary between countries. In the last decade the world saw a significant change in the pattern of TBI-related deaths causes. In High Income Countries (HIC) there was a substantial increase in fall related TBI deaths (affecting mainly the elderly), whereas in Low Medium Income Countries (LMIC) the main cause of fatal TBI is still traffic road accidents with young adults (GBD Neurology, 2019).

After the injury, this condition poses a dramatic impact on patients, their families and society. Amongst TBI survivors, some will live with long-lasting consequences such as physical disabilities, dementia, cognitive impairment, psychiatric disorders and will require long-term rehabilitation treatments (Stocchetti & Zanier, 2016). The US Centers for Disease Control and Prevention has estimated an average decrease in life expectancy in surviving TBI patients of 9 years (CDC, 2022). An

additional and less well-known index that measures the overall burden of a disease/condition is the YLD (Years Lost to Disability). In 2016, TBI caused 8.1 million YLDs worldwide, corresponding to age-standardised rates of 111 per 100 000 people. YLD and also YLL (Years of Life Lost) reflects better the health public consequences of this brain injury (Maas et al., 2017).

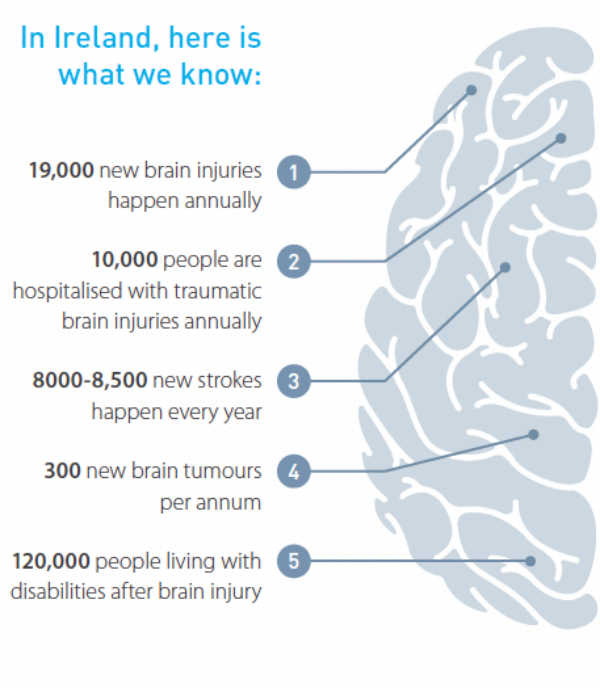

Figure 1-1. Epidemiological data regarding brain injury and patient outcomes in Ireland
An annual report published by the Acquired Brain Injury Ireland foundation including quantitative data regarding traumatic and non-traumatic cases of brain injury. (Acquired Brain Injury Ireland, 2019).

1.2 TBI Biomarkers: The Current State of the Art

A biomarker is defined as a substance which is objectively measured in body fluids and that indicates normal or pathological biological responses. A biological marker can be used as an adjunct of clinical evaluation and represents a powerful tool to optimise diagnosis, monitor disease progression and improve outcome prediction in different clinical scenarios (Gan et al., 2019).

In the context of TBI, an enormous heterogeneity is observed in the sex, age, previous health status of patients, and the mechanism and severity of trauma in patients. Additionally, a single mild TBI can lead to a wide range of individual responses from being asymptomatic to significant neurologic disability. This heterogeneity reiterates the need of a patient-based assessment which will permit for an individualized, tailored management and treatment plan more precise than broad protocols.

Clinical scenarios in which the use of a TBI biomarker could be advantageous include: document concussion when the history is unclear, predict intracranial damage after a mild TBI and help in the decision to indicate a CT head, aid in return to play/work decisions, and predict poor outcome after a moderate/severe brain injury (Gan et al., 2019). Additionally, it has been demonstrated that the risk of neurodegenerative diseases such as Alzheimer's disease (AD) and Parkinson's disease (PD) is

increased after a brain injury (Delic et al., 2020; Gardner et al., 2018; Li et al., 2021; Ramos-Cejudo et al., 2018) and the risk of secondary infections is also higher in these patients (Harrison-Felix et al., 2012; Lee & Rincon, 2012; Schwulst et al., 2013; Scott et al., 2013; Sharma et al., 2019). These post-injury long term consequences have been linked to a sustained inflammatory response after the primary injury (Simon et al., 2017). A blood-based test that could not only reflect tissue damage but also demonstrate the functional state of the immune system would guide us to provide a better care for these patients, and moreover, would aid in the prognosis assessment and development of targeted treatments.

There is current ongoing research into blood and cerebral spinal fluid (CSF) biomarkers for TBI. However, as TBI is a diverse and variable condition its complexity hinders the identification of a unique substance that could reflect accurately its whole heterogeneity (Huie et al., 2021; Kawata et al., 2016; Zetterberg & Blennow, 2016). The primary drawback from the current TBI biomarkers candidates is the lack of specificity. While promising as TBI biomarkers, most are also increased due to traumas not involving the central nervous system (CNS). There are a number of biomarker candidates under investigation for application to TBI, these biomarkers and their characteristics and limitations are discussed below (Figure 1-2).

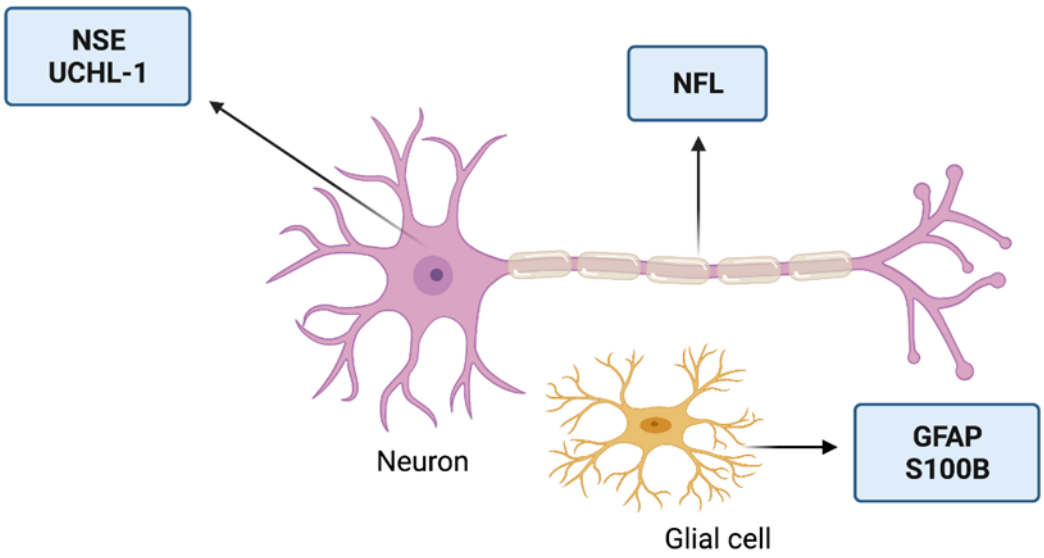

Figure 1-2. Candidate biomarkers for Traumatic Brain Injury
Potential TBI biomarkers currently include neurofilament light (NFL), neuron-specific enolase (NSE), ubiquitin C-terminal hydrolase-L1 (UCH-L1), S100B and glial fibrillary acidic protein (GFAP). NFL is a biomarker for axonal injury, whereas NSE and UCHL1 are proteins enriched in neuronal soma and are putative biomarkers for neuronal injury. GFAP and S100B are secreted from activated astrocytes following TBI. Image created with BioRender.com

S100 calcium binding protein B (S100B) is a protein most abundant in glial cells of the CNS, predominately in astrocytes. S100B also has extracerebral origin (adipose tissue and skeletal muscle) and these findings may affect the interpretation of its serum levels after TBI. Several

clinical studies have demonstrated that increased circulating S100B is associated with poor TBI outcomes, and it has been incorporated in the Scandinavian guidelines of initial management of head injuries in adults. Minkkinen et al., demonstrated the validity of using S100b as a tool for screening TBI patients, which has the added potential to reduce unnecessary CT scanning and costs (Kleindienst et al., 2007; Minkkinen et al., 2019; Undén et al., 2013).

Glial fibrillary acidic protein (GFAP) is an intermediate filament protein of the astrocytic cytoskeleton, which is released into the bloodstream after injury-induced astroglial damage. GFAP is a promising biomarker which was approved in 2018 by US Food and Drug Administration (FDA) to be used with ubiquitin carboxy-terminal hydrolase L1 (UCH-L1) for aiding in the clinical decision of obtaining head computed tomography (CT) scan in patients with mild TBI (Abdelhak et al., 2022; Anderson et al., 2020; Bazarian et al., 2018; Mondello et al., 2011; Mondello et al., 2021).

Ubiquitin carboxy-terminal hydrolase-L1 (UCH-L1) is a de-ubiquitinating enzyme specifically expressed in neurons. A blood test which combines UCH-L1 and GFAP was approved by FDA and has been in use in the clinical setting since 2018. Mondello at al. has demonstrated that patients with diffuse injuries present with higher UCH-L1 levels than GFAP with a possible explanation for this profile being that astrocytes are more resistant to ischemia and other stressors than neurons. A predominance of neuronal death is postulated to occur in diffuse injuries (Anderson et al., 2020; Bazarian et al., 2018; Mondello et al., 2011).

***Neuron- Specific Enolase (NSE*)** is an enzyme involved in glycolytic energy metabolism in the brain and is released from neurons following injury. Although NSE is relatively specific for neuronal cells, it is also found in neuroendocrine carcinomas. It has been demonstrated that following TBI NSE levels are elevated in the serum (Wolf et al., 2013), however there is not sufficient evidence to recommend its use in the clinical practice thus far (Mondello et al., 2021).

Neurofilament light (NFL) are proteins exclusively expressed in neurons that are released in the CSF and blood upon axonal damage. They are highly specific for neuronal cell damage and are gaining increasing interest not only in TBI research but also in different neurological disorders which also involve neuroaxonal damage such as multiple sclerosis, stroke, amyotrophic lateral sclerosis and Parkinson disease. The introduction of fourth generation assays (single-molecule array) enabled highly sensitive detection of NFL in blood across a wide range of concentrations, even in mild disease (Khalil et al., 2018). There is growing clinical evidence indicating that NFL could be a potential TBI blood-based biomarker with good diagnostic utility and even better prognostic value (Gao et al., 2020; Shahim, Politis, van der Merwe, Moore, Chou, et al., 2020). Shaim et al., recently demonstrated that NFL has a better correlation with the rate of MRI brain atrophy for subacute and chronic TBI when compared to GFAP, tau and UCH-L1 (Shahim, Politis, van der Merwe, Moore, Ekanayake, et al., 2020).

While these biomarkers just discussed offer promising potential as TBI diagnostic and prognostic tools, there is also an urgent need to find a way to fully and successfully integrate these tools into the clinical decision-making process. While there may previously have been an emphasis on finding an unique, singular biomarker, several studies have demonstrated that instead of choosing a sole biomarker as a "TBI signature", a better approach would be to assess multiple biomarkers simultaneously (Huie et al., 2019; Thelin et al., 2019; Zetterberg & Blennow, 2016). A combination of various biomarkers with different cellular origin would give us information on different pathological mechanisms as well as the involvement of different organ systems. As a result, this would increase predictive value and improve the accuracy to diagnosis and anticipate recovery post-TBI.

In an important difference from the biomarkers of cellular damage described above, our study aimed at developing a functional blood-based TBI biomarker. Several studies have shown that brain injury culminates in persistent systemic and neuroinflammation and moreover, TBI victims present with increased risk to infections (Harrison-Felix et al., 2012; Schwulst et al., 2013; Scott et al., 2013; Sharma et al., 2019). The main goal of this project is to use a simple and robust assay to demonstrate the profound and prolonged changes in the innate immune responses provoked by mild to moderate TBI.

1.3 TBI and the Immune System: Central and Peripheral Responses

TBI is a heterogeneous condition as it involves a complex diversity of pathological responses and depends on multiple factors such as patient age, sex and comorbidities. It is essential to consider the severity and mechanism of the *primary injury*, which is defined as the direct mechanical damage to the brain tissue and its surroundings; as well as the impact of the *secondary injury,* which includes any additional insult such as hypoxaemia, hypotension and inflammation. Thus, predicting outcome following TBI is an incredibly challenging task (Jassam et al., 2017).

The primary injury consists of brain contusion, intracranial haemorrhage, epidural and subdural haematoma, axonal shearing, vasculature damage and blood-brain-barrier (BBB) disruption which occur at the time of trauma and vary according to the severity. The secondary injury, on the other hand, occurs within minutes and may persist for potentially years after the initial trauma and involves numerous biochemical cascades, such as glutamate excitotoxicity, mitochondrial dysfunction, central and peripheral immune system activation, increased oxidative stress, among others. These secondary processes can exacerbate neurodegeneration and neurological impairment (Simon et al., 2017).

Immediately after the injury, damage-associated molecular patterns (DAMPs) are released from cells due to membrane disruption or actively secreted by monocytes or macrophage. Examples of DAMPs include ATP, heat shock proteins (HSPs), and HGMB1. These proteins, also knowns as alarmins, bind to DAMP sensors like receptor for advanced glycation end products (RAGE) and Toll-like receptor (TLR) and induce microglia and astrocytes activation, and release of pro-inflammatory cytokines such as tumour necrosis factor alpha (TNFα), IL-6, IL-1β and IL-18 (Jassam et al., 2017). Microglial and astrocyte activation in the acute phase result in increased debris clearance and tissue repair (Figure 1-3). This response is favourable in the beginning; however, it may become exacerbated and detrimental with time, resulting in chronic increased levels of proinflammatory substances such as

reactive oxygen species (ROS) and cytokines, and ultimately promoting tissue damage and progressive neurodegeneration (Hanscom et al., 2021; Loane et al., 2014).

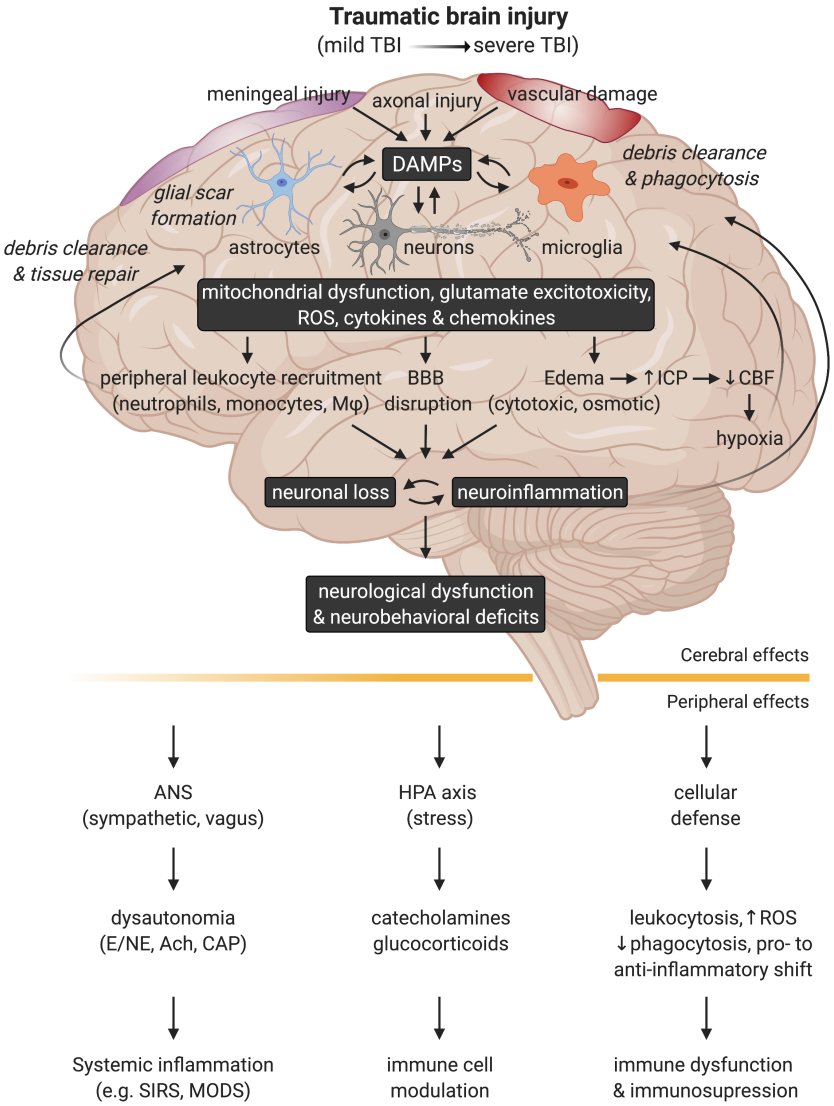

Figure 1-3. TBI induces central and peripheral immune responses
Illustration demonstrating the molecular and signalling sequalae and outcomes in CNS and peripheral responses to TBI. Abbreviations: Traumatic Brain Injury (TBI), Damage associate molecular patterns (DAMPs), Reactive Oxygen Species (ROS), Blood-brain-barrier (BBB), Intracranial pressure (ICP), Cerebral Blood Flow (CBF). *Reproduced and modified from Hanscom et al., 2021.*

TBI results in cytotoxic oedema due to sustained intracellular water collection and vasogenic oedema due to BBB disruption (Jha et al., 2019). Both will lead to increased intracranial pressure (ICP) and reduced cerebral flow (CBF), enhancing the deficit in energy supply to the brain, cell death and neuroinflammation, ultimately leading to neurological dysfunction and deficits in motor, cognitive, and affective function.

It has been demonstrated that TBI has a substantial impact on the peripheral immune system (McDonald et al., 2020; Sabet et al., 2021). The peripheral compartment is represented by recruited immune cells that traffic through the blood to the brain (mainly monocytes and neutrophils initially) and also by lymphoid organs such as spleen, thymus and bone marrow which incur substantial modifications that persist chronically post-injury, as shown by some recent studies (Ritzel et al., 2018). The disruption of the BBB enables the infiltration of peripheral immune cells into the brain. Neutrophils are the first immune cell to arrive to the injury site and represent a critical innate immune response. They have a potent array of microbicidal mechanisms including phagocytosis, release of chemokines, proteinase, cytokines, and ROS, but in the context of a sterile injury the release of these products will perpetuate secondary tissue damage (Trivedi et al., 2021).

TBI is also known to affect the autonomic nervous system (ANS) and the hypothalamic-pituitary-adrenal (HPA), both of which are intrinsically associated with the systemic immune response following a head injury. During acute TBI, a massive release of catecholamines epinephrine and norepinephrine (E/NE) occurs, also known as “sympathetic storm”, which is associated with the release of glucocorticoids known to be involved in modulation of systemic immune function. A surge in catecholamines would result in the entry of marginated neutrophils into the circulation. A peak in glucocorticoid levels would stimulate bone marrow cellular production and release of immune cells into the blood stream (Hazeldine et al., 2015). TBI may also disrupt some mechanisms of cellular defence resulting in immunosuppression, which will be discussed in further depth in the next section.

1.4 TBI and Peripheral Immune Suppression

Several papers have shown that following experimental TBI in mice and TBI patients there are impairments in systemic immune responses (Doran et al., 2020; Hazeldine et al., 2015; Husain et al., 2020; Marks et al., 2013; Ritzel et al., 2018; Schwulst et al., 2013; Sharma et al., 2019). These findings are extremely relevant considering that secondary infections result in increased mortality rates, longer hospital stays and poor neurological outcomes.

Doran et al., demonstrated that acutely brain injured mice (3 days post-injury) infected with *Streptococcus pneumoniae* had impaired lung-infiltrating monocytes responses. These cells produced lower levels of IL1ß, TNFα and ROS in response to *Streptococcus pneumoniae* when compared to sham mice, which reflected an immunosuppressed state. They also showed that at 60 days following injury infected mice had increased mortality, exacerbated motor function impairments and neuroinflammation and dysfunctional monocyte responses (Doran et al., 2020). TBI mice at either acute or chronic time points were unable to respond to *Streptococcus pneumoniae* and control inflammation. Ritzel et al., showed that although ROS baseline levels are increased at 60 days following brain injury in mice, upon stimulation bone marrow neutrophils and monocytes did not release ROS as expected in chronically injured mice when compared to sham mice (Ritzel et al., 2018).

Liao at al., investigated inflammatory mediators’ plasma levels and oxidative activity of circulating neutrophils in the blood from TBI patients, trauma control patients (general trauma with no CNS involvement) and uninjured subjects. These authors found that in the immediate hours and up to

14 days following TBI, neutrophils exhibit increased ROS generation in their resting state (Liao et al., 2013). This enhancement in basal ROS levels was attributed to a TBI-induced increase expression in $gp91^{phox}$, which is a subunit of the ROS generating enzyme nicotinamide adenine dinucleotide phosphate (NADPH) oxidase, also known as NOX. Interestingly, this study also described an impaired phagocytic activity of neutrophils in TBI patients throughout the entire observation period. In a study of TBI patients admitted to hospitals with moderate or severe brain trauma, Marks et al. found a significant impairment of the oxidative burst on day 9 post-injury and significant decreased phagocytic activity at day 3, 6 and 9 (Marks et al., 2013).

TBI induces a widespread suppression of innate and adaptive immune responses that culminates in increased risk of hospital-acquired infections and multiple organ dysfunction (Hazeldine et al., 2015; Kourbeti et al., 2012). In addition to that, the long-term sequalae of TBI on systemic immunity are also largely unknown. The mechanisms underlying these processes are not fully understood and further studies exploring the TBI-induced peripheral dysfunction are required to comprehend this cross talk and to guide tailored clinical therapeutic interventions to improve TBI patient prognosis.

1.5 TBI and NOX2 Activity

As previously described, following the primary brain injury, a complex cascade of secondary injury including edema, hypoxia, central and peripheral inflammation take place. These pathological mechanisms can have profound and persistent consequences to TBI survivors. One of the main contributors to the secondary injury is oxidative stress and there is growing interest in investigating these pathways (Husain et al., 2020; Kumar et al., 2016; Liao et al., 2013; Ma et al., 2018). The production and release of ROS occurs under physiological conditions; however, in TBI and other pathological conditions an imbalance between ROS/ROS scavengers can contribute to tissue damage and worsening of neurological outcomes.

ROS are produced by many cellular organelles such as mitochondria, peroxisome and endoplasmic reticulum. However, this project focused on ROS produced by NADPH oxidase 2 (NOX2), which is an enzymatic complex with the sole function of producing ROS. It has been demonstrated that NOX2 is chronically activated after TBI and plays a critical role in exacerbating the primary injury (Kumar et al., 2016). Thus, NOX2 has emerged as potential target in the management of these patients.

Briefly, NOX2 is comprised of the multiple subunits, including membrane-bound subunits ($gp91^{phox}$, $p22^{phox}$), cytosolic subunits ($p40^{phox}$, $p47^{phox}$, $p67^{phox}$) and regulatory Rac2. Upon stimulation, there is assembly and activation of the NOX2 complex, which involves translocation of cytosolic units to the membrane, phosphorylation of $p47^{phox}$, and finally the conversion of oxygen to superoxide via NADPH-dependent oxygen reduction. While there are seven isoforms of the NOX enzyme, NOX2 is the most studied and is highly associated with TBI (Figure 1-4) (Liao et al., 2013; Ma et al., 2018).

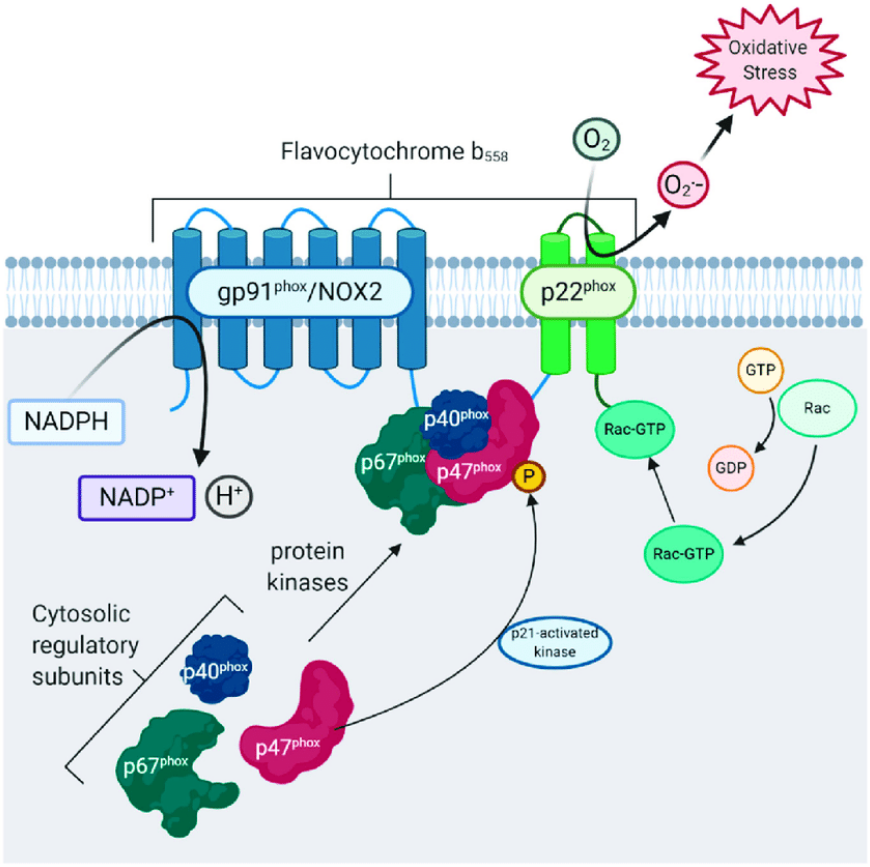

Figure 1-4. NOX2 activation and complex assembly
Upon stimulation, the cytosolic subunits p40^{phox}, p47^{phox}, p67^{phox} and regulatory Rac2 translocate to the plasma membrane and assemble a complex with the membrane bound subunits gp91^{phox} and p22^{phox}. A key step for this process is the phosphorylation of p47^{phox} by p21-activated kinase. *Reproduced and modified from Simpson et al., 2020*.

NOX2 plays a key role in host defense against bacterial infection, but it also regulates others cellular processes such as cytokine/chemokine signalling (Sun et al., 2020). Deficits in protein subunits of NOX2 result in an innate immune deficiency called Chronic Granulomatous Disease (CGD). CGD affects mainly the phagocyte compartment (i.e. neutrophils, monocytes, and macrophages) and it presents with impaired superoxide production that is essential for microbicidal activity; therefore, it culminates in increased susceptibility to bacterial and fungal infections (Rastogi et al., 2017). There is a wide spectrum of clinical manifestations in CGD ranging from mild to life-threatening infections and that is because CGD can be genetically heterogeneous. CYBB variants (gp91^{phox}) for example present with more severe disease than patients with NCF1 (p47^{phox}) defects (Chiriaco et al., 2016).

The current gold standard diagnostic test for CGD is the dihydrorhodamine (DHR) flow cytometry assay as it corelates with NOX2 activity (Richardson et al., 1998). DHR123 is an uncharged non-fluorescent dye which in the presence of ROS is oxidized to fluorescent R123. This is a simple assay that consists in the *ex vivo* stimulation of phagocytes in a whole blood sample with an oxidative burst stimulant such as phorbol myristate acetate (PMA) and measures ROS release in monocytes and neutrophils using an appropriate gating strategy.

As DHR123 is a widely used and simple assay and there is a documented correlation between this dye and the NOX2 enzymatic activity, it could potentially be applied as a biomarker in TBI. However, DHR123 is not specific for NOX2 as it reacts not only with superoxide anion (NOX product) but also other oxidants, making it unsuitable for quantitative or kinetic studies (Quinn et al., 2007). In order to circumvent this limitation, use of DHR123 as a biomarker in either preclinical or clinical studies would need to incorporate a means of simultaneously assessing NOX2 activity/expression and ROS release in baseline and stimulated states, such as inclusion of a NOX2 specific antibody.

1.6 Role of NOX2 Activity in Neurodegenerative Diseases

NOX2 and Amyotrophic lateral sclerosis (ALS)

ALS is a neurodegenerative disorder affecting primarily the motor system, in the brain, brain stem and spinal cord leading to progressive muscle weakness and wasting. Some studies have shown that NOX2 exacerbates disease progression in the $SOD1^{G93A}$ transgenic mice, a widely used mouse model of ALS. NOX2 expression and activation was shown to be significantly upregulated in microglia in the spinal cord of $SOD1^{G93A}$ mice compared to controls (Wu et al., 2006). The authors demonstrated that NOX2 deletion in $SOD1^{G93A}$ transgenic mice prolonged survival and slowed disease progression, suggesting that NOX2 activity contributes to the degeneration of motor neurons and disease progression in ALS. In a clinical study, NOX2 activity from peripheral neutrophils and monocytes was directly measured in fresh whole blood of a cohort of 83 ALS patients using the Phagoburst™ assay which measures mean fluorescent intensity (MFI) DHR123 following different stimulation conditions by flow cytometry. The authors did not identify a significant difference in NOX2 activity between ALS patients and matched controls. However, ALS patients with lower NOX2 activity (low DHR123 oxidation) were found to have a significant longer survival (Marrali et al., 2014).

NOX2 and Alzheimer's disease (AD)

NOX2 has also been associated with AD pathology mechanisms. Increased NADPH oxidase activity was found in post-mortem brains of AD patients (Butterfield & Boyd-Kimball, 2018) and a recent study demonstrated that NOX2 knockout aged mice had less Aβ deposition and plaque formation compared to aged wild-type controls (Geng et al., 2020). ROS levels were also decreased in NOX2 knockout mice, showing that ROS released in the aged mice was NOX2-dependent. It has also been found that Aβ activates microglia, consequently, though the production of toxic and inflammatory mediators such as nitric oxide, cytokines and ROS. Therefore, NOX activation can be mediated by inflammatory factors, such as Aβ, TNF-α, and interleukins, proteins also involved in AD pathology. The activation of microglial cells and NOX can then produce more inflammatory mediators, causing a vicious cycle which damages the neurons and causes chronic neurodegeneration (Fragoso-Morales et al., 2021).

NOX2 and Multiple Sclerosis (MS)

In contrast to other neurodegenerative diseases, MS is an autoimmune disease that results in the destruction of the myelin sheath and the neuronal loss is secondary to the myelin loss. MS presents typical features of inflammation as it is characterized by infiltration of leukocytes in the brain and spinal cord (Sorce et al., 2017). It has been demonstrated that superoxide released by microglia plays a key role in the progression of MS. A recent study investigated the effect of NOX2 gene ablation on the inflammatory response in a mouse experimental autoimmune encephalomyelitis (EAE) model and demonstrated that NOX2 deficiency attenuates demyelination, neuronal damage and disease severity (Hu et al., 2021). An important clinical study demonstrated upregulation of the subunits $gp91^{phox}$, $p22^{phox}$, and $p47^{phox}$ in activated microglia in classical active lesions in autopsy brains of patients with MS, which suggest that oxidative burst is important in the pathogenesis of MS (Fischer et al., 2012).

1.7 NOX2/ROS Assay Development

NOX2 activator

In this project we used phorbol 12-myristate 13-acetate (PMA) and ionomycin to induce respiratory burst in leukocytes. PMA is a potent Protein Kinase C (PKC) activator and has been shown to induce respiratory burst by NOX2 through stimulation of PKC (Cox et al., 1985). Some studies revealed that PKC induces phosphorylation of $p47^{phox}$ and translocation of $p47^{phox}$ and $p67^{phox}$ to the plasma membrane, enabling the complex assembly and superoxide generation (El-Benna et al., 2009; Nauseef et al., 1991; Rastogi et al., 2017) (Figure 1-4). Ionomycin is a calcium ionophore which synergizes with PMA in enhancing the activation of PKC.

NOX2 inhibitors

Most of the NOX inhibitors (i.e. VAS2870, GKT136901, GKT137831) reported are non-specific for the NOX isoforms. Some inhibit upstream pathways of ROS, while others act as oxidant scavengers or produce artifacts in the assay. When assessing NOX inhibitors, it is important to use methods that measure both consumption of the substrates (NADPH and O_2) and the products of the reaction (O^{2-}) (Reis et al., 2020). Hirano et al. characterized a novel NOX2 inhibitor, GSK2795039, which inhibits both the formation of superoxide anion and utilization of the substrates. Importantly, this drug was selective over other NOX isoforms, xanthine oxidase, and endothelial nitric oxide synthase enzymes. GSK2795039 is orally available, non-toxic, CNS-permeable and inhibits NOX2 activity *in vivo*. We used GSK2795039 in our experiments *in vitro* to assess the specificity of our NOX2/ROS TBI biomarker.

In this project we also used Diphenyleneiodonium chloride (DPI), a widely used inhibitor, as a broad antioxidant in order to compare against the effects of a NOX2 specific inhibitor (Reis et al., 2020). DPI inhibits ROS release by accepting an electron from flavin adenine dinucleotide (FAD). Consequently, DPI inhibits NOX and other flavoenzymes such as nitric oxidase synthase, xanthine

oxidase, mitochondrial complex I, and cytochrome P-450 reductase. DPI has high toxicity, low solubility and bind irreversibly to flavin limiting its utility in *in vivo* studies (Hirano et al., 2015).

1.8 Hypothesis and Specific Aims

The hypothesis of this study was that TBI has profound and persistent effects on the peripheral immune responses leading to immunosuppression and increased susceptibility to infections among TBI survivors. We wanted to determine how oxidative stress participates in these processes by assessing NOX2 activity and ROS generation in blood leukocytes.

Therefore, the goals of this Research Masters Project were to:

1) Develop a robust panel to measure NOX2/ROS activity by combining DHR123 (ROS dye) and a specific antibody against NOX2 *in vitro*.
2) Apply the NOX2/ROS flow cytometry assay in the blood samples from experimental TBI mice in different time points following injury.

Ultimately, this project aims to translate our preclinical research around NOX2/ROS as a hallmark of systemic chronic inflammation in human TBI, and to determine whether NOX2/ROS activity in blood could be a predictive biomarker of injury severity and long-term outcomes in TBI patients.

CHAPTER 2: MATERIALS AND METHODS

2.1 Materials

2.1.1 Complete Roswell Park Memorial Institute (cRPMI) Medium

500 ml RPMI 1640 Medium, GlutaMAX™ (Gibco, 61870010)
10% Fetal Bovine Serum (FBS; Sigma-Aldrich, F9665)
1% Penicillin/Streptomycin (Sigma-Aldrich, P4333)

2.1.2 Cell Differentiation Media

Complete RPMI (GlutaMAX™, 2.1.1)
DMSO 1.3% (v/v) (Sigma-Aldrich, 472301)

2.1.3 FACS Buffer

485ml Phosphate buffered Saline (Sigma-Aldrich, D8537)
10ml EDTA (Sigma-Aldrich, E6511)
5ml FBS (Sigma-Aldrich, F9665)

2.1.4 Western Blot Lysis Buffer

10 µl Phosphatase inhibitor cocktail 1 (Sigma-Aldrich, P2850)
10 µl Phosphatase inhibitor cocktail 2 (Sigma-Aldrich, P5726)
10 µl Protease Inhibitor cocktail (Sigma-Aldrich, P8340)
100 µl PierceTM RIPA buffer (Thermo Scientific, 89900)

2.1.5 Tris-buffered Saline (TBS) 10X

63.04 g Tris HCL (Trizma; Sigma-Aldrich, T1503)
175.32 g Sodium Chloride (Sigma-Aldrich, S9888)
2 L dH2O
pH to 7.5

2.1.6 Western Blot Wash Buffer TBS-Tween 20 (TBST)

100ml TBS (2.1.5)
900ml dH2O
0.5 ml Tween 20 (Sigma-Aldrich, P1379)

2.1.7 Western Blot Blocking Buffer 5% Milk in TBST

5 g Skim milk powder (Sigma-Aldrich, 70166)
100 ml TBST (2.1.6)

2.1.8 Western Blot Blocking Buffer 5% BSA in TBST

5g Bovine serum albumin (Sigma-Aldrich, A3059)

100ml TBST (2.1.6)

2.1.9 Separating Gel Buffer (1.5M)

90.8 g Tris base (Sigma-Aldrich, T1503)

1 g Sodium Dodecyl Sulfate (SDS) (Sigma-Aldrich, 436143)

450 ml dH2O

pH to 8.8

2.1.10 Stacking Gel Buffer (1M)

15.13 g Tris base (Sigma-Aldrich, T1503)

1 g SDS (Sigma-Aldrich, 436143)

200 ml dH2O

pH to 6.8

2.1.11 Stripping Buffer

15 g Glycine (Sigma-Aldrich, G8898)

1 g SDS (Sigma-Aldrich, 436143)

10 ml Tween 20 (Sigma-Aldrich, P1379)

pH to 2.2

2.1.12 Subcellular Fractionation Lysis Buffer

20mM Hepes, pH 7.2

80mM Potassium Chloride (Sigma-Aldrich, P5405)

1mM Ethylenediaminetetraacetic acid (Sigma-Aldrich, E7889)

1mM EGTA

1mM DTT

250mM Sucrose (BDH Laboratory Supplies, BDH9308)

200ug/ml Digitonin

Protease Inhibitor (Sigma-Aldrich, P8340)

dH_2O

2.1.13 General Reagents

Reagent	Catalogue number	Supplier
Acrylamide	A3059	Sigma-Aldrich

Ammonium Sulfate	472301	Sigma-Aldrich
TEMED	61870010	Gibco
Trypan Blue	T8154	Sigma-Aldrich

2.1.14 Reagents for *in vitro* Stimulation and Treatment

Reagent	Working concentration	Catalogue number	Supplier
Ionomycin	1.34uM	10634	Sigma-Aldrich
Phorbol 12-myristate 13-acetate (PMA)	81nM	P8139	Sigma-Aldrich
Diphenyleneiodonium chloride (DPI)	0.1 - 5 µM	D2926	Sigma-Aldrich
GSK2795039	1 - 25 µM	HY-18950	MedChemExpress

2.1.15 Separating Gels for Western Blot

Reagent	10% gel	12% gel	15% gel
30% Acrylamide	3.3 ml	4 ml	5 ml
dH2O	4.0 ml	3.3 ml	2.3 ml
Buffer (2.1.11) pH 6.8	2.5 ml	2.5 ml	2.5 ml
10% Ammonium sulfate	100 µl	100 µl	100 µl
10% SDS	100 µl	100 µl	100 µl
TEMED	4 µl	4 µl	4 µl

2.1.16 Stacking Gel 4%for Western Blot

Reagent	Volume
30% Acrylamide	2.8 ml
dH2O	660 µl
Buffer (2.1.11) pH 6.8	500 µl
10% Ammonium sulfate	40 µl
10% SDS	40 µl
TEMED	4 µl

2.1.17 Primary Western Blot Antibodies

Antibody	Molecular Weight (kDa)	Block	Host	Working Dilution	Catalogue number	Supplier
ß-actin	42	5% Milk in TBST	Mouse	1:50,000	A1978	Sigma-Aldrich
Caveolin	22	5% Milk in TBST	Mouse	1:200	sc-53564	Santa Cruz
gp91	60/91	5% Milk in TBST	Mouse	1:200	sc-130543	Santa Cruz
p-Ser345 (phospho-p47)	44	5% BSA in TBST	Rabbit	1:1000	SAB4504721	Sigma-Aldrich
$p22^{phox}$	22	5% Milk in TBST	Mouse	1:500	sc-271968	Santa Cruz
$p40^{phox}$	40	5% Milk in TBST	Mouse	1:200	sc-48388	Santa Cruz
$p47^{phox}$	47	5% Milk in TBST	Mouse	1:1000	sc-17844	Santa Cruz
$p67^{phox}$	67	5% Milk in TBST	Mouse	1:200	sc-374510	Santa Cruz

2.1.18 Secondary Western Blot Antibodies

Antibody	Working dilution	Catalogue number	Supplier
Goat Anti-Mouse	1:5000	115-035-003	Jackson ImmunoResearch
Goat Anti-Rabbit	1:5000	111-035-003	Jackson ImmunoResearch

2.1.19 Other Western Blot Reagents

Reagent	Catalogue number	Supplier
30 % Acrylamide/Bis solution 37.5:	1610158	Bio-Rad
4x Lamelli Sample Buffer	1610747	Bio-Rad
2-Mercaptoethanol	M3701	Sigma-Aldrich
TEMED	T7024	Sigma-Aldrich
110x Tris/Glycine Buffer	1610734	Bio-Rad
10x Tris/Glycine/SDS Buffer	1610772	Bio-Rad
WesternBrightTM ECL-spray Western blot detection system	K-12049-D50	Advansta
WesternBrightTM Quantum Chemiluminescent HRP Substrate kit	K-12042-D10	Advansta

2.1.20 FACS Antibodies

Specificity	Clone	Fluorochrome	Working dilution	Catalogue number	Supplier
CD45	30-F11	PE	1:200	12-0451-83	eBioscience
CD11b	M1/70	PE-Cy7	1:200	552850	BD Biosciences
Ly6G	1A8	BV421	1:200	127627	Biolegend
Ly6C	AL-21	BV605	1:200	563011	BD Biosciences
NOX2/gp91^{phox}	Polyclonal	Alexa Fluor 647	1:100	bs-3889R-A647	Bioss

2.1.21 Other FACS Reagents

Reagent	Catalogue number	Supplier
Anti-mouse CD16/32 Fc block	553141	BD Biosciences

CountBright Absolute Counting Beads	C36950	Invitrogen
Dihydrorhodamine 123	D23806	Invitrogen
FoxP3 Transcription Factor Staining Buffer Set	00-5523-00	eBioscience
LIVE⁄DEAD® Fixable Near-IR Dead Cell Stain	L10119	Thermo Fisher
Lysing buffer	555899	BD Biosciences
One Comp eBeads	01-1111-42	eBioscience
Paraformaldehyde (16%)	28906	Thermo Fisher

2.2 Methods

2.2.1 HL-60 Cell Culture and Differentiation

2.2.1.1 Culture

HL-60 cells are promyeloblasts isolated from the blood from a woman with acute promyelocytic leukaemia. This cell line can be differentiated along macrophage or neutrophil lineage (Babatunde et al., 2021; Brackman et al., 1995; Zucker et al., 1983) and is widely used as a model system for the analysis of human neutrophil behaviour (Birnie, 1988; Hauert et al., 2002). Considering that myeloid cells are the major producers of ROS during inflammation, this cell line was chosen as a tool to investigate ROS produced by NADPH oxidase 2. HL-60 cells used in this study were kindly provided by Dr. Rebecca Amet (Trinity College Dublin).

Cells were cultured in RPMI Glutamax™ supplemented with 10% FBS and 1% (v/v) penicillin/streptomycin at 37°C with 5% CO_2. Single cell suspensions were cultured in T175 flasks for 2 days and then centrifugated with subsequent resuspension at $1x10^5$ viable cells/ml. Cell density was maintained between $1x10^5$ and $1x10^6$ viable cells/mL and cells between passage 5-20 were used for experimentation.

2.2.1.2 Differentiation

There is extensive evidence in the literature (Collins et al., 1978; Fleck et al., 2005; Millius & Weiner, 2010) regarding the role of DMSO in the differentiation of HL-60 cells into a granulocyte profile. We performed several experiments with this cell line in order to optimize conditions (density, treatment duration) for differentiation. In our protocol HL-60 cells were seeded at $5x10^5$ cells/ml in T175 flasks with 1.3% v/v DMSO in complete RPMI Glutamax for 3-5 days without media change.

2.2.1.3 Cell Counting

Viable cells were counted by diluting 10ul of cells in 90ul Trypan Blue solution 0.4% (Sigma-Aldrich, 2.1.13). The mixture (10ul) was then placed in a haemocytometer. Live (viable) cells do not take the dye whereas dead (non-viable) cells are permeable and are stained as intense blue. The density (cells/ml) was determined by multiplying the average number of viable cells by the dye dilution factor (10) and by 10^4 to calculate the number of cells/ml.

2.2.2 Pharmacological Stimulation and Inhibition of Reactive Oxygen Species Generation

The stimulation model chosen to induce ROS release in HL-60 cells in this study was 81nm PMA and 1.34uM Ionomycin for 60 minutes at 37°C, 5% CO_2. Concentrations were based on David Loane's group previous experiments (Ritzel et al., 2018) and time of stimulation was decided based on repeated time-response experiments demonstrated in the results section (Figure 3-1B). To assess inhibition of ROS generation, differentiated HL-60 (dHL-60) cells were stimulated with PMA/Ionomycin and co-treated with GSK2795039 (MedChemExpress; 1-25μM; 1h; 37°C, 5% CO_2) or diphenyleneiodonium chloride (DPI; Sigma-Aldrich; 0.1- 5μM; 1h; 37°C, 5% CO_2). Cells were then prepared for flow cytometry analysis.

2.2.3 Western Blotting

Preparation of total cell lysates was performed as follows. Briefly, dHL-60 cells ($10x10^6$ cells/ml) were transferred to 5ml tubes and centrifuged for 5 minutes (1350 rpm; 5 min; 4°C). Supernatants were discarded and the pellet was resuspended in Western blot lysis buffer (2.1.4). Cell lysates were incubated for 20 minutes on ice and then sonicated (6 pulses of 1 second duration each), after which the lysate was centrifuged (15,000 rpm; 15 mins; 4°C) to pellet the insoluble material. Supernatants (cell lysates containing soluble proteins) were collected and transferred to 1.5ml microcentrifuge tube. Protein concentrations were quantified using the Pierce™ BCA Protein Assay kit (Thermo Scientific, 10678484) and all samples were then normalised to [1ug/ul] using RIPA, 4x Lamelli buffer (2.1.19) and ß-mercaptoethanol (2.1.19).

Samples were denatured (95°C; 5mins) before being loaded 15-20ug (15-20ul) per sample onto 10-15 % gels (2.1.15) and undergoing electrophoresis. Proteins were transferred from the gels to nitrocellulose membranes using a Trans-Blot Turbo Transfer System (Bio-Rad, 1704150). After transfer was completed, membranes were washed twice with TBS-T (2.1.6, 5 minutes) and then blocked for 1 hour in 5% milk in TBS-T (2.1.7) at room temperature. The membranes were then incubated with the respective primary antibodies in TBS-T (2.1.6) overnight at 4°C. Membranes were then washed in TBS-T (3 times, 5 minutes) and incubated in the appropriate HRP-conjugated secondary antibody in TBS-T for 2 hours at room temperature. Finally, membranes were washed three times in TBS-T (5 minutes, room temperature), and proteins were visualized using enhanced chemiluminescence (WesternBrightTM ECL-spray, 2.1.19). Protein bands were quantified by densitometric analysis using Image Lab software v6.0.1 build 34.

2.2.4 Subcellular Fractionation

Subcellular fractionation was performed to investigate compartmentalization of proteins thought to play a role in the generation of ROS in activated dHL-60 cells. Briefly, dHL-60 cells ($40x10^6$ cells/ml) were transferred to 5ml tubes and centrifuged at 1350 rpm for 5 min (Figure 2-1 and 2-2). Supernatants were discarded and the pellet was resuspended in 500ul of subcellular fractionation lysis buffer (2.1.12) and incubated on ice for 20 minutes. The pellet was then passed through a 25G needle 25 times and incubated on ice for an additional 15 minutes. Samples were centrifuged at 1000xg for 5 minutes to pellet down the nuclei fraction; the supernatant, containing cytoplasm, plasma membranes and mitochondria, was saved on ice for later steps. The nuclei pellet was resuspended in 500ul of subcellular fractionation lysis buffer (2.1.12), passed through a 27G needle 20 times, incubated on ice for 15 minutes, centrifuged again at 1000xg for 5 minutes. These steps were repeated once more, and 2 washes were performed. The final nuclear pellet was resuspended in 75ul of Western blot lysis buffer (2.1.4). The supernatant containing cytoplasm, plasma membrane, and mitochondria saved previously was centrifuged at 12000xg for 10 minutes to pellet down the mitochondrial fraction; the supernatant from this spin (saved for downstream steps) contained cytoplasm and plasma membrane proteins. The mitochondrial pellet was washed and centrifuged at 12000xg for 10 minutes twice, finally being resuspended in 75uL of Western blot lysis buffer (2.1.4). The supernatant containing cytoplasm and plasma membrane fractions was concentrated using 3 kDa filter units (Millipore, UFC200324) to a final volume of 200ul and then ultracentrifuged at 50000 rpm (equivalent to 100000xg) for 1 hour. The supernatant from this first ultracentrifugation spin contained cytoplasm proteins and was stored on ice. The pellet from the first ultracentrifugation spin was washed and spun at 50000 rpm for 45 minutes and the new resulting pellet containing plasma membrane proteins was resuspended in Western blot lysis buffer (2.1.4). All the centrifugations in this protocol were done at 4^oC and samples were kept on ice all times.

Nuclear, mitochondrial, and total cell lysates (positive control) samples were sonicated on ice for 12 pulses of 1 second duration each. Protein quantification and western blotting of samples for visualization of proteins and qualitative analysis were performed as previously described in the Western blotting section above.

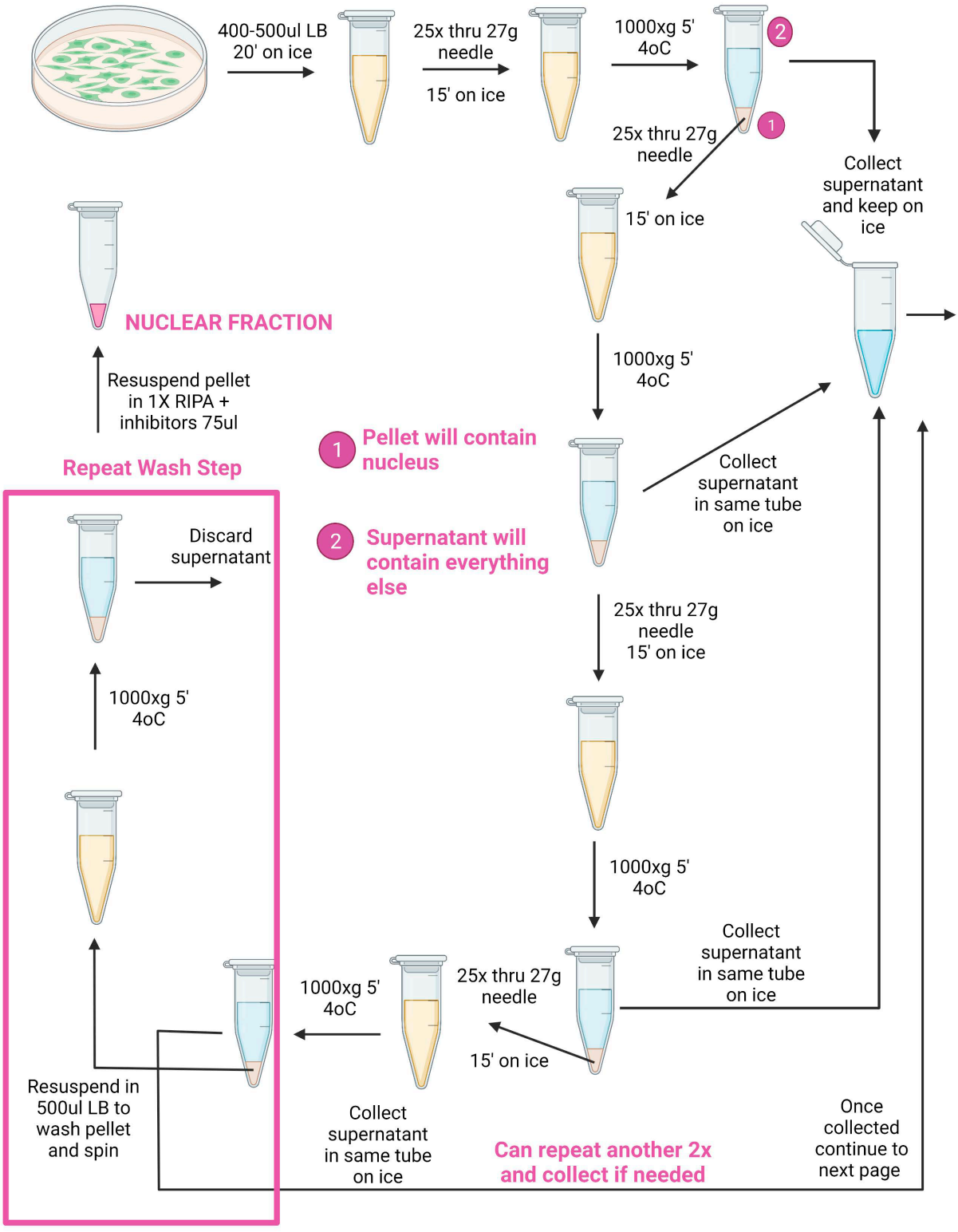

Figure 2-1. Subcellular fractionation protocol schematic
Image created with BioRender.com.

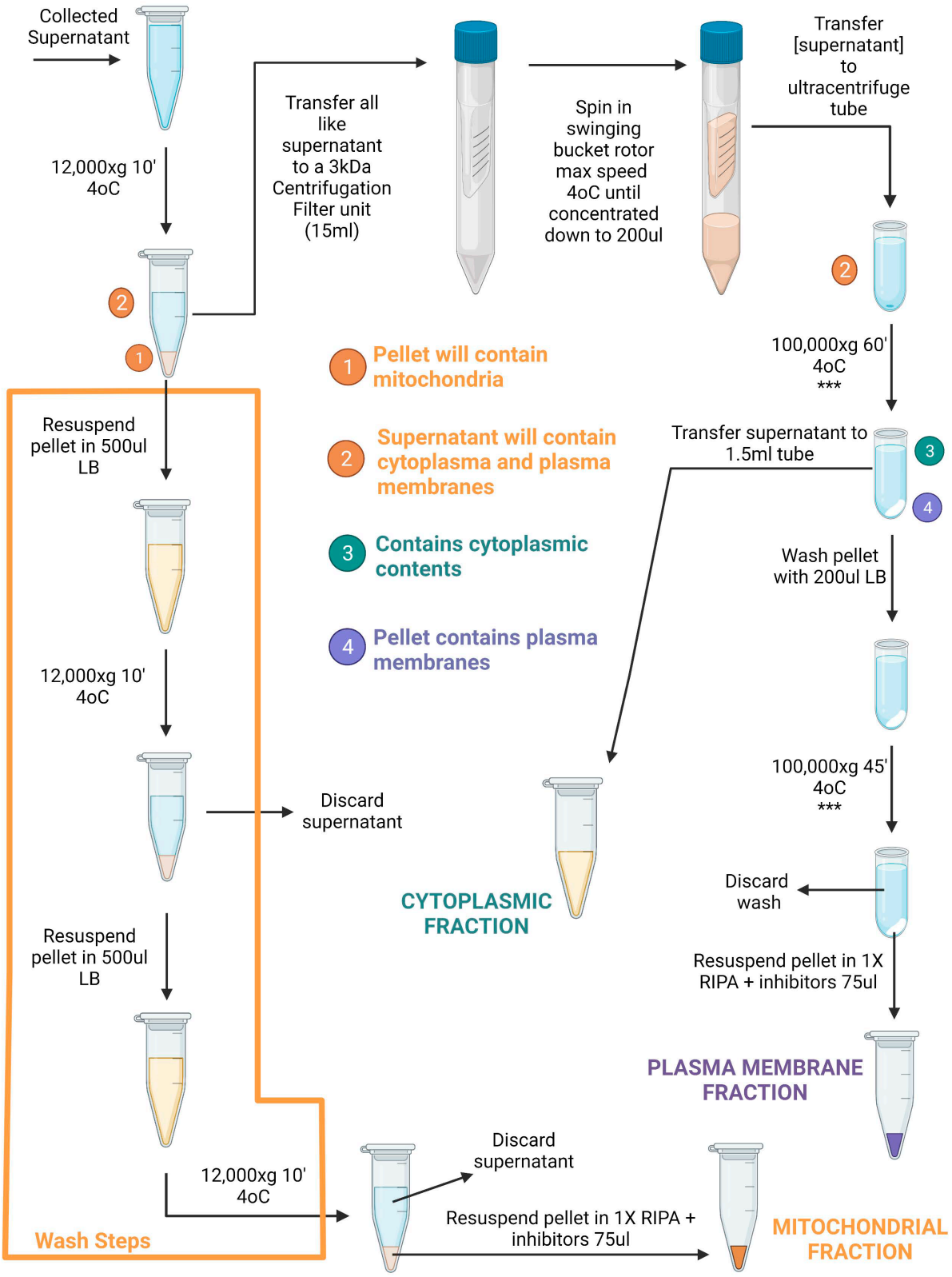

Figure 2-2. Subcellular fractionation protocol schematic
Continuation of subcellular fractionation protocol from Figure 2-1. Image created with BioRender.com.

2.2.5 Experimental Traumatic Brain Injury

2.2.5.1 Animals and Experimental Design

C57BL/6JOlaHsd mice were bred by the Comparative Medicine Unit (CMU), Trinity College Dublin. Mice were maintained under guidelines and regulations of the Health Products Regulatory Authority and experiments were carried out under license with the approval of Trinity College Dublin Animal Research Ethics Committee. Experiments were conducted with 7–9-week-old male mice. Mice were sacrificed by anaesthetic overdose (isoflurane) followed by terminal blood collection (cardiac puncture) and transcardial perfusion by a trained researcher.

At 7-9 weeks of age, male C57BL/6JOlaHsd mice (n=4-5/group *Cohort 1*; n=5-6/group *Cohort 2*; n=5-6/group *Cohort 3*) were subjected to either sham surgery (incision only) or controlled cortical impact (CCI) (Figure 2-3). Mice were daily weighted and assessed for health and wellbeing. On day 1 post injury (cohort 1), day 7 post injury (cohort 2) or day 14 post injury (cohort 3) animals were weighed, anaesthetized with 4.5% isoflurane, and ~0.5ml of blood was collected via cardiac puncture into heparin-coated tubes for flow cytometry analysis. Isoflurane was then reduced to 1.5% and the spleen was removed, weighed, and transferred to tubes containing ice cold RPMI.

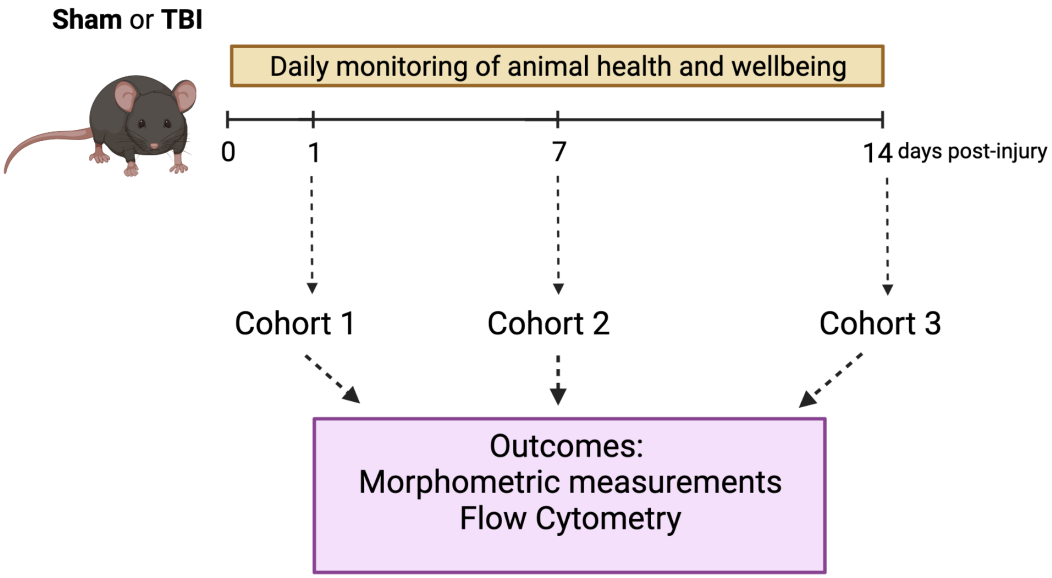

Figure 2-3. Experimental design
Mice were subjected to sham (incision only) or TBI (CCI) after which blood, spleen, thymus and brain tissue were collected at 1-, 7-, and 14-days post-injury for flow cytometry and molecular analyses. Mice were weighed daily and monitored for health and wellbeing. Image created with Biorender.com

The mice were then transcardially perfused with 50ml ice-cold 0.9% saline. Perfused brains were removed and rapidly dissected on a cutting mat chilled to 4°C. The contralateral and ipsilateral hippocampus, cortex (3mm around the impact), and cerebellum were isolated, flash frozen in liquid nitrogen and stored at -70°C for later use in gene expression analyses. Thymus was also removed following saline perfusion, flash frozen in liquid nitrogen and stored at -70°C freezer for future studies

2.2.5.2 Controlled Cortical Impact

In this study CCI model (68099Ⅱ, RWD, Guangdong, China) was used to induce mild- to moderate-level traumatic brain injury in adult male mice (Ritzel et al., 2018) (Figure 2-4). Briefly, mice were anesthetized with isoflurane dispensed from a precision vaporizer (R500, RWD, Guangdong, China) in 100% O_2 (induction 3%, maintenance at 1.5%) through a chamber (induction) and nose mask (maintenance). After skin preparation with alternating scrubs of 2% chlorohexidine and 70%ethanol, a line infiltration of 50uL of 0.083% bupivacaine (W/V) was given subcutaneously before the incision to ensure analgesia. A 10mm midline incision was made over the skull and the skin and fascia were reflected. A 5mm craniotomy was made on the central aspect of the left parietal bone, taking care so as not to disrupt the underlying dura. The impactor tip was extended to its full stroke distance, positioned over the surface of the exposed dura, and set to impact the cortical surface. Mild- to moderate-level CCI was then induced by using an impactor velocity of 3m/s, deformation depth of 1mm, and 0.18 sec dwell time. Approximately, 100uL of 0.083% bupivacaine (W/V) was placed at the craniotomy site before wound closure to ensure post-operative analgesia. The incision was closed with 7-0 sutures and anaesthesia terminated. Mice received 1ml of normal saline intraperitonially for fluid replacement and were placed into a heated chamber (Harvard Apparatus) for 45 minutes post-injury to maintain core body temperature. All surgical procedures were performed using aseptic techniques. The control group for this procedure was a sham surgery that involved anaesthesia and skin incision, but no craniotomy or physical trauma using the CCI apparatus. Recovery from anaesthesia and post-operative behaviour during the acute phase every 5-10 minutes up to 1 hour after surgery was recorded. Return of righting reflex (RORR) which is the time taken by a mouse to return to prone position after being placed in supine position, was recorded for all mice after anaesthesia was terminated. An assessment form was completed for each animal daily post-surgery to monitor the animal health and wellbeing. This form included body weights, BAR (Bright, Alert, Responsive) score, incision conditions (signs of swelling/redness/discharge), and Pain Assessment Scoring (Table 1).

Score	Behaviour	Action
0	Normal behaviour	No action
1	Mild behaviour and physiological changes (slightly depressed behaviour, minor guarding of incision site)	Observe animal closely
2	Moderate pain (includes score of 1 plus swelling/redness/discharge at surgical site, reluctance to move, guarding with vocalization or aggression)	Observe animal closely and contact DV/ACUO for advice
3	Severe pain/distress (includes scores of 1 & 2 plus immobility,	Humanely euthanize and report.

	dehiscence of incision, profound dehydration/weight loss)	
4	Moribund	Humanely euthanize and report

Table 1. Animal daily assessment
Parameters and interpretation of scoring with action points. Abbreviations: DV, Designated Veterinarian; ACUO, Animal Care and Use Officer.

Seizure activity is sometimes induced following CCI and mice were monitored for the development of seizures post-injury. Animals with excessive and prolonged seizures accompanied by tonic flexion and extension of the limbs were removed from the study and humanely euthanized. In our study one mouse from the TBI cohort 1 and a second mouse from TBI cohort 3 developed progressive worsening seizures in the immediate post-operative period (within 1 hour) and were humanely euthanized.

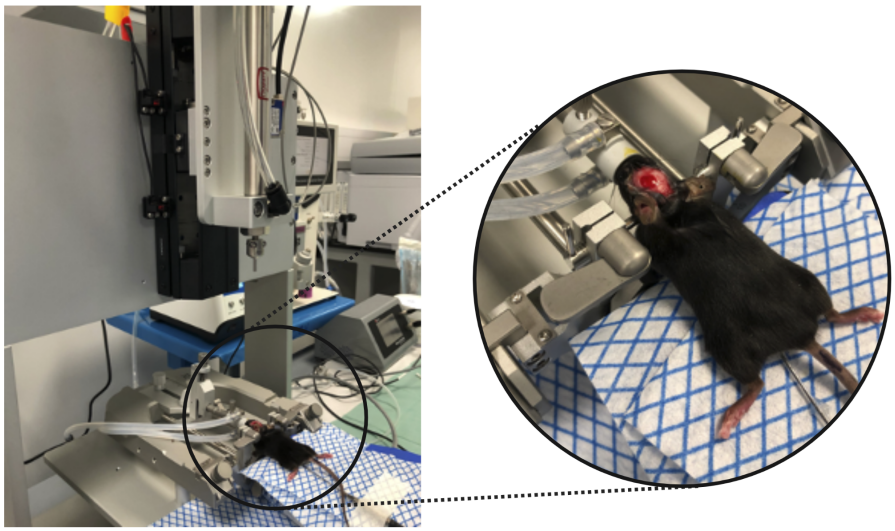

Figure 2-4. Controlled cortical impact device
Mice were mounted on the ear bars with their bodies placed on covered heated pads. Temperature was monitored throughout the procedure via a rectal temperature probe. This picture shows a mouse under anaesthesia (maintained through nose mask) seconds after the injury was induced.

2.2.6 Flow Cytometry Studies

2.2.6.1 Blood Preparation

Blood (~0.5ml) was collected via cardiac puncture of deeply anaesthetized mice into heparin-coated tubes. Two aliquots of 200µL of blood were transferred to two FACS tubes per mouse (to serve as control and stimulated tubes). Lysing buffer (2ml, 2.1.21) was added to all the samples to lyse the

red blood cells and incubated for 15 minutes at room temperature. Samples were then spun at 1350 rpm at 4°C for 5 minutes and supernatants were decanted. Pellets were resuspended with 1ml of Lysing buffer and incubated for 15 minutes at room temperature. A second spin was performed, and pellets were resuspended in 500µl of RPMI Glutamax without FBS (2.1.1). Cell pellets were then characterized using flow cytometry as described in the Flow Cytometry protocol below in section 2.2.6.3.

2.2.6.2 Spleen Preparation

Spleens were isolated from freshly perfused mice and transferred to tubes with ice-cold RPMI and homogenized using the flat end of the plunger of a 1ml syringe to mince the organ through a 70 µm cell strainer (Fisher Scientific, 352350). Cells were washed through the strainer with 10ml of RPMI without serum and centrifuged at 1350 rpm for 5 minutes at 4°C. The supernatants were carefully removed and discarded without disturbing the pellet. Pellets were then resuspended in 1ml of Lysis Buffer and incubated at room temperature for 2 minutes. RPMI (9ml) was added to each tube and the cell solution was spun at 1350 rpm at 4°C for 5 minutes. The final pellets were resuspended in 1.2ml of RPMI without serum. Two aliquots of 500µL of the solution were transferred to FACS tubes per mouse (to serve as control and stimulated samples). The samples were then processed as indicated in the flow cytometry protocol described below in section 2.2.6.3.

2.2.6.3 Flow Cytometry Protocol

Single-cell suspensions prepared from *in vitro* cultures (dHL-60 cells $1x10^6$ cells/ml) or from *in vivo* studies (blood and spleen) were analysed by multi-colour flow cytometry in FACS tubes. For detection of ROS, cells were stained with DHR123 (2.1.21; 1:500) and stimulated with 81nm PMA (2.1.21) and 1.34uM ionomycin (2.1.21) for 60 minutes (dHL-60 cells) or for 30minutes (blood and spleen) at 37°C, 5% CO2. The stimulation reaction was stopped with cold PBS and cells were pelleted by centrifugation at 1350 rpm for 5 minutes at 4°C. The pellet was resuspended in 50µl/tube of Live/Dead Near Infrared (2.1.21; 1:600 in PBS) and incubated for 15 min in the dark at room temperature. After this step cells were washed with PBS and spun at 1350 rpm for 5 minutes at 4°C. Surface staining was carried out for 20 minutes on ice in the dark using fluor-conjugated antibodies diluted in FACS buffer in the presence of Fcγ receptor blocking antibody to prevent non-specific binding. A surface stain master mix was made by adding appropriate dilutions (1:100-500) of the appropriate fluor-conjugated antibodies to FACS buffer (2.1.3) and 50µL was then added to each sample. Cells were washed twice with FACS buffer following surface staining. For intracellular staining with the NOX2 antibody (2.1.20), cells were first fixed with 50µl/tube of FoxP3 Fixation/Permeabilization solution (2.1.21) for 30 minutes at room temperature and then washed twice with 1X Permeabilization buffer (2.1.21). Fifty microliters of the NOX2 antibody solution (1:100 in 1X Permeabilization buffer) was then added to each sample and cells were stained in the dark for 1 hour on ice. After NOX2 staining, the cells were washed twice with 1X Permeabilization buffer and then washed again, twice, with FACS buffer. Supernatants were discarded and cells were re-suspended in FACS buffer (200µl/tube) and

stored at 4ºC in dark until analysed by the flow cytometer. dHL-60 cells were counted as described in methods section 2.2.1; for blood and spleen samples cell count estimations were performed using counting beads (2.1.21) according to the manufacturer's instructions. dHL-60 cells were gated on live/single cells as demonstrated in Figure 3-1A. In blood and spleen samples the gating strategy shown in Figure 3-10A was used to identify monocyte ($CD45^+CD11b^+Ly6C^+Ly6G^-$) and neutrophil ($CD45^+CD11b^+Ly6C^-Ly6G^+$) populations (complete gating strategy provided in Supplemental Figure 2).

2.2.6.4 Flow Cytometry Data Analysis

Data were acquired using BD FACSCanto II or BD LSRFortessa™ (BD Biosciences) and analysed using FlowJo™ v10.8 Software (BD Life Sciences). Compensation was calculated using single stained cells or compensation beads. Fluorescence minus one (FMO) controls were used for gating strategies. Mean Fluorescence Intensity (MFI) of the cells was measured on single live cells.

2.2.7 Statistical Analysis

All quantitative data were expressed as mean ± standard error of the mean (SEM). Experimental data were analysed by unpaired two-tailed student's t test (two data sets) or by one-way ANOVA with post hoc Tukey's multiple comparisons test (three or more data sets). Weight loss curves were analysed by repeated measures two-way ANOVA with post hoc Šídák's multiple comparisons test. Linear regression was performed to find the relationship between the MFI DHR123 and MFI NOX2 in *in vivo* and in *vitro* studies. Statistical analyses were performed using GraphPad Prism v9.3.1, GraphPad software (San Diego, California, USA) with a $p<0.05$ being considered statistically significant.

CHAPTER 3: RESULTS

3.1 - NOX2/ROS assay development in a neutrophil-like cell line

3.1.1 Dihydrorhodamine 123 (DHR123) can be used as a ROS probe in PMA/ionomycin stimulated neutrophils-like cells

There is extensive research using DHR123 as a ROS indicator (Djiadeu et al., 2017; Jirapongsananuruk et al., 2003; Quinn et al., 2007; Sacco et al., 2020). In this study we aimed to determine the potential of this dye as a component of our biomarker assay. Initially the goal was to optimize cell culture and differentiation conditions, duration of PMA/ionomycin stimulation and DHR123 flow cytometry data interpretation. HL-60 cells were initially treated with 1.3% DMSO for 3-5 days to induce differentiation into neutrophil-like cells, as described in the methods section. Following that, cells were counted and transferred to FACS tubes, stained for DHR123, and stimulated with 81nM PMA and 1.34uM ionomycin for 5, 10, 30 and 60 minutes. PMA and ionomycin concentrations were chosen based on previous experiments from Loane lab (Ritzel et al., 2018). Cells were fixed with 4% PFA and then analysed by flow cytometry for mean fluorescence intensity of DHR123. It was noticed during FACS analysis that DMSO treatment induced the generation of two subpopulations (Figure 3-1A and 3-1C), but since no superficial marker was used in these experiments to differentiate the populations, a decision was made to perform all the analysis in the live cells gate.

PMA/ionomycin stimulation significantly increased ROS release in differentiated HL-60 (dHL-60) cells after 30 minutes and 60 minutes (****$p<0.0001$), when compared to controls (Figure 3-1B). A subsequent analysis in the subpopulations mentioned previously (Figure 3-1C) demonstrated that the population with the higher FSC-A produced more ROS compared to the population with the lower FSC-A. This finding could be interpretated as the “High-FSC-A” being the true differentiated HL-60 population (Babatunde et al., 2021). However, superficial markers such as CD11b and LTB4 will need to be included in future experiments to allow for further characterization. Combining these subpopulations in the gate of live cells did not affect the final result.

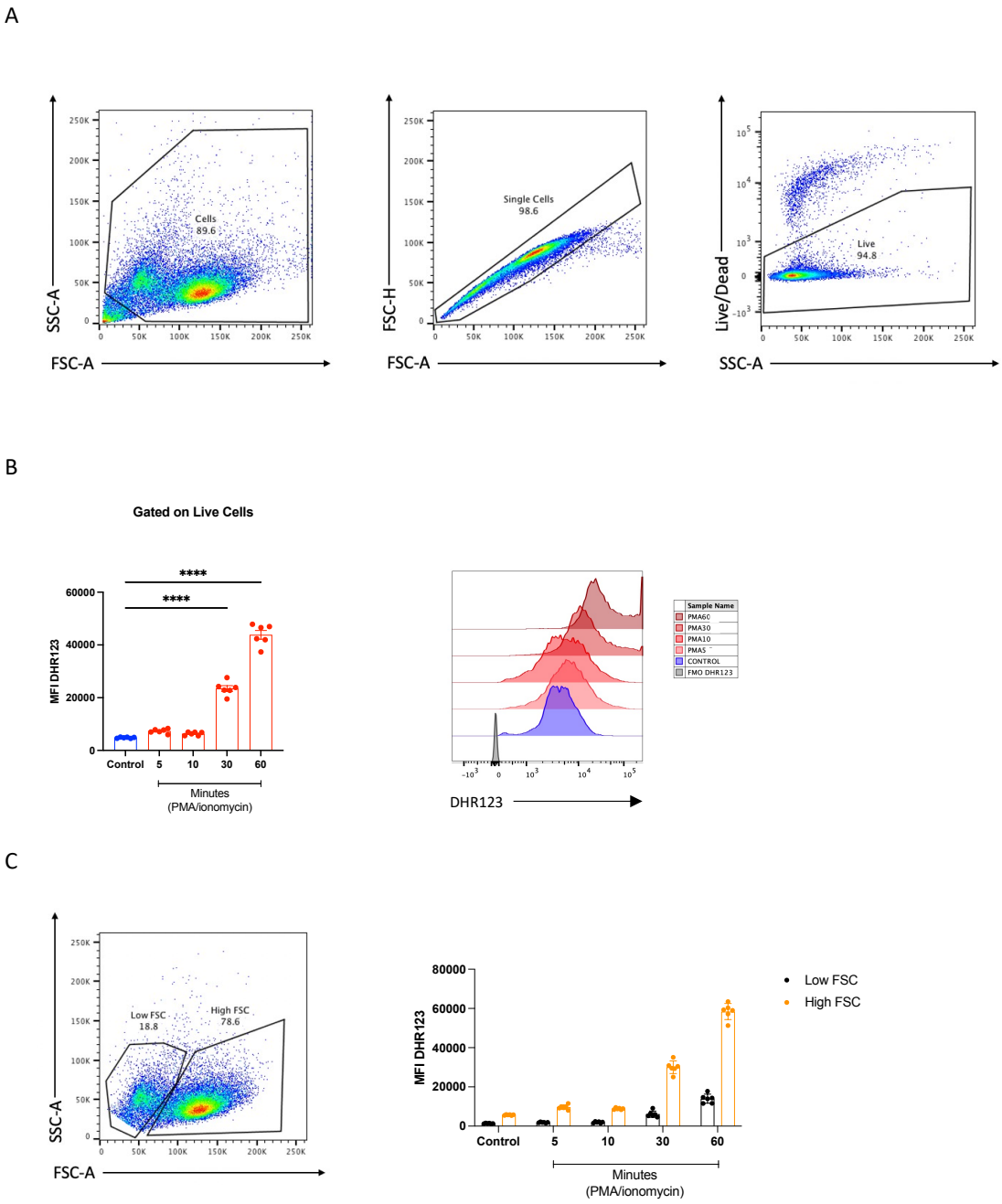

Figure 3-1. Reactive Oxygen Species (ROS) release induced by PMA/ionomycin in dHL-60 cells
HL-60 cells were differentiated with 1.3% DMSO (v/v) for 5 days and then stimulated with PMA 81nM and ionomycin 1.34uM for 5, 10, 30 and 60 minutes. After the stimulation period cells were fixed and analysed by flow cytometry for Mean Fluorescence Intensity of DHR123, a ROS dye. A) Gating strategy used in Flow Cytometry studies; B) Time-dependent ROS release (MFI DHR123) after PMA/ionomycin stimulation by live dHL-60 cells. C) HL-60 subpopulations noted after DMSO induced differentiation showed different levels of ROS release. Data are mean ±SEM (n=6 per group). ****p<0.0001 versus control by one-way ANOVA with post hoc Tukey's multiple comparisons test.

3.1.2 NAPDH Oxidase 2 (NOX2) is activated upon PMA/ionomycin stimulation of dHL-60 cells

We successfully demonstrated above that PMA/ionomycin induces ROS release in dHL-60 cells. However, there are multiple sources of ROS within the cellular apparatus, with NOX2 being one of them and the major focus of this research. As DHR123 does not bind specifically to NOX2-driven ROS it was necessary to assess whether PMA/ionomycin stimulation was activating NOX2 in dHL-60 cells. The NADPH oxidase (NOX2) complex requires a particular activation process through interaction of its subunits (Figure 3-2A). Briefly, the cytosolic subunits ($p40^{phox}$, $p47^{phox}$, and $p67^{phox}$) translocate to the plasma membrane and anchor to the membrane bound subunits ($gp91^{phox}$ and $p22^{phox}$) to enable the complex assembly and function. Another crucial step is the phosphorylation of $p47^{phox}$, which enables its interaction with $p22^{phox}$.

HL-60 cells were differentiated with 1.3% DMSO for 3-5 days and then stimulated with 81uM PMA and 1.34uM ionomycin for 0, 5, 10, 30 and 60 minutes. Total cell lysates were used for protein expression analysis via western blotting. Upon PMA/ionomycin stimulation there is increased phosphorylation of $p47^{phox}$ at the serine 345 residue after 5 minutes when compared to controls (normalized to total $p47^{phox}$) (Figure 3-2B). This increase in phospho-$p47^{phox}$ (ser345) was reduced by 30 minutes and returned to baseline control levels 60 minutes following treatment (Figure 3-2B).

As translocation of subunits is a critical component in NOX2 complex assembly, we next performed subcellular fractionation to examine the cellular location of subunits during temporal PMA/ionomycin stimulation of dHL-60 cells. HL-60 cells were differentiated with 1.3% DMSO (v/v) for 3-5 days and then stimulated with 81nM PMA and 1.34uM ionomycin for 0, 30, and 60 minutes. After the stimulation, cells were gently lysed in a subcellular fraction buffer and subjected to differential centrifugation in order to separate nuclear, mitochondrial, cytoplasmic, and plasma membrane proteins. Total cell lysate was used as a positive control, while β-actin and caveolin were used as cytoplasm and plasma membrane markers, respectively (Figure 3-2C). Results indicate that with prolonged exposure to PMA/ionomycin stimulation there is increased protein expression of the membrane bound subunits: $p22^{phox}$ and $gp91^{phox}$. Translocation of the cytosolic subunits ($p40^{phox}$, $p47^{phox}$ and $p67^{phox}$) from the cytoplasm to the plasma membrane is observed upon PMA/ionomycin stimulation. Additionally, these subunits also exhibited increased expression in the cytoplasmic fraction indicating either an increase in protein translation and/or gene expression. These results corroborate the hypothesis that PMA/ionomycin stimulation of dHL-60 cells enables NOX2 complex assemble and activation through key changes in their subunits including phosphorylation, translocation, and elevated protein expression.

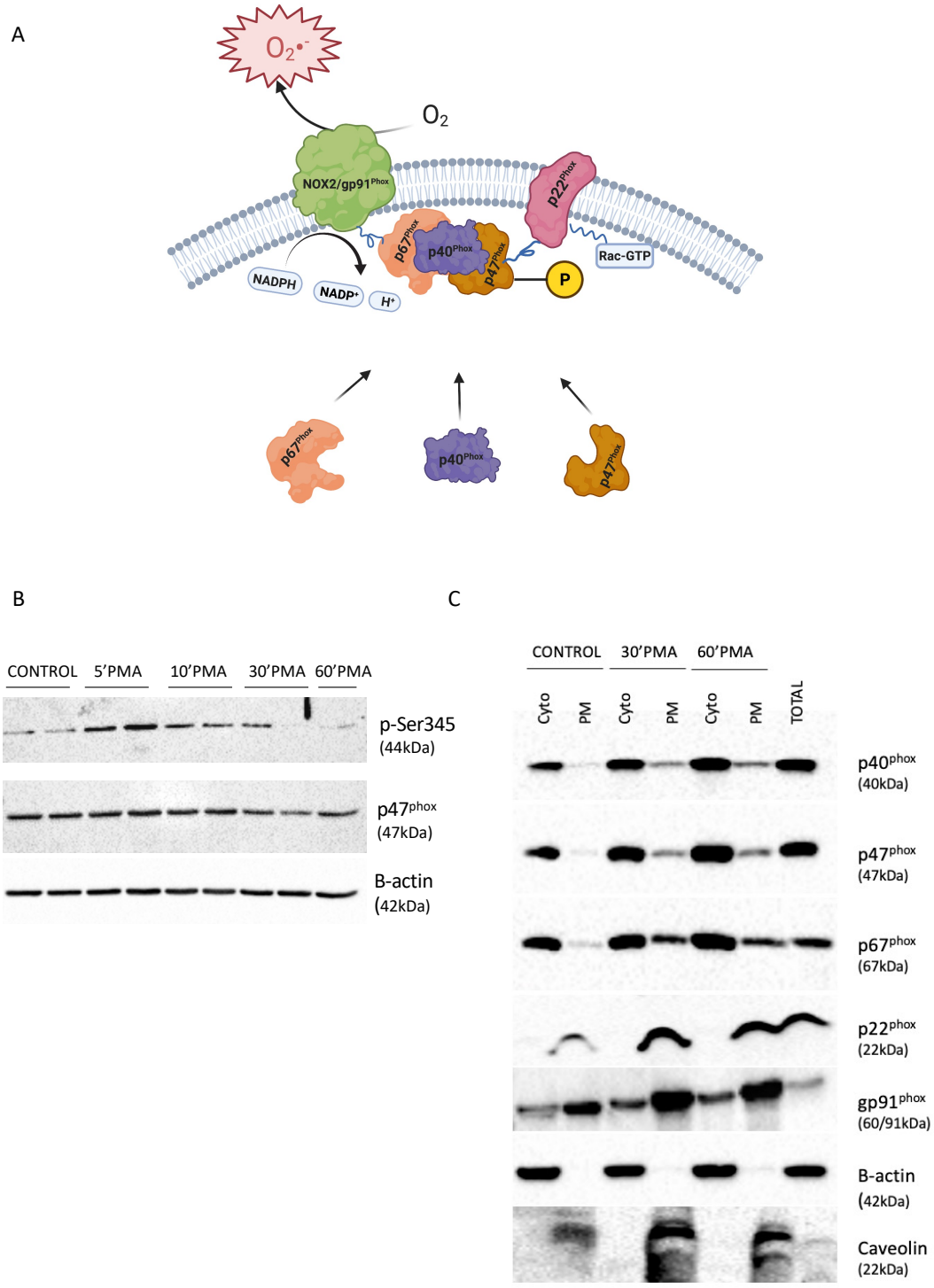

Figure 3-2. PMA/Ionomycin stimulation causes ROS release through NAPDH (NOX2) activation
The complex assembly is seen by phosphorylation of p47phox, translocation of p40phox, p47phox and p67phox to the plasma membrane and increased expression of p22phox and gp91phox in the plasma membrane. A) Schematic: NADPH oxidase (NOX2) activation schematic representation: the generation of superoxide anion (O2-) is based on the translocation of p40phox, p47phox and p67phox and on the phosphorylation of p47phox subunit. HL-60 cells were differentiated with 1.3% DMSO (v/v) for 5 days and then stimulated with PMA 81nM and ionomycin 1.34uM for 0, 5, 10, 30 and 60 minutes. B) Total cell lysates were used for qualitative Western Blot analysis of p47phox phosphorylation. C) HL-60 cells were differentiated with 1.3% DMSO (v/v) for 5 days and then stimulated with PMA 81nM and ionomycin

1.34uM for 0, 30 and 60 minutes. After the stimulation, cells were lysed and submitted to a subcellular fractionation protocol for Western Blot. A total cell lysate (right) was used as positive control. β-actin and Caveolin were used as cytoplasm and plasma membrane markers, respectively.

3.1.3 DPI and GSK2795039 reduce PMA/ionomycin-induced ROS in a concentration-dependent manner in dHL-60 cells

Additional experiments were performed to determine the optimal duration of PMA/ionomycin for examination of ROS generation. 60 minutes was selected as the optimal duration of PMA/ionomycin stimulation. With the concentration and timing of stimulation established, our next aim was to test the effect of two pharmacological ROS inhibitors on the stimulated dHL-60 cells using MFI DHR123 by flow cytometry. Firstly, we assessed the effect of diphenyleneiodonium chloride (DPI), a broad antioxidant which is non-specific for NOX2 (Figure 3-3A) and secondly, we examined the effect of GSK2795039, a novel NOX2 inhibitor (Figure 3-3B). dHL-60 cells were co-treated with 81uM PMA, 1.34uM ionomycin, and either DPI (0.1, 0.5, 1, 5μM) or GSK2795039 (1, 5, 10, 25μM) for 60 minutes. DPI (0.5μM) and GSK2795039 (25μM) alone were used as the drug controls. PMA/Ionomycin increased ROS generation compared to controls (C, D ****$p<0.0001$). DPI significantly attenuated PMA/ionomycin-induced ROS production in a concentration-dependent manner from 0.5μM (++++$p<0.0001$; Figure 3-3C). GSK2795039 significantly reduced PMA/ionomycin-induced ROS production in a concentration-dependent manner from 1μM (++++$p<0.0001$; Figure 3-3D). PMA/ionomycin stimulation significantly decreased cell viability (****$p<0.0001$) (Figure 3-3E, F), which was not rescued by treatment with either DPI (Figure 3-3E, F) or GSK (Figure 3-3F).

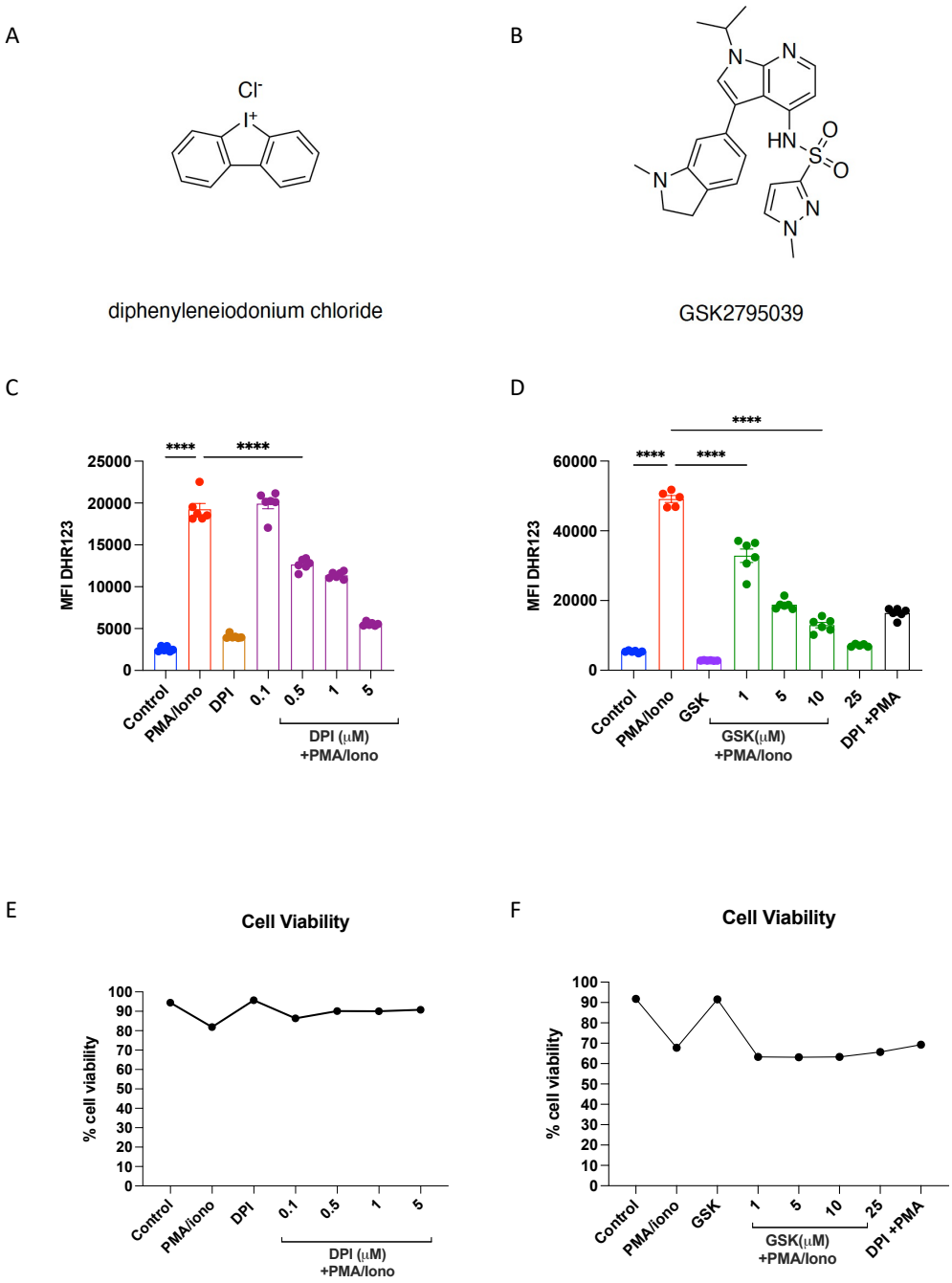

Figure 3-3. DPI and GSK2795039 attenuates ROS release induced by PMA/ionomycin in dHL-60 cells in a dose-dependent manner

The chemical structure of GSK2795039 (A) and Diphenyleneiodonium chloride (DPI)(B). HL-60 cells were differentiated with 1.3% DMSO (v/v) for 5 days and then co-treated with PMA 81nM, ionomycin 1.34uM and Diphenyleneiodonium (DPI) (0.1, 0.5, 1, 5μM) or GSK2795039(1, 5, 10, 25μM) for 60 minutes. DPI (0.5μM) and GSK2795039 (25μM) were used as the drug controls. ROS levels were measured by flow cytometry for Mean Fluorescence Intensity of DHR123. Trends for PMA/ionomycin induced decrease in cell viability were not rescued by either DPI (E, F) or GSK (F). Data are mean ±SEM (n=6 per group). ****p<0.0001versus control, +p<0.05; ++p<0.01; +++p<0.001; ++++p<0.0001 versus PMA/ionomycin by one-way ANOVA with post hoc Tukey's multiple comparisons test.

3.1.4 DHR123 is sensitive to intra- and extracellular ROS generation

To further characterize DHR123 as a ROS probe we examined cellular production of ROS in different compartments (intra- and extracellular). There are two different pools of NOX2, one in the plasma membrane and other in the phagosome membrane. This means that depending on the agonist the assembly of the NOX2 complex can either lead to extracellular ROS release or to the intracellular release. In theory, DHR123 should measure mainly intracellular ROS, as it diffuses across the cell membrane, but some of the hydrogen peroxide (H_2O_2) released extracellularly may also pass through the plasma membrane and bind with the probe intracellularly.

Here, we sought to address this aspect of DHR123 behaviour by adding Superoxide Dismutase (SOD) and catalase to the experiment. SOD catalyses the reduction of O^{2-} to H_2O_2, while catalase catalyses the reduction of H_2O_2 to H_2O (Figure 3-4A). Therefore, when these two membrane-impermeable enzymes are included in reaction mixtures they remove O^{2-} and H_2O_2 release extracellularly, leaving ROS generated specifically in intracellular compartments to be measured (Dao et al., 2020).

Differentiated HL-60 were pre-treated with SOD (25, 50, 100units) or catalase (25, 50, 100µg) (Figure 3-4B) or a combination of SOD 50U and catalase 50µg (Figure 3-4C) for 15 minutes and then stimulated for 60 minutes with PMA 81nM, ionomycin 1.34uM. SOD alone caused increased DHR123 fluorescence signal in a concentration-dependent manner (+$p<0.05$; ++$p<0.01$; +++$p<0.001$; ++++$p<0.0001$ versus PMA/ionomycin), whereas catalase decreased DHR123 signal with increasing concentrations. These findings demonstrate that DHR123 is sensitive to H_2O_2 levels, but it is not possible to conclude that H_2O_2 is the only oxidant that can change the fluorescence of this substrate. The presence of SOD 50U and catalase 50µg combined reduced the extracellular ROS concentration resulting in significantly attenuated the PMA/ionomycin induced DHR123 MFI. This result indicates that DHR123 is sensitive to extracellular, as well as intracellular ROS (Quinn et al., 2007).

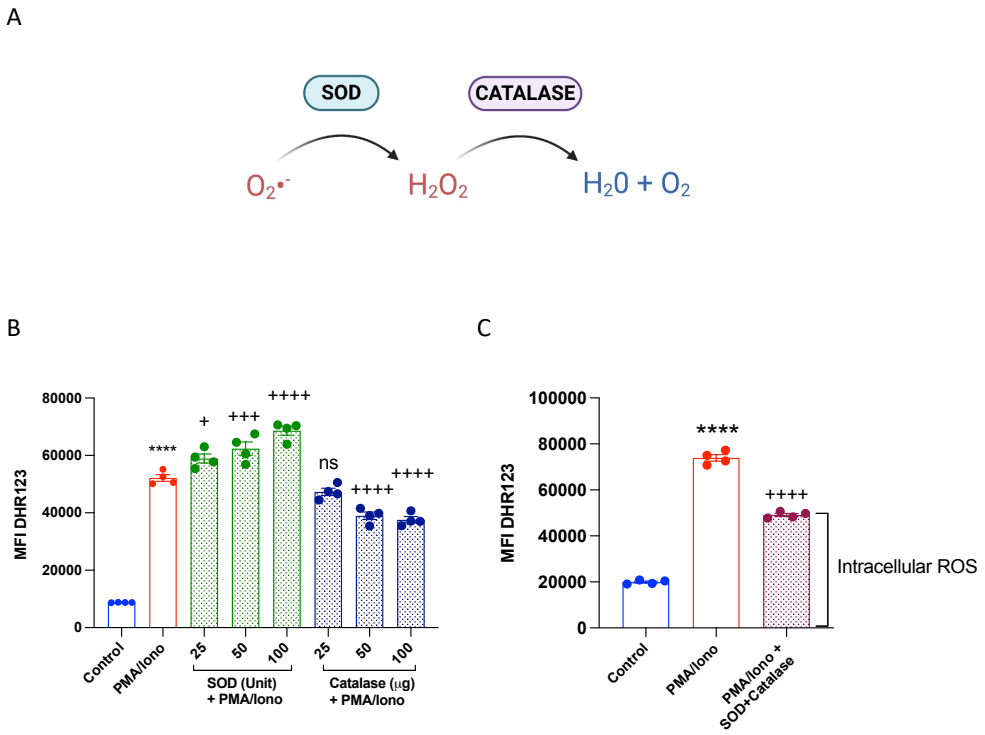

Figure 3-4. DHR123 is sensitive to intra and extracellular ROS generation
A) Schematic: Superoxide dismutase (SOD) catalyses the reduction of O_2^- to H_2O_2 and catalase catalyses the reduction of H_2O_2 to H_2O. The addition of these 2 enzymes to the experiment removes extracellularly released O_2^- and H_2O_2 leaving ROS generated specifically in intracellular compartments to be measured. B) HL-60 cells were differentiated with 1.3% DMSO (v/v) for 5 days. Cells were then pre-treated with SOD (25, 50, 100units) or catalase (25, 50, 100µg) (B) or SOD 50U and catalase 50µg (C) for 15 minutes and stimulated for 60 minutes with PMA 81nM, ionomycin 1.34uM. Data are mean ±SEM (n=4 per group). ****p<0.0001versus control, +p<0.05; ++p<0.01; +++p<0.001; ++++p<0.0001 versus PMA/ionomycin by one-way ANOVA with post hoc Tukey's multiple comparisons test.

3.1.5 GSK2795039 treatment decreases ROS production and NOX2 (gp91^{phox}) expression

Our next aim in the biomarker assay development was to combine DHR123, a general ROS probe, with a specific NOX2 marker and correlate these two. The specific marker chosen was an antibody against the gp91^{phox} subunit (Alexa Fluor 647, Bioss). To include the NOX2 antibody in this experiment a few adjustments were necessary in the protocol because this antibody binds to the intracellular portion of the subunit requiring intracellular staining step. Titration of the NOX2 antibody was also performed to find the optimal concentration for these cell line (Supplemental Figure 1).

HL-60 cells were differentiated with 1.3% DMSO (v/v) for 3-5 days and then co-treated with PMA 81nM, ionomycin 1.34uM and GSK2795039 10µM for 60 minutes. Cells were stained for DHR123, Live/Dead, intracellular gp91^{phox} and analysed by flow cytometry. GSK2795039 optimal concentration (10µM) was chosen based on our previous experiments (Figure 3-3D). GSK2795039 significantly reduced NOX2 expression (MFI NOX2) (+p<0.05) and ROS levels (MFI DHR123) (++++p<0.0001) compared to the PMA/ionomycin stimulated cells (Figure 3-5A and 3-5B). A linear regression analysis

was carried out to investigate the relationship between MFI DHR123 and MFI NOX2. We found a significant relationship ($p < 0.001$) between these two variables ($R^2 = 0.59$) (Figure 3-5C). Further experiments investigating the specificity of the NOX2 antibody would be interesting, such as using NOX2 knockout cells (CGD neutrophils) as negative controls.

Our *in vitro* experiments represented the cornerstones of the development of our TBI NOX2/ROS functional biomarker. The encouraging results we had combining DHR123 and NOX2 antibody in a flow cytometry panel lead us to the next step, the application of the optimized NOX2/ROS flow cytometry assay in tissues from sham and TBI animals.

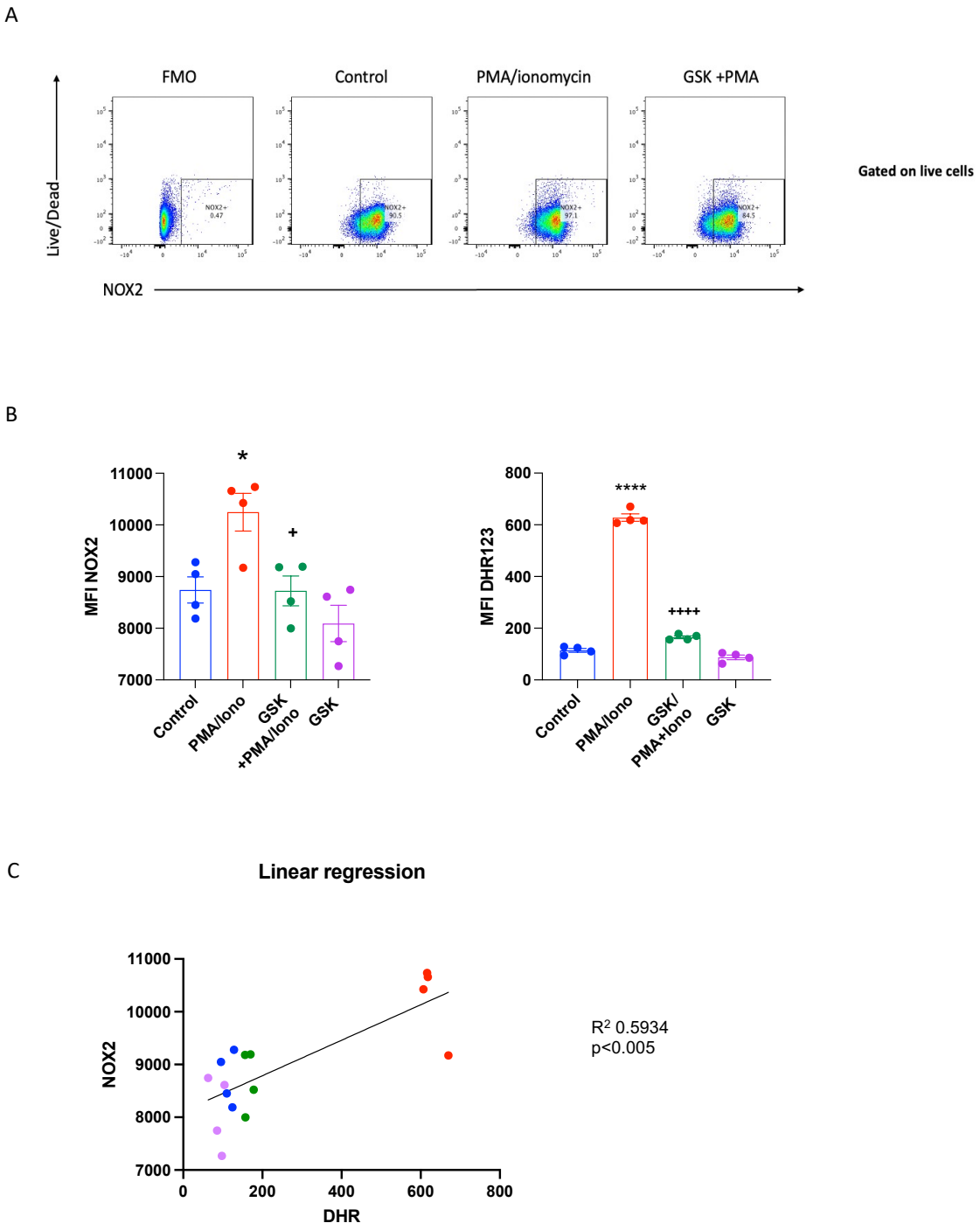

Figure 3-5. GSK2795039 treatment decreases ROS production and NOX2 (gp91^{phox}) expression
HL-60 cells were differentiated with 1.3% DMSO (v/v) for 5 days and then co-treated with PMA 81nM, ionomycin 1.34µM and GSK2795039 10µM for 60 minutes. Cells were stained for DHR123, Live/Dead, intracellular gp91^{phox} and analysed by flow cytometry. (A) Representative FACS plots. (B) Results are expressed as MFI of NOX2 (gp91^{phox}) and MFI of DHR123 (ROS levels) . (C) Linear regression between MFI NOX2 values and MFI DHR123 values – p value < 0.0005, R^2 = 0.5934. Dots are colour-coded for each group. Data are mean ± SEM (n=4/group). *p<0.05; ****p<0.0001 versus control, +p<0.05; ++p<0.01; +++p<0.001; ++++p<0.0001 versus PMA/ionomycin by one-way ANOVA with post hoc Tukey's multiple comparisons test.

3.2 - NOX2/ROS biomarker assay applied to TBI mice

In the previous section (3.1) we described the development of a flow cytometry assay to measure NOX2 activity and ROS release at the same time using a neutrophil-like cell line. We combined DHR123 (ROS) with a NOX2 specific antibody (anti-gp91^{phox}) in the same panel and we were able to demonstrate a significant correlation between these two factors. Having established that, our next goal was to apply the same protocol in the blood from brain injured mice to demonstrate that this assay could be used as a NOX2/ROS blood-based functional biomarker. Several preclinical studies have shown that TBI induces changes in peripheral organs including those involved in the systemic immune response (Doran et al., 2020; Hanscom et al., 2021; Ritzel et al., 2018). The spleen plays a crucial role in peripheral immune responses and is known to be affected by brain injury (Rasouli et al., 2011). Therefore, we decided to include the spleen in our investigation of immunophenotypic and functional changes induced by experimental TBI.

3.2.1 TBI induced macroscopic neuroinflammation changes in different time points post-injury

Young adult male mice were subjected to either sham surgery (incision only) or controlled cortical impact (CCI). On day 1 (cohort 1), day 7 (cohort 2) or day 14 (cohort 3) post-injury, mice were euthanized, and brain, blood, and spleen were collected as described in Chapter 2 for further analysis. Before dissecting the brains, we took pictures to perform a macroscopic evaluation of these organs and compare them in the different cohorts and conditions (Figure 3-6; TBI vs sham).

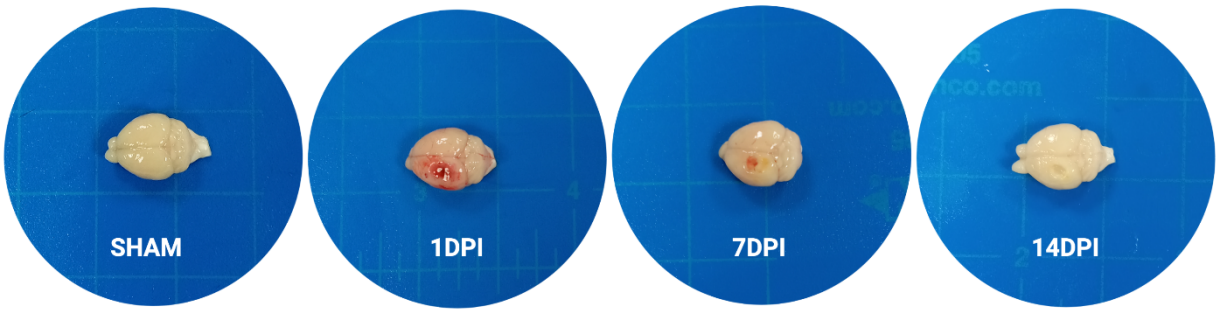

Figure 3-6. Mild to moderate-level TBI pathoprogression at the site of injury in mice
Representative images of brains from sham and TBI mice at 1-, 7- and 14-days post injury. Injury progression from initial tissue damage with associated vasculature damage and haemorrhage (1-day post-injury), to resolution and clearance of haemorrhage and necrotic tissue (7-days post-injury), to the chronic progressive loss of white matter at the injury site (14-days post-injury).

Although an immunohistochemistry study with stereological analysis of lesion volume would be the best method to characterize the effect of TBI on these brains, it is still possible to describe some temporal macroscopic changes. After 1 day of injury, brains presented with signs of acute inflammation such as edema and more blood content visible (due to leakage of blood into the cortical tissue resulting

from vasodilatation, increased vascular permeability and damage of the vasculature) despite being perfused as described in Chapter 2. At 7 days post-injury the cavity in the cortex appeared to be more defined and there was less blood overall (subacute phase). Two weeks after injury, the impact site seemed increased in size compared to other time points, due to the scarring process leading to brain tissue loss. The pictures from our study correlate well with previous preclinical studies examining lesion volume expansion after experimental TBI (Loane et al., 2014; Mao et al., 2020; Turtzo et al., 2014; Zhao et al., 2018).

3.2.2 TBI did not significantly alter body or spleen weights at both acute and chronic time points following injury

Experimental TBI has been reported to result in significant body weight loss at acute time points following the initial insult (Hanscom et al., 2021). Additionally, TBI induces a systemic immune response involving a splenic contribution (Rasouli et al., 2011). Systemic inflammation is typically associated with an increase in spleen size and weight, however, data regarding morphological changes in the spleen following TBI have been largely overlooked and not reported in the preclinical literature (Ritzel et al., 2018). We examined changes in body weight and spleen weights at all time points following injury.

Sham and TBI mice lost similar amounts of weight, at a similar speed, with peak weight loss occurring 1 day after injury in cohorts 2 and 3. In cohort 1 it is also possible to observe a peak weight loss but there is no statistical significance between sham and TBI (cohort 1: p=0.5). There was no different in the comparison Sham vs TBI in cohorts 2 and 3 within time (*cohort 2*: Injury effect: p=0.4786; *cohort 3*: Injury effect: p= 0.6062). By the end of the third day, all mice were close to their initial weight in cohorts 2 and 3. Weight loss was analysed by repeated measures Two-Way ANOVA in cohorts 2 and 3 to determine the interactions of time and injury, followed by *post-hoc* adjustments using a Sidak's multiple comparison test. Data in cohort 1 was analysed by paired t test (Figure 3-7).

At 1-, 7-, and 14-days post-injury, spleens were removed immediately following blood collection and prior to transcardial perfusion and weighed before being processed for Flow Cytometry analysis. No significant changes in spleen weights were found between the sham and TBI (Figure 3-8; TBI vs sham, A: p = 0.0894, B: p = 0.4666, C: p = 0.1102). We did not observe any other gross macroscopic changes to these spleens.

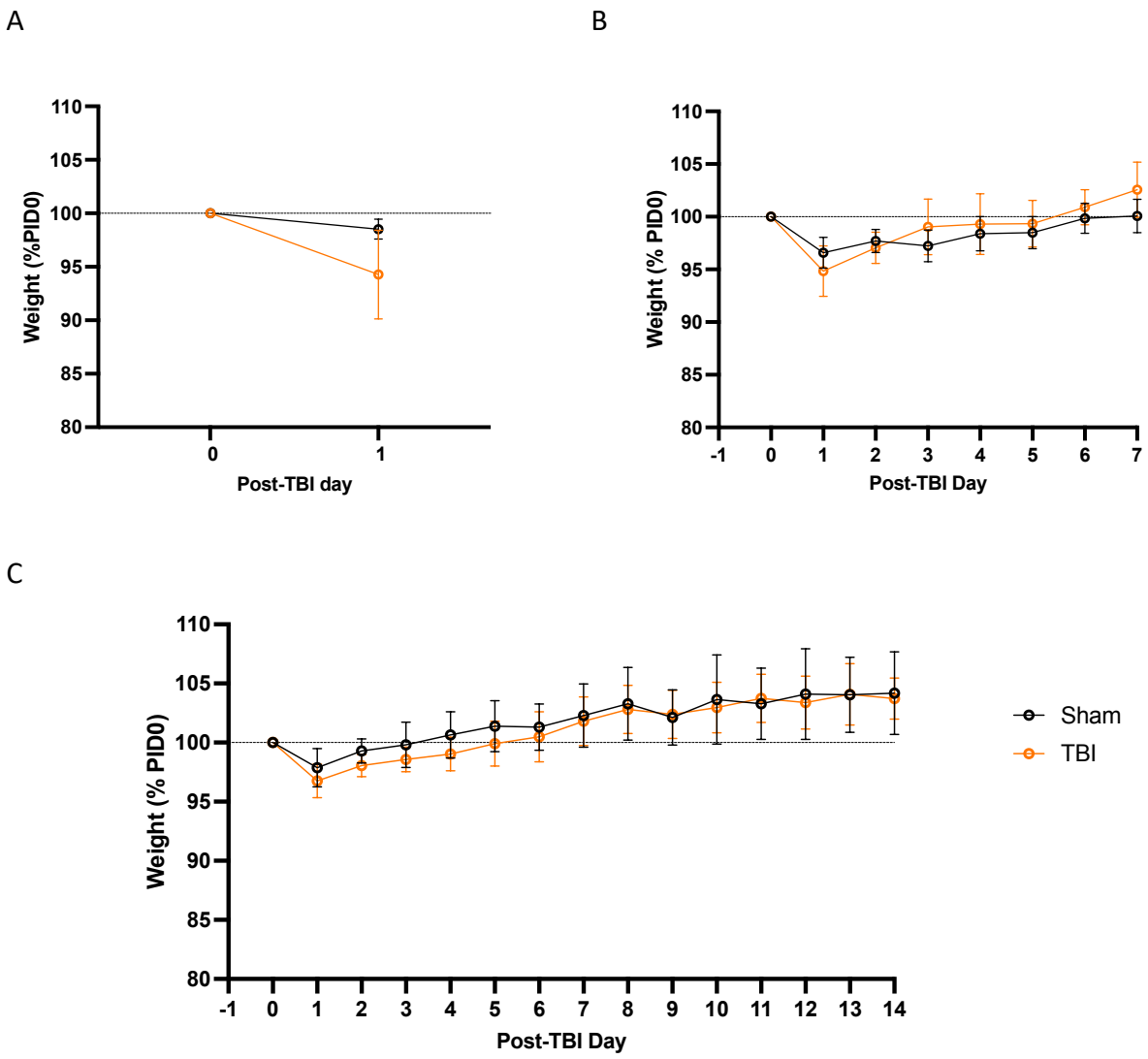

Figure 3-7. Alteration of body weights following experimental TBI
Graphic representation of temporal changes in body weight in sham and TBI mice from cohort 1 (1 day post-injury; A), cohort 2 (7-days post-injury; B), and cohort 3 (14-days post-injury; C). TBI did not significantly exacerbate the amount of body weight lost or alter physiological weight gained over time compared to sham. Data expressed as mean ± SEM (A: *cohort 1, Injury effect: p=0.5,* n= 4-5*; cohort 2, Injury effect: p=0.479,* n= 5-6; *cohort 3*, *Injury effect: p0.6062,* n=5-6) by repeated measures two-way ANOVA with post hoc Tukey's multiple comparisons test (cohorts 2 and 3) and paired t test (cohort 1).

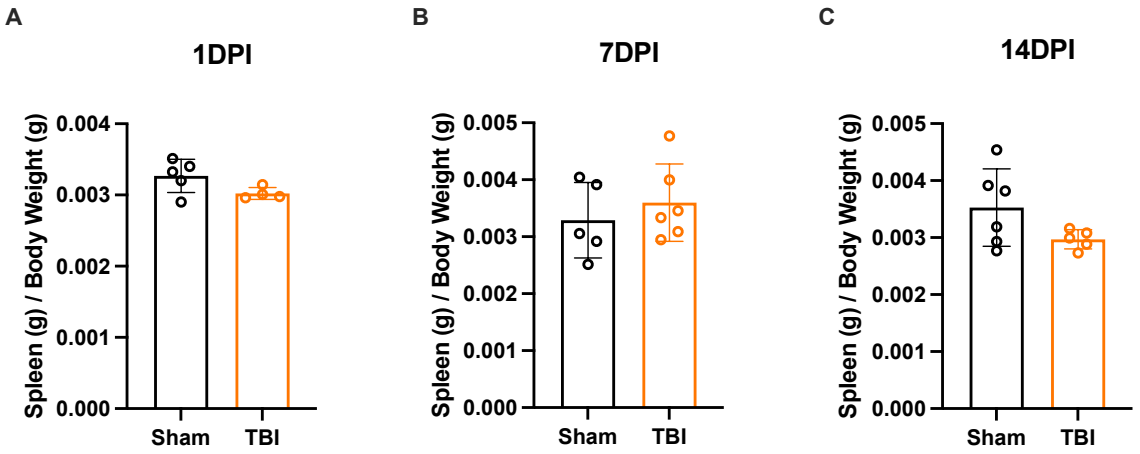

Figure 3-8. Experimental TBI did not significantly alter spleen weight
Traumatic brain injury did not induce significant changes in spleen weight (normalized to body weight) compared to sham controls at 1-, 7-, or 14-days post-injury (A, B, C, respectively). Data expressed as mean ± SEM and statistical significance analysed by unpaired two-tailed t-test. No statistical significance was found between the experimental groups at any time point analysed.

3.2.3 TBI prolonged the return of righting reflex

Righting reflex is defined as the time required for the animal to return to all four paws after being placed in a supine position. This is a binary measure widely used for assessing arousal/recovery of consciousness in rodents (Solt et al., 2011; Yarnell et al., 2016). In our study recovery of righting reflex (RORR) was recorded for all mice after exposure to isoflurane was terminated. TBI was found significantly increased RORR compared to sham (RR time sham: 259.3s, RR time TBI: 827.4s, $p<0.0001$ vs sham; Figure 3-9). As assessment of RORR occurred immediately following sham- and TBI-surgery for all mice, data from all cohorts was combined for analysis.

One confounding factor that could have affected these results could be the average duration of isoflurane exposure per procedure. The average time for CCI surgeries was 42:40 minutes and the average time for sham surgeries was 26:54 minutes. The timing of isoflurane exposure for sham mice should have been matched to exposure times for CCI surgeries within each cohort; however, due to time constraints sham mice were removed from isoflurane exposure following completion of sham surgery rather than allowed to remain under isoflurane longer to match a CCI surgery. Furthermore, there is some criticism regarding using RORR as a measure of return of consciousness (Gao & Calderon, 2020; Vincent et al., 2021) and this will be discussed separately in Chapter 4.

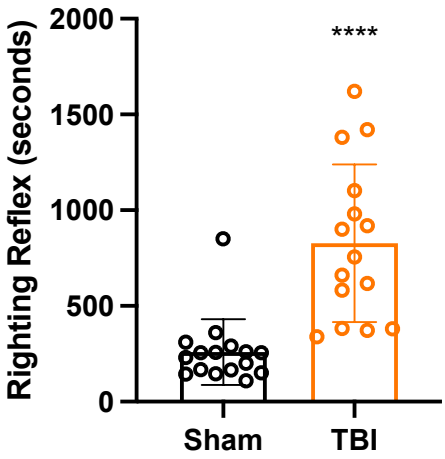

Figure 3-9. TBI increased righting reflex recovery
Recovery of righting reflex was significantly delayed in TBI compared to sham mice. Mice from all cohorts were combined for analysis (sham: n = 16; TBI: n = 15). Data expressed as mean ± SEM and analysed for statistical significance using the two-tailed, unpaired student t-test (Sham: 259.3s; TBI: 827.4s; difference of means: 568.1 ± 112.2 (95% CI: 338.7 to 797.5) **** p<0.0001 vs sham).

3.2.4 Absolute counts of neutrophils and monocytes in the blood remained unaltered following experimental TBI

Blood was collected via cardiac puncture under anaesthesia at 1-, 7-, and 14-days post-injury and cells were prepared for flow cytometry analysis as described in Chapter 2. Cell counts were performed using counting beads and cells were stained for surface CD45, CD11b, Ly6C, Ly6G. A standardized gating strategy (Figure 3-10A) was used to identify monocytes ($CD45^+CD11b^+Ly6C^+Ly6G^-$) and neutrophils ($CD45^+CD11b^+Ly6C^-Ly6G^+$) populations. Cell-specific fluorescence minus one (FMO) controls were used to determine the positivity of each antibody. The absolute number of $Ly6C^+$ monocytes and $Ly6G^+$ neutrophils subsets per 200uL of blood are represented (Figure 3-10B).

There was no statistical difference in numbers of $Ly6C^+$ monocytes when comparing sham and TBI mice at any time points. At 24 hours post-injury there was a significant decrease in absolute numbers of blood neutrophils in the TBI group (-2579 ± 980.4 *p= 0.0390 vs sham; Figure 3-10B) and no difference was observed at 7 and 14 days post-injury. This decrease in neutrophils counts after TBI is not consistent with previous published studies (Ritzel et al., 2018) and it was not expected. We decided to analyse this data separately using unpaired t-test based on the caveat that the samples from each cohort were obtained and processed for flow cytometry in different dates.

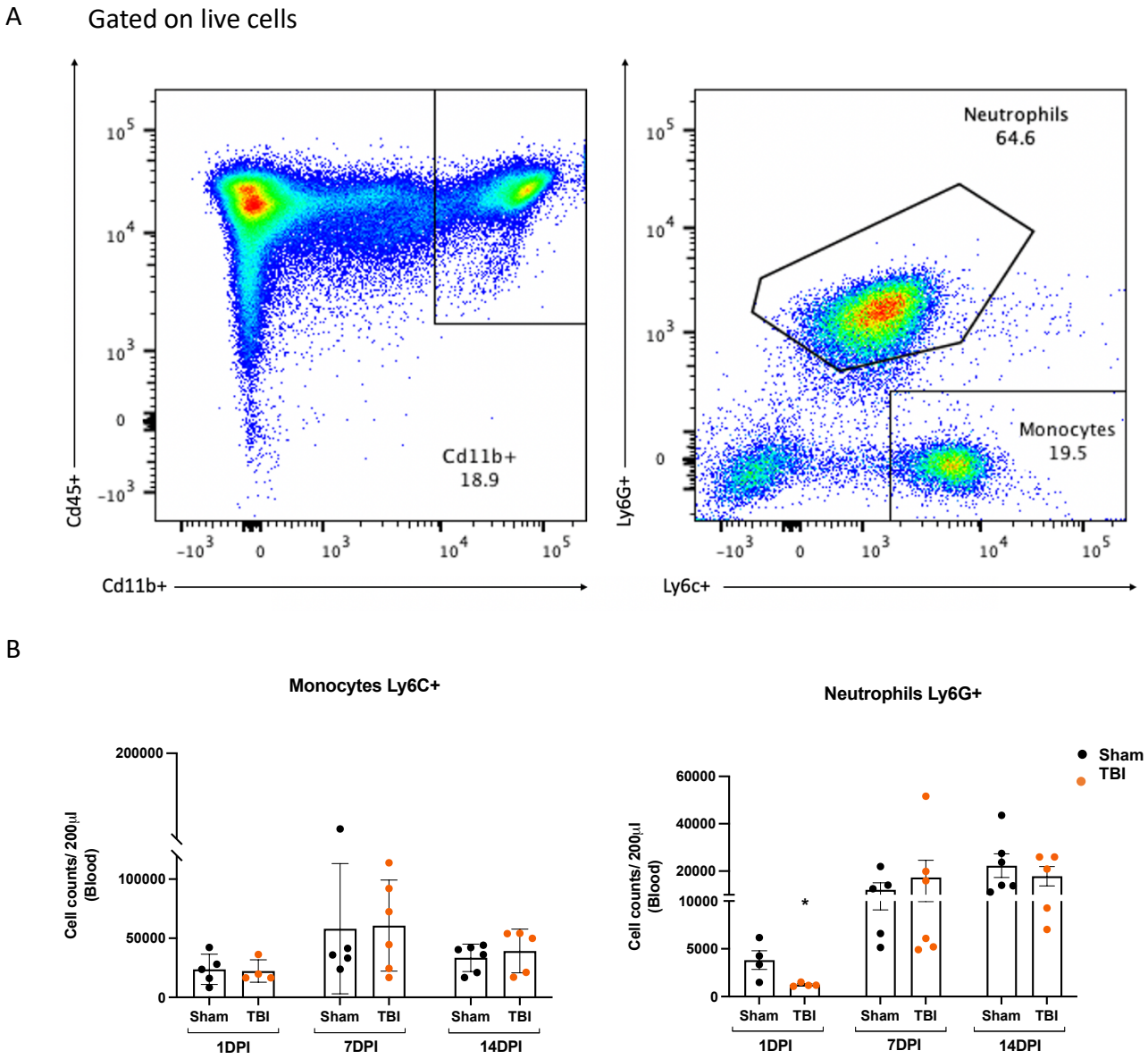

Figure 3-10. Leukocyte composition in the blood at different time points after TBI
Representative FACS plots of the gating strategy to identify Ly6C$^+$ monocytes and Ly6G$^+$ neutrophils populations in the blood (A). Briefly, cells were gated on single cells, live cells, CD45$^+$ and CD11b$^+$ cells. Monocytes were then gated on CD45$^+$CD11b$^+$Ly6C$^+$Ly6G$^-$ and neutrophils gated on CD45$^+$CD11b$^+$Ly6C$^-$Ly6G$^+$ (Complete gating strategy in the Supplemental Figure 2). The absolute Ly6C$^+$ monocytes and Ly6G$^+$ neutrophils counts were assessed in the blood at the indicated time points after TBI (B). For all experiments, n = 4–6/group. Data expressed as mean ± SEM relative to sham and statistical significance analysed by unpaired student t- test.

3.2.5 NOX2/ROS blood-based functional biomarker in the CCI model of experimental TBI

Respiratory burst consists of a rapid release of high concentrations of ROS by the innate phagocytes (Nguyen et al., 2017). This can be generated by NOX2 enzyme complex and it plays an important role in the defense against bacterial infection. The absence of this response leads to increased risk of infection while its exacerbation causes excessive inflammation and tissue damage (Husain et al., 2020; Kumar et al., 2016).

In this study we used PMA/ionomycin as a respiratory burst inducer. Considering that the CCI injury is the primary brain injury, the *ex vivo* stimulation with PMA/ionomycin would represent a second hit for the immune system of these animals. This "second hit" could be translated as any other insult after TBI, the main example being a secondary infection. It has been demonstrated that experimental TBI results in chronic alterations in the systemic immune response. Ritzel et al. showed that basal ROS levels in the blood are increased after 60 days post-injury which reflects persistent inflammation at chronic time points (Ritzel et al., 2018). Furthermore, stimulation of monocytes and neutrophils in the bone marrow with PMA/ionomycin did not respond as expected at this chronic injury time point. Compared to sham, TBI mice had a decreased bone marrow ROS release after stimulation, meaning that although baseline levels were high, after a second hit immune cell responses were impaired at 60 days of injury. Here, we sought to replicate these results in the blood, of which samples are less invasive and easier to obtain in clinical practice. Simultaneously, we aimed to correlate ROS release and NOX2 activity in the same assay to create a robust functional biomarker.

3.2.5.1 Respiratory burst and NOX2 activity are impaired in circulating neutrophils at 14 days post-TBI

To assess the effects of mild-to-moderate TBI in NOX2/ROS activity of circulating monocytes and neutrophils, adult male mice were subjected to either sham surgery (incision only) or CCI. Mice were sacrificed at 1-, 7- and 14-days post-injury and blood was collected via cardiac puncture under anaesthesia. Blood samples were then processed for flow cytometry analysis as described in Chapter 2. A standardized gating strategy (Figure 3-10A) was used to identify Ly6C+ monocytes and neutrophils populations. MFI DHR123 was used to measure ROS production and MFI NOX2 was used to determine NOX2 activity/expression. Considering that samples from different cohorts were not generated and analysed in flow cytometry on the same date, we judged that combining all the data in the same statistical analysis would not be appropriate. Therefore, these results are presented in separated graphs.

Upon stimulation with PMA/ionomycin, circulating neutrophils released significant amounts of ROS in both groups (sham and TBI) when compared to controls at 1 day post-injury (DPI) (cohort 1: sham control vs sham PMA/ionomycin: *p=0.0462; TBI control vs TBI PMA/ionomycin: *p=0.030) but there was no difference in response comparing sham (stimulated) versus TBI (stimulated) (Figure 3-11A) . Regarding NOX2 activity/expression there was no significant effect of stimulation on these cells (*cohort 1:* sham control vs sham PMA/ionomycin: p=0.560; TBI control vs TBI PMA/ionomycin: p=0.999)

(Figure 3-11B). A simple linear regression was carried out to estimate the relation between MFI DHR123 and MFI NOX2 and this was non-significant (p=0.4227; R^2=0.04334) (Figure 3-11C).

At 7 DPI there was a significant increase in ROS released by neutrophils in the PMA/ionomycin group both in sham and TBI mice (cohort 2: sham control vs sham PMA/ionomycin: ***p=0.0001; TBI control vs TBI PMA/ionomycin: ****p<0.001) but no statistical difference when comparing sham (stimulated) and TBI (stimulated) (p=0.7206) (Figure 3-11D). NOX2 activity was not affected in the sham group (p=0.0566) but it was increased significantly in the TBI group after stimulation (*p=0.0159) (Figure 3-11E). Simple linear regression was performed and resulted in a significant relation between MFI DHR123 and MFI NOX2 (p=0.0014; R^2=0.4078; Figure 3-11F).

At 14 DPI circulating neutrophils from sham mice had a significant increase both in ROS levels (cohort 3: ****p<0.0001) and NOX2 activity upon stimulation (cohort 3: **p=0.0083). However, TBI neutrophils failed to respond to PMA/ionomycin both in ROS production (TBI control vs TBI PMA/ionomycin: p=0.1048) and NOX2 activity (TBI control vs TBI PMA/ionomycin: p=0.1455). Interestingly, when comparing sham versus TBI (PMA/ionomycin sham versus PMA/ionomycin TBI), there was a significant decrease in MFI DHR123 in the PMA/ionomycin group (*p=0.0124). In this experiment, we demonstrated that at 14 DPI neutrophils from TBI mice had an impaired response to stimulation compared to sham mice (Figure 3-11G and H). The simple linear regression in this cohort resulted in a significant relation between MFI DHR123 and MFI NOX2 (p=0.0043; R^2=0.3553) (Figure 3-11I).

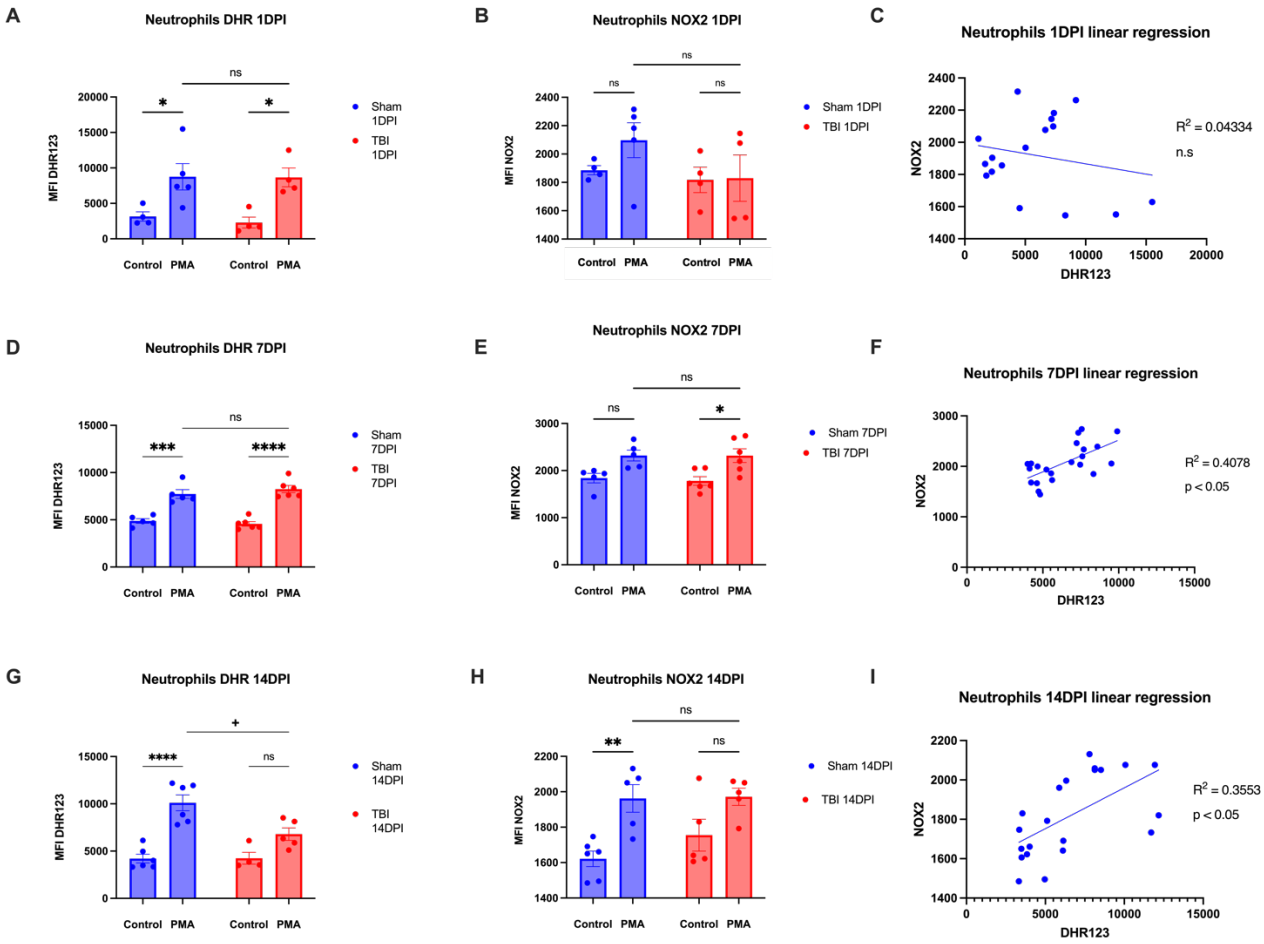

Figure 3-11. Temporal assessment of NOX2/ROS activity in circulating neutrophils following experimental TBI

C57BL/6JOlaHsd male mice (n=4-5/group *Cohort1: 1DPI*; n=5-6/group *Cohort 2: 7DPI*; n=5-6/group *Cohort 3: 14DPI*) were subjected to either sham surgery (incision only) or controlled cortical impact (CCI). Blood was collected via cardiac puncture at 1, 7, and 14 days following injury and cells were processed for flow cytometry analysis. Cells were stained for DHR123, CD45, CD11b, Ly6C, and Ly6G; and intracellular NOX2 ($gp91^{phox}$). Neutrophils were gated as $CD45^{+}CD11b^{+}Ly6C^{-}Ly6G^{+}$. Respiratory burst (A, D, G) and NOX2 activity (B, E, H) were measured following PMA/ionomycin stimulation for 30 minutes; data are expressed in MFI. For all experiments, n = 4–6/group. The association between ROS levels and NOX2 activity was assessed at each time point by linear regression analyses (C, F, I). Data are expressed as mean ±SEM with *p<0.05; **p<0.01; ***p<0.001; ****p<0.0001 vs. control and +p<0.05 vs PMA by two-way ANOVA with Tukey's multiple comparisons test post hoc.

3.2.5.2 Respiratory burst and NOX2 activity are impaired in blood monocytes after 14 days post-TBI

Here we sought to address the same outputs (MFI DHR123 and MFI NOX2) in gated Ly6C+ monocytes in the blood from sham and TBI mice. Gating strategy was demonstrated in Figure 3-10A. At 1 DPI (cohort 1), circulating monocytes from TBI mice significantly increased ROS production in the PMA/ionomycin group compared to control (*p=0.0238). The same trend was observed in the sham mice but failed to reach statistical significance (p=0.3539) (Figure 3-12A). There was no change in NOX2 activity in any of the experimental groups in cohort 1 (Figure 3-12B). Simple linear regression correlating MFI DHR123 and MFI NOX2 was also not significant (p=0.7846; R^2=0.005137) (Figure 3-12C). At 7 DPI (cohort 2), there were no significant results when comparing control versus PMA/ionomycin neither in sham versus TBI in either ROS levels (Figure 3.12D) and NOX2 expression/activity (Figure 3-12E). Linear regression comparing the two variables MFI DHR123 and MFI NOX2 was not significant (p=0.079; R^2=0.1472) (Figure 3-12F).

At 14 DPI (cohort 3), PMA/ionomycin stimulation in circulating monocytes from sham mice significantly increased ROS production (cohort 3: *p=0.0126; Figure 3-12G) and NOX2 activity (cohort 3: *p=0.0228); Figure 3.12H) when compared to control group. Surprisingly, in the TBI group monocytes failed to respond to stimulation compared to control in both outputs: MFI DHR123 (p=0.969) and MFI NOX2 (p=0.516). This impairment in respond to PMA/ionomycin stimulation was also seen in neutrophils from cohort 3, however here there were no significant changes in the PMA groups when comparing sham versus TBI. The simple linear regression in cohort 3 resulted in a significant relation between MFI DHR123 and MFI NOX2 (p=0.0009; R^2=0.4489; Figure 3-12I).

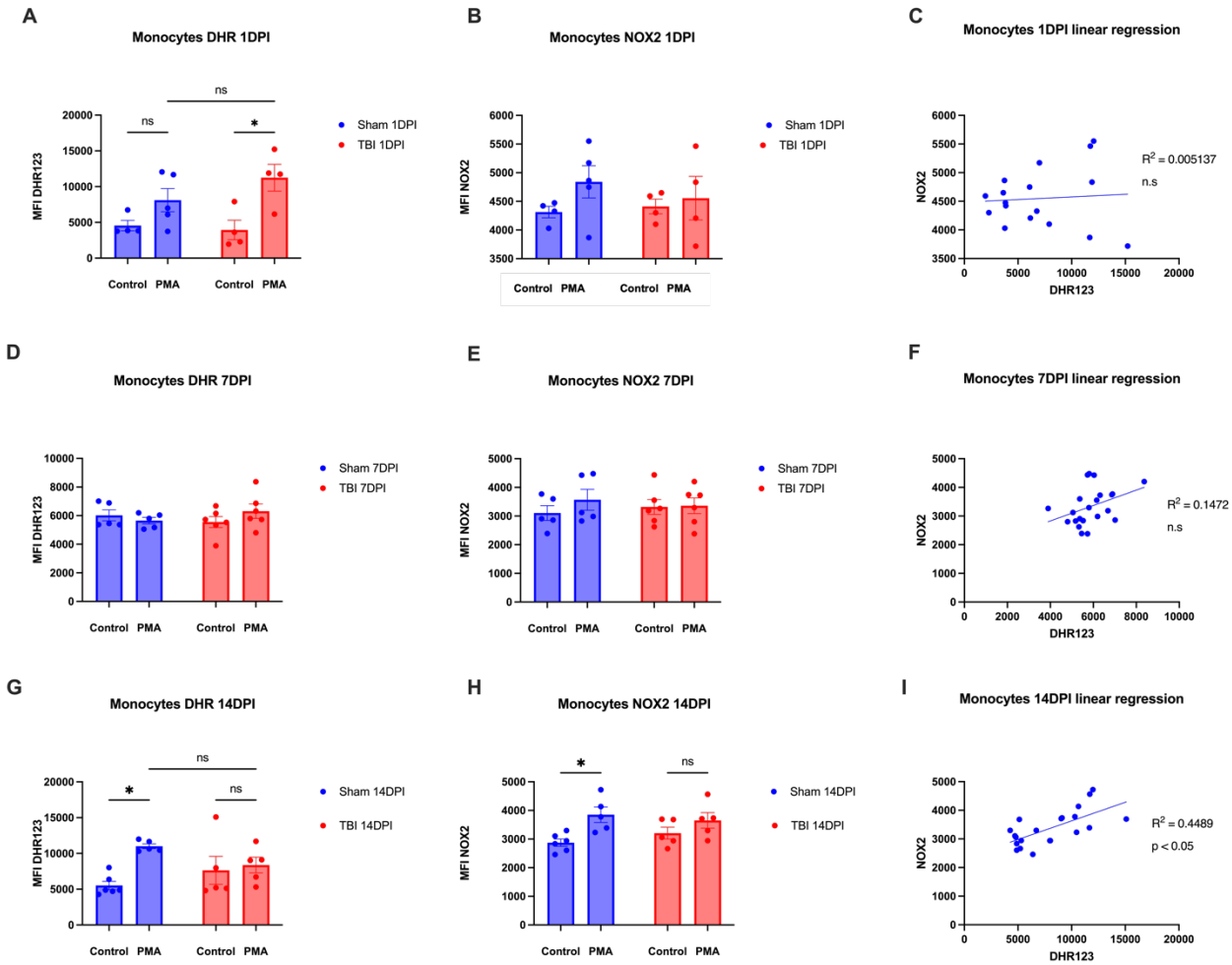

Figure 3-12. NOX2/ROS activity assessment in blood monocytes after 1, 7, and 14 days following TBI

C57BL/6JOlaHsd male mice (n=4-5/group *Cohort1: 1DPI*; n=5-6/group *Cohort 2: 7DPI*; n=5-6/group *Cohort 3: 14DPI*) were subjected to either sham surgery (incision only) or controlled cortical impact (CCI). Blood was collected via cardiac puncture under anaesthesia and cells were processed for flow cytometry analysis. Cells were stained for DHR123, CD45, CD11b, Ly6C, and Ly6G; and intracellular NOX2 ($gp91^{phox}$). Monocytes were gated as $CD45^{+}CD11b^{+}Ly6C^{+}Ly6G^{-}$. Respiratory burst (A, D, G) and NOX2 activity (B, E, H) were measured following PMA/ionomycin stimulation for 30 minutes; ; data are expressed in MFI. For all experiments, n = 4–6/group. The association between ROS levels and NOX2 activity was assessed at each time point by linear regression analyses (C, F, I). For all experiments, n = 4–6/group. Data are mean ±SEM relative to control *p<0.05; **p<0.01; ***p<0.001; ****p<0.0001 by two-way ANOVA with with post hoc Tukey's multiple comparisons test.

We also assessed the effect of mild-to-moderate TBI in the spleen. The protocol used was the same used for the blood samples, described in Chapter 2. Spleens were removed immediately after blood collection and prior to transcardial perfusion and processed for Flow Cytometry analysis. Cells were stimulated with PMA/ionomycin for 30 minutes and stained with DHR123 and with superficial markers (CD45, CD11b, Ly6C, Ly6G) and intracellular $gp91^{phox}$ (NOX2). The gating strategy used was the same used in blood samples (Figure 3-10). The PMA/ionomycin stimulation did not seem to have worked on the spleen samples and this might reflect an issue with the cell preparation protocol, which might need adjustments to the spleen due to the higher number of cells when compared to blood. This data is presented in Supplemental – Figures 3 and 4.

CHAPTER 4: DISCUSSION

TBI should be seen as a systemic condition owing to the fact that following the initial insult, multiple central and peripheral interactions take place with profound effects on other organs such as lungs, spleen, heart and immune system (McDonald et al., 2020). The circulatory system functions as the conduit of the immune system, where numerous cellular, molecular, and signalling factors are released to facilitate the response of the systemic immune response. Importantly, these factors released into the circulation due to TBI could potentially function as biomarkers providing important information related to injury severity and status, as well as prognosis. There is increasing interest within the TBI field regarding identification of TBI biomarkers. Several studies have been published recently with the common goal of finding a substance that correlates with injury and injury severity and is also readily measured in body fluids (CSF or blood) in order to improve diagnosis accuracy and management of these patients (Abdelhak et al., 2022; Czeiter et al., 2020; Frankel et al., 2019; Mondello et al., 2021). Most of these biomarkers though are mainly based on the breakdown of cellular components (neurons, astrocytes, glia) and are measured at acute time points in patients with mild TBI to augment CT findings. In our study, the focus was to develop a blood-based test that would reflect the function of the immune system after TBI upon a challenge, such as an infection, at chronic time points. We did not aim here to aid in diagnosis of TBI but rather prognosis, considering that an impaired immune system post-injury will increase the risk of acquiring secondary infections and will result in poorer outcomes.

Oxidative stress is an important component of the complex cascade in post-injury immune responses and contributes to persistent systemic and neuroinflammation that occurs as part of secondary injury (Kumar et al., 2016). NOX2 is a key player in this scenario, being one of the main sources of ROS. Activation of NOX2 occurs under homeostatic physiological conditions. However, it's activation can become detrimental, contributing to secondary injury and chronic neurodegeneration, leading to worse overall outcomes. Thus, the duality of the roles of NOX2 in varying states provides a rationale of targeting its activity as a potential biomarker and importantly, a promising treatment pathway (Ma et al., 2018).

The goal of our functional TBI biomarker was to measure NOX2 activity and ROS simultaneously and correlate the two at different time points following trauma. To assess NOX2 activity we used a specific antibody against the main subunit ($gp91^{phox}$) that composes the enzymatic complex. To determine ROS levels, we used DHR123 which is a ROS dye widely used in research, but also is the gold standard diagnostic test for CGD, an inherited immunodeficiency in NOX2-dependent phagocytes (Chapter 1) (Sacco et al., 2020).

Firstly, we tested and optimized the NOX2/ROS flow cytometry assay using differentiated HL-60 cells, a neutrophil-like cell line. After differentiation with DMSO, dHL-60 cells express all the components of NADPH oxidase and its behaviour is similar to primary neutrophils (Kuwabara et al., 2015). The rationale for utilizing this cell line lies in the fact that neutrophils are key members of the innate immune response and have an important role in initiating the inflammation process. Neutrophils also rely on the activation of NOX and the generation of ROS for their microbicidal activity (Nguyen et al., 2017).

Our initial studies demonstrated that PMA/ionomycin induced a robust and significant ROS release (increased MFI DHR123) by these cells in a temporal manner. As DHR123 is not specific for NOX2 produced ROS, we assessed whether our stimulation protocol was activating NOX2 by western blot. Our western blot results demonstrated that PMA/ionomycin increased phosphorylation of $p47^{phox}$ within 5 minutes and provoked translocation of $p40^{phox}$, $p47^{phox}$ and $p67^{phox}$ to the membrane as well as increased protein expression of $p22^{phox}$ and $gp91^{phox}$ (in the membrane fraction) and $p40^{phox}$, $p47^{phox}$ and $p67^{phox}$ (in the cytoplasm fraction). Our subcellular fractionation results represent a *n* of 1 and should be repeated in the future to confirm findings.

We also assessed DHR123's behaviour as a ROS probe. In theory, this dye should measure mainly intracellular ROS, because it diffuses passively through the membrane and localizes in the mitochondria. However, it has been shown that extracellularly released H_2O_2 can cross the plasma membrane and react with DHR123 inside the cell, which may affect data interpretation (Quinn et al., 2007). In our experiments we confirmed that DHR123 is sensitive to both intra and extracellular release ROS by removing extracellular ROS using SOD and catalase. Another drawback that came to light from our DHR123 data analysis is that different oxidants (O_2^-, H_2O_2, $ONOO^-$) can change its fluorescence signal, rendering it unsuitable for quantitative or kinetic studies. Even with the limitations of DHR123, we still believe it is a good generic redox sensitive probe and its extensive use in the clinical setting to diagnose CGD (Jirapongsananuruk et al., 2003; Sacco et al., 2020) substantiates its significant relationship with NOX2 activity, albeit non-specific. Another method to assess respiratory burst activity routinely used is the cytochrome c reduction assay (Husain et al., 2020). This assay relies on the cytochrome c reduction by the superoxide anion that can be quantitatively monitored spectrophotometrically. Although it has the advantage of being able to measure the main product of NOX2-generated ROS, the superoxide anion, it is still not possible to confirm that this assay is specific for NOX2 considering that other NOXs also produce O^{2-}.

To further evaluate the ROS component of our TBI biomarker we used two antioxidants. The first was DPI, a broad antioxidant which inhibits ROS release by accepting an electron from flavin and consequently affecting all the flavin-dependent enzymes such as NOX, nitric oxidase synthase, xanthine oxidase, mitochondrial complex I, and cytochrome P-450 reductase. The second was GSK2795039, a novel small molecule drug that is known to be a potent and specific NOX2 inhibitor by blocking both the formation of ROS and the utilization of the enzyme substrates, NADPH and oxygen both *in vitro* and *in vivo* (Hirano et al., 2015; Wang & Luo, 2020). DPI and GSK2795039 decreased PMA/ionomycin-stimulated ROS release in dHL-60 cells in a concentration-dependent manner.

The last step of our *in vitro* biomarker assay development involved the inclusion of a NOX2 specific marker in the panel to combine with DHR123. We successfully demonstrated a significant correlation between MFI DHR123 and MFI NOX2 ($gp91^{phox}$) which encouraged us to move forward in our project and apply this assay to experimental TBI studies in mice.

Preclinical TBI studies in mice have shown that brain injury induces vasculature damage, blood-brain barrier disruption, microglia and astrocytes activation, cell death, demyelination, and grey and white matter atrophy (Loane et al., 2014; Mao et al., 2020; Mohamed et al., 2021). Neuroimaging and histopathological studies demonstrated a progressive increase in lesion size after moderate-level CCI,

our TBI model, and although we did not perform specific assessments it was possible to observe that the volume of the lesion was increased over time by gross examination of the brains at 14 days following injury. TBI induces brain tissue loss not only at the lesion site but also in areas distant from the contusion such as ipsilateral and contralateral hippocampus (Loane et al., 2014; Pischiutta et al., 2018). Such important histopathological events, that become even more pronounced in chronic time points post-injury, demonstrate that neuroinflammation and neurodegeneration processes are progressive and persistent. These findings reproduce what has been shown in the brains of TBI survivors (Ariza et al., 2006) and reiterates the need of exploring chronic consequences of TBI, with the ultimate goal of discovering novel therapeutic targets.

In our preclinical *in vivo* studies, experimental animals were assessed daily for health and wellbeing. Sham and TBI mice lost similar amounts of weight, at a similar speed, with peak weight loss occurring 1 day post-injury in all cohorts. This data is consistent with data measuring body weight changes from previous studies (Hanscom et al., 2021). We also found that TBI significantly delayed return of righting reflex (RORR). RORR is a binary measure that assesses the time it takes to the animal to return to all fours after being placed in a supine position and is the gold standard tool to evaluate level of arousal in rodents. Although widely used in animal models of a variety of neurological disorders, including TBI (Yarnell et al., 2016), evidence suggests that RORR is dissociable from cortical patterns of wakefulness (Gao & Calderon, 2020) and does not reflect recovery of cognitive function (Vincent et al., 2021). RORR should be associated with other behaviours tests such as quivering, standing posture after perturbation, and weight-bearing on limbs, to provide a reliable assessment of the level of consciousness after TBI. Due to time constraints, we did not match surgery time in sham mice to CCI mice leading to a longer isoflurane exposure in the TBI group, which might have affected these results. In future experiments, we will allow sham mice to remain under inhaled anaesthesia for a longer time, so it matches a CCI surgery and also combine RORR with other behavioural parameters such as weight bearing to assess level of consciousness.

An intrinsic relationship between brain injury and spleen has been reported by several studies, referred to by some authors as “the brain-spleen inflammatory coupling” (Rasouli et al., 2011). The spleen is a crucial peripheral lymphoid organ which acts as a filter of the circulatory system in removing foreign material from the blood and is also responsible for the mononuclear phagocyte response preventing infections by encapsulated bacteria and intracellular microorganisms. In addition to its role in protecting against infections, the spleen is also associated with exacerbated inflammation after brain trauma or ischaemia. Following TBI there is an increase in the sympathetic tone with expressive release of catecholamines in the blood that is sensed by spleen resident macrophages and culminates in secretion of pro-inflammatory cytokines into the systemic circulation, ultimately exacerbating the inflammatory response in the brain. Based on this process, it has been shown that post-injury splenectomy can decrease mortality and improve cognitive function in animal models (Li et al., 2011; McDonald et al., 2020; Rasouli et al., 2011).

Our studies assessed whether TBI had an effect on the spleen weight of rodents, which is an indicator of an inflammatory response to various noxious, infectious, or traumatic stimuli (Rasouli et al., 2011). In the current literature the effect of TBI on spleen size/weight is poorly described and there are

some conflicting results. Ritzel et al demonstrated significant splenomegaly in TBI mice by the third day post-injury compared to sham mice with a return to baseline weight by 60 days following injury (Ritzel et al., 2018). Most importantly, the authors showed that the increase in spleen weight was associated with acute rise in myeloid cells numbers. However, it remains unclear if this rise is due to increased traffic of myeloid cells or increased splenic cell production. Preclinical studies using stroke models showed atrophy of the spleen after injury which was related to a massive migration of splenocytes into systemic circulation, thereby enhancing neuroinflammation (Seifert et al., 2012). In our studies, there was no significant change in spleen weights when comparing sham and TBI mice.

It is important to mention that some differences found in our experiments compared to previous studies from our lab could be explained by some changes in the protocols such as: a different CCI device was used in this project; severity of the hit – in our experiments mild to moderate versus moderate level in Ritzel et al., 2018; and most importantly, the strain of mice used here was C57BL/6JOlaHsd whereas in previous studies C57BL/6 strain was studied.

TBI has been shown to cause acute changes in the peripheral immune response in animal models and humans. Leucocytosis is the hallmark of systemic response to physical trauma and has been described at 1- to 3-days post-injury (Liao et al., 2013; Ritzel et al., 2018; Saber et al., 2020). In our experiments, we did not see a significant increase in number of circulating monocytes in TBI mice at any of the examined time points compared to sham mice. Interestingly, we did observe a decrease in neutrophils counts in the blood at 1 day post-injury. This result is not consistent with the literature and should be repeated before further conclusions to be drawn.

A number of studies have described how oxidative stress plays a key role in the secondary injury of TBI pathogenesis (Kumar et al., 2016; Liao et al., 2013). Although respiratory burst is a physiological and protective response, in conditions such as TBI, an imbalance between ROS versus ROS scavengers becomes evident in favour of a pro-oxidative response with significant progression of the initial injury. Increasing evidence suggests that NOX2, being an enzymatic complex with the sole function of producing ROS and known to be activated in TBI, is a promising therapeutic target for TBI (Kumar et al., 2016; Liao et al., 2013; Ma et al., 2018; Wang & Luo, 2020).

The current study examined ROS release and NOX2 activity/expression in baseline and stimulated states of neutrophils and monocytes from the blood of sham and TBI mice at different time points (1,7, and 14 DPI). Additionally, we performed linear regression analyses between MFI DHR123 (ROS probe) and MFI NOX2 ($gp91^{phox}$ antibody) to assess the correlation between these two probes with the main goal of establishing our panel as a credible, reliable, and effective functional biomarker for TBI.

Our experimental design was based on previous results from the Loane group, which demonstrated a biphasic pattern in basal ROS levels in blood monocytes and neutrophils following TBI. There was a significant increase at day 3, decrease at day 7 followed by a second peak at day 60 after injury (Ritzel et al., 2018). In a recent human study, authors demonstrated that among TBI patients there was increased baseline levels of blood neutrophils ROS with a peak at 1 day post-injury compared to uninjured patients and trauma controls, which was attributed to enhanced expression of $gp91^{phox}$ (Liao et al., 2013). Unfortunately, due to the nature of our experimental design, we were unable to

compare the data between different time points as our samples were both generated and processed for flow cytometry on different days, therefore we performed statistical analysis within the same cohort only. We did not see a statistical difference in sham vs. TBI mice in basal ROS levels (MFI DHR123) or in NOX2 activity, both in blood neutrophils and monocytes up to 2 weeks post-injury. At 14 days post-injury, it was possible to observe an increased trend in MFI NOX2 when comparing TBI to sham mice, but this did not reach statistical significance. In future experiments, we aim to have cohorts with 30, 60 and 180 days post-injury to have a better understanding of the basal NOX2 activity in chronic TBI.

Like most aspects of TBI, there is a temporal difference in neural and systemic responses, including the peripheral immune response. TBI is highly associated with peripheral immunosuppression (Hazeldine et al., 2015; Husain et al., 2020; Ritzel et al., 2018; Schwulst et al., 2013). Different from the initial peak in basal ROS levels in the acute phase of TBI, at more chronic stages of TBI an impairment in the respiratory burst activity has been demonstrated (Schwulst et al., 2013; Sharma et al., 2019). Marks et al. showed that at 9 days following TBI, ROS production by neutrophils from injured patients was lower when compared to healthy matched controls. This fact could explain the increased susceptibility of TBI patients to later (or subsequent) infections (Husain et al., 2020; Marks et al., 2013).

Previous work from our group demonstrated that at acute time points (3 days post-injury) phagocytes in the bone marrow from sham and TBI responded equally to stimulation (Ritzel et al., 2018). However, at 2 months after injury an impairment of the respiratory burst activity, which is the main target in our studies, was shown. To assess the functional status of the circulating myeloid cells after brain injury and, therefore, determine the peripheral immune response to a second challenge, we stimulated our blood and spleen samples with PMA/ionomycin to induce a strong respiratory burst. The focus was on the blood myeloid cells in this study, owing to the fact that in the clinical setting a blood-based biomarker is more appropriate, and sampling is less invasive. Additionally, we included a NOX2 antibody in the panel to simultaneously estimate ROS production and NOX2 activity.

The most exciting finding of this study was the observation that upon stimulation at 14 days post-injury the peripheral immune system already shows signs of impairment, whereas previously this impairment was observed at 60 days post-injury (Ritzel et al., 2018). Blood neutrophils from injured mice did not respond as expected after PMA/ionomycin stimulation in both outputs: MFI DHR123 and MFI NOX2. Circulating monocytes from TBI mice also demonstrated a deficit in ROS production after stimulation, but NOX2 activity remained unaffected in this cell population at 14 days post-injury. These are promising results corroborating our hypothesis that after TBI the peripheral immune response becomes dysfunctional with time. Future studies should examine other cohorts such as 30, 60 and 180 days post-injury as well as other immune organs, to more fully capture the temporal and spatial alteration of systemic immune responses and function following TBI.

We also demonstrated through linear regression analyses that the association between ROS generation (MFI DHR123) and NOX2 activation (MFI NOX2) became statistically significant at 7 days in circulating neutrophils and at 14 days post-injury in monocytes. A possible explanation for this could be that at acute time points other sources of ROS, that are not NOX2, also play important roles and contribute significantly to ROS being detected by DHR123. At chronic time points after TBI, when NOX2 is known to be persistently activated (Kumar et al., 2016; Liao et al., 2013; Ma et al., 2018) and

contributes to the aggravation of the primary injury, it may function as the primary source of ROS. Confirmation of findings by repeating the study will need to be carried out. Additionally, inclusion of more chronic time points into future studies to evaluate whether this NOX2/ROS panel is a potential functional biomarker for chronic TBI should be considered.

Curiously, stimulation of whole spleen samples yielded no significant differences neither in ROS release nor in NOX2 activity/expression after stimulation. This is most likely due to background caused by the myriad of cell types in the cell suspension. In the future, the protocol for the spleen preparation should be optimized and magnetic or flow cytometric cell sorting of specific cell subsets should be incorporated to allow for better discriminate in splenic cell populations.

This project faced some challenges throughout its course but undoubtedly the COVID-19 pandemic was a major drawback. Due to these unprecedent times we had to pause the experiments in a few occasions and the *in vivo* work was delayed. Despite the obstacles we had successful results in the NOX2/ROS assay development in a neutrophil-like cell line and we were able to apply the protocol in samples from TBI mice.

The *in vivo* results presented in this thesis reflect one set of experimental data and should be repeated to consolidate our findings. Due to time constraints, we had three cohorts in this study (1,7 and 14 days post TBI) and the samples were not generated and processed for flow cytometry on the same day. Based on this caveat we decided to adjust the statistical analysis accordingly to not compromise our results. The future goal of the lab is to repeat this experiment and include chronic time points such as 30, 60 and 180 days post-injury to elucidate chronic sequelae of TBI in the peripheral immune response. Additionally, we aim to generate samples for flow cytometry from different cohorts on the same day enabling a more accurate statistical analysis.

Another proposed future experiment is to use different assays to measure ROS generation, cytochrome C reduction assay being the main one, considering it measures superoxide anion release (NOX final product) and it enables kinetic and quantitative studies. In addition to that, stimuli more physiological than PMA/ionomycin to induce respiratory burst should be considered.

To further characterise the NOX2/ROS blood-based TBI biomarker, a specificity study should be performed using a NOX2 inhibitor such as GSK2795039. GSK2795039 is a novel and promising drug as it is orally available, non-toxic, CNS-permeable and it has been shown to inhibit NOX2 activity *in vivo* (Hirano et al., 2015). It has been recently used in TBI *in vivo* studies with encouraging results (Wang & Luo, 2020). To understand completely the role of NOX2 in TBI pathology these findings should be correlated with injury severity and long-term neurological and behavioural function. Future experiments testing GSK2795039 *in vivo* might lead us to its potential therapeutic use in clinical TBI.

Here we used a NOX2/ROS blood-based assay to evaluate the functional status of circulating myeloid cells post TBI and we had encouraging results. We strongly believe that this biomarker could be translated to the clinical setting considering that DHR123 has been routinely used as a diagnostic test for CGD patients and it is an easy test to perform.

The connection between TBI and a dysfunctional systemic immune response has been increasingly documented and long-term consequences of this link need to be better investigated. TBI patients are at higher risk of acquiring secondary infections which is associated with increased morbidity

and mortality and worsened neurological outcomes. An accurate assessment of the "immunosuppressed state" of these patients will be a crucial tool providing us with a greater understanding of the physiological and pathological responses relevant to host defense and would help us identify specific populations at higher risk. TBI patients with impaired respiratory burst will face an additional challenge in their condition. A functional TBI biomarker would allow us to act on infection prevention, vigilance and moreover encourage research on targeted treatments.

REFERENCES

Abdelhak, A., Foschi, M., Abu-Rumeileh, S., Yue, J. K., D'Anna, L., Huss, A., Oeckl, P., Ludolph, A. C., Kuhle, J., Petzold, A., Manley, G. T., Green, A. J., Otto, M., & Tumani, H. (2022). Blood GFAP as an emerging biomarker in brain and spinal cord disorders. *Nat Rev Neurol*. https://doi.org/10.1038/s41582-021-00616-3

Anderson, T. N., Hwang, J., Munar, M., Papa, L., Hinson, H. E., Vaughan, A., & Rowell, S. E. (2020). Blood-based biomarkers for prediction of intracranial hemorrhage and outcome in patients with moderate or severe traumatic brain injury. *J Trauma Acute Care Surg*, *89*(1), 80-86. https://doi.org/10.1097/ta.0000000000002706

Ariza, M., Serra-Grabulosa, J. M., Junqué, C., Ramírez, B., Mataró, M., Poca, A., Bargalló, N., & Sahuquillo, J. (2006). Hippocampal head atrophy after traumatic brain injury. *Neuropsychologia*, *44*(10), 1956-1961. https://doi.org/10.1016/j.neuropsychologia.2005.11.007

Babatunde, K. A., Wang, X., Hopke, A., Lannes, N., Mantel, P. Y., & Irimia, D. (2021). Chemotaxis and swarming in differentiated HL-60 neutrophil-like cells. *Sci Rep*, *11*(1), 778. https://doi.org/10.1038/s41598-020-78854-6

Bazarian, J. J., Biberthaler, P., Welch, R. D., Lewis, L. M., Barzo, P., Bogner-Flatz, V., Gunnar Brolinson, P., Büki, A., Chen, J. Y., Christenson, R. H., Hack, D., Huff, J. S., Johar, S., Jordan, J. D., Leidel, B. A., Lindner, T., Ludington, E., Okonkwo, D. O., Ornato, J., . . . Jagoda, A. S. (2018). Serum GFAP and UCH-L1 for prediction of absence of intracranial injuries on head CT (ALERT-TBI): a multicentre observational study. *Lancet Neurol*, *17*(9), 782-789. https://doi.org/10.1016/s1474-4422(18)30231-x

Birnie, G. D. (1988). The HL60 cell line: a model system for studying human myeloid cell differentiation. *Br J Cancer Suppl*, *9*, 41-45. https://www.ncbi.nlm.nih.gov/pubmed/3076064

Brackman, D., Lund-Johansen, F., & Aarskog, D. (1995). Expression of cell surface antigens during the differentiation of HL-60 cells induced by 1,25-dihydroxyvitamin D3, retinoic acid and DMSO. *Leuk Res*, *19*(1), 57-64. https://doi.org/10.1016/0145-2126(94)00061-e

Brazinova, A., Rehorcikova, V., Taylor, M. S., Buckova, V., Majdan, M., Psota, M., Peeters, W., Feigin, V., Theadom, A., Holkovic, L., & Synnot, A. (2021). Epidemiology of Traumatic Brain Injury in Europe: A Living Systematic Review. *J Neurotrauma*, *38*(10), 1411-1440. https://doi.org/10.1089/neu.2015.4126

Butterfield, D. A., & Boyd-Kimball, D. (2018). Oxidative Stress, Amyloid-β Peptide, and Altered Key Molecular Pathways in the Pathogenesis and Progression of Alzheimer's Disease. *J Alzheimers Dis*, *62*(3), 1345-1367. https://doi.org/10.3233/jad-170543

Chiriaco, M., Salfa, I., Di Matteo, G., Rossi, P., & Finocchi, A. (2016). Chronic granulomatous disease: Clinical, molecular, and therapeutic aspects. *Pediatr Allergy Immunol*, *27*(3), 242-253. https://doi.org/10.1111/pai.12527

Collins, S. J., Ruscetti, F. W., Gallagher, R. E., & Gallo, R. C. (1978). Terminal differentiation of human promyelocytic leukemia cells induced by dimethyl sulfoxide and other polar compounds. *Proc Natl Acad Sci U S A*, *75*(5), 2458-2462. https://doi.org/10.1073/pnas.75.5.2458

Cox, J. A., Jeng, A. Y., Sharkey, N. A., Blumberg, P. M., & Tauber, A. I. (1985). Activation of the human neutrophil nicotinamide adenine dinucleotide phosphate (NADPH)-oxidase by protein kinase C. *J Clin Invest*, *76*(5), 1932-1938. https://doi.org/10.1172/jci112190

Czeiter, E., Amrein, K., Gravesteijn, B. Y., Lecky, F., Menon, D. K., Mondello, S., Newcombe, V. F. J., Richter, S., Steyerberg, E. W., Vyvere, T. V., Verheyden, J., Xu, H., Yang, Z., Maas, A. I. R., Wang, K. K. W., & Büki, A. (2020). Blood biomarkers on admission in acute traumatic brain injury: Relations to severity, CT findings and care path in the CENTER-TBI study. *EBioMedicine*, *56*, 102785. https://doi.org/10.1016/j.ebiom.2020.102785

Dao, V. T., Elbatreek, M. H., Altenhöfer, S., Casas, A. I., Pachado, M. P., Neullens, C. T., Knaus, U. G., & Schmidt, H. (2020). Isoform-selective NADPH oxidase inhibitor panel for pharmacological target validation. *Free Radic Biol Med*, *148*, 60-69. https://doi.org/10.1016/j.freeradbiomed.2019.12.038

Delic, V., Beck, K. D., Pang, K. C. H., & Citron, B. A. (2020). Biological links between traumatic brain injury and Parkinson's disease. *Acta Neuropathol Commun*, *8*(1), 45. https://doi.org/10.1186/s40478-020-00924-7

Djiadeu, P., Azzouz, D., Khan, M. A., Kotra, L. P., Sweezey, N., & Palaniyar, N. (2017). Ultraviolet irradiation increases green fluorescence of dihydrorhodamine (DHR) 123: false-positive results for reactive oxygen species generation. *Pharmacol Res Perspect*, *5*(2), e00303. https://doi.org/10.1002/prp2.303

Doran, S. J., Henry, R. J., Shirey, K. A., Barrett, J. P., Ritzel, R. M., Lai, W., Blanco, J. C., Faden, A. I., Vogel, S. N., & Loane, D. J. (2020). Early or Late Bacterial Lung Infection Increases Mortality After Traumatic Brain Injury in Male Mice and Chronically Impairs Monocyte Innate Immune Function. *Crit Care Med*, *48*(5), e418-e428. https://doi.org/10.1097/CCM.0000000000004273

El-Benna, J., Dang, P. M., Gougerot-Pocidalo, M. A., Marie, J. C., & Braut-Boucher, F. (2009). p47phox, the phagocyte NADPH oxidase/NOX2 organizer: structure, phosphorylation and implication in diseases. *Exp Mol Med*, *41*(4), 217-225. https://doi.org/10.3858/emm.2009.41.4.058

Faul, M., & Coronado, V. (2015). Epidemiology of traumatic brain injury. *Handb Clin Neurol*, *127*, 3-13. https://doi.org/10.1016/b978-0-444-52892-6.00001-5

Fischer, M. T., Sharma, R., Lim, J. L., Haider, L., Frischer, J. M., Drexhage, J., Mahad, D., Bradl, M., van Horssen, J., & Lassmann, H. (2012). NADPH oxidase expression in active multiple sclerosis lesions in relation to oxidative tissue damage and mitochondrial injury. *Brain*, *135*(Pt 3), 886-899. https://doi.org/10.1093/brain/aws012

Fleck, R. A., Romero-Steiner, S., & Nahm, M. H. (2005). Use of HL-60 cell line to measure opsonic capacity of pneumococcal antibodies. *Clin Diagn Lab Immunol*, *12*(1), 19-27. https://doi.org/10.1128/cdli.12.1.19-27.2005

Fragoso-Morales, L. G., Correa-Basurto, J., & Rosales-Hernández, M. C. (2021). Implication of Nicotinamide Adenine Dinucleotide Phosphate (NADPH) Oxidase and Its Inhibitors in Alzheimer's Disease Murine Models. *Antioxidants (Basel)*, *10*(2). https://doi.org/10.3390/antiox10020218

Frankel, M., Fan, L., Yeatts, S. D., Jeromin, A., Vos, P. E., Wagner, A. K., Wolf, B. J., Pauls, Q., Lunney, M., Merck, L. H., Hall, C. L., Palesch, Y. Y., Silbergleit, R., & Wright, D. W. (2019).

Association of Very Early Serum Levels of S100B, Glial Fibrillary Acidic Protein, Ubiquitin C-Terminal Hydrolase-L1, and Spectrin Breakdown Product with Outcome in ProTECT III. *J Neurotrauma*, *36*(20), 2863-2871. https://doi.org/10.1089/neu.2018.5809

Gan, Z. S., Stein, S. C., Swanson, R., Guan, S., Garcia, L., Mehta, D., & Smith, D. H. (2019). Blood Biomarkers for Traumatic Brain Injury: A Quantitative Assessment of Diagnostic and Prognostic Accuracy. *Front Neurol*, *10*, 446. https://doi.org/10.3389/fneur.2019.00446

Gao, S., & Calderon, D. P. (2020). Robust alternative to the righting reflex to assess arousal in rodents. *Sci Rep*, *10*(1), 20280. https://doi.org/10.1038/s41598-020-77162-3

Gao, W., Zhang, Z., Lv, X., Wu, Q., Yan, J., Mao, G., & Xing, W. (2020). Neurofilament light chain level in traumatic brain injury: A system review and meta-analysis. *Medicine (Baltimore)*, *99*(38), e22363. https://doi.org/10.1097/md.0000000000022363

Gardner, R. C., Byers, A. L., Barnes, D. E., Li, Y., Boscardin, J., & Yaffe, K. (2018). Mild TBI and risk of Parkinson disease: A Chronic Effects of Neurotrauma Consortium Study. *Neurology*, *90*(20), e1771-e1779. https://doi.org/10.1212/wnl.0000000000005522

Geng, L., Fan, L. M., Liu, F., Smith, C., & Li, J. (2020). Nox2 dependent redox-regulation of microglial response to amyloid-β stimulation and microgliosis in aging. *Sci Rep*, *10*(1), 1582. https://doi.org/10.1038/s41598-020-58422-8

GBD Neurology- Global, regional, and national burden of traumatic brain injury and spinal cord injury, 1990-2016: a systematic analysis for the Global Burden of Disease Study 2016. (2019). *Lancet Neurol*, *18*(1), 56-87. https://doi.org/10.1016/s1474-4422(18)30415-0

Hanscom, M., Loane, D. J., Aubretch, T., Leser, J., Molesworth, K., Hedgekar, N., Ritzel, R. M., Abulwerdi, G., Shea-Donohue, T., & Faden, A. I. (2021). Acute colitis during chronic experimental traumatic brain injury in mice induces dysautonomia and persistent extraintestinal, systemic, and CNS inflammation with exacerbated neurological deficits. *J Neuroinflammation*, *18*(1), 24. https://doi.org/10.1186/s12974-020-02067-x

Hanscom, M., Loane, D. J., & Shea-Donohue, T. (2021). Brain-gut axis dysfunction in the pathogenesis of traumatic brain injury. *J Clin Invest*, *131*(12). https://doi.org/10.1172/JCI143777

Harrison-Felix, C., Kolakowsky-Hayner, S. A., Hammond, F. M., Wang, R., Englander, J., Dams-O'Connor, K., Kreider, S. E., Novack, T. A., & Diaz-Arrastia, R. (2012). Mortality after surviving traumatic brain injury: risks based on age groups. *J Head Trauma Rehabil*, *27*(6), E45-56. https://doi.org/10.1097/HTR.0b013e31827340ba

Hauert, A. B., Martinelli, S., Marone, C., & Niggli, V. (2002). Differentiated HL-60 cells are a valid model system for the analysis of human neutrophil migration and chemotaxis. *Int J Biochem Cell Biol*, *34*(7), 838-854. https://doi.org/10.1016/s1357-2725(02)00010-9

Hazeldine, J., Lord, J. M., & Belli, A. (2015). Traumatic Brain Injury and Peripheral Immune Suppression: Primer and Prospectus. *Front Neurol*, *6*, 235. https://doi.org/10.3389/fneur.2015.00235

Hirano, K., Chen, W. S., Chueng, A. L., Dunne, A. A., Seredenina, T., Filippova, A., Ramachandran, S., Bridges, A., Chaudry, L., Pettman, G., Allan, C., Duncan, S., Lee, K. C., Lim, J., Ma, M. T., Ong, A. B., Ye, N. Y., Nasir, S., Mulyanidewi, S., . . . Rutter, A. R. (2015). Discovery

of GSK2795039, a Novel Small Molecule NADPH Oxidase 2 Inhibitor. *Antioxid Redox Signal*, *23*(5), 358-374. https://doi.org/10.1089/ars.2014.6202

Hu, C. F., Wu, S. P., Lin, G. J., Shieh, C. C., Hsu, C. S., Chen, J. W., Chen, S. H., Hong, J. S., & Chen, S. J. (2021). Microglial Nox2 Plays a Key Role in the Pathogenesis of Experimental Autoimmune Encephalomyelitis. *Front Immunol*, *12*, 638381. https://doi.org/10.3389/fimmu.2021.638381

Huie, J. R., Diaz-Arrastia, R., Yue, J. K., Sorani, M. D., Puccio, A. M., Okonkwo, D. O., Manley, G. T., & Ferguson, A. R. (2019). Testing a Multivariate Proteomic Panel for Traumatic Brain Injury Biomarker Discovery: A TRACK-TBI Pilot Study. *J Neurotrauma*, *36*(1), 100-110. https://doi.org/10.1089/neu.2017.5449

Huie, J. R., Mondello, S., Lindsell, C. J., Antiga, L., Yuh, E. L., Zanier, E. R., Masson, S., Rosario, B. L., & Ferguson, A. R. (2021). Biomarkers for Traumatic Brain Injury: Data Standards and Statistical Considerations. *J Neurotrauma*, *38*(18), 2514-2529. https://doi.org/10.1089/neu.2019.6762

Husain, M., Becker, E. J., Jr., Bone, N. B., Schmitt, A., Pittet, J. F., & Zmijewski, J. W. (2020). NOX2 decoy peptides disrupt trauma-mediated neutrophil immunosuppression and protect against lethal peritonitis. *Redox Biol*, *36*, 101651. https://doi.org/10.1016/j.redox.2020.101651

Jassam, Y. N., Izzy, S., Whalen, M., McGavern, D. B., & El Khoury, J. (2017). Neuroimmunology of Traumatic Brain Injury: Time for a Paradigm Shift. *Neuron*, *95*(6), 1246-1265. https://doi.org/10.1016/j.neuron.2017.07.010

Jha, R. M., Kochanek, P. M., & Simard, J. M. (2019). Pathophysiology and treatment of cerebral edema in traumatic brain injury. *Neuropharmacology*, *145*(Pt B), 230-246. https://doi.org/10.1016/j.neuropharm.2018.08.004

Jirapongsananuruk, O., Malech, H. L., Kuhns, D. B., Niemela, J. E., Brown, M. R., Anderson-Cohen, M., & Fleisher, T. A. (2003). Diagnostic paradigm for evaluation of male patients with chronic granulomatous disease, based on the dihydrorhodamine 123 assay. *J Allergy Clin Immunol*, *111*(2), 374-379. https://doi.org/10.1067/mai.2003.58

Kawata, K., Liu, C. Y., Merkel, S. F., Ramirez, S. H., Tierney, R. T., & Langford, D. (2016). Blood biomarkers for brain injury: What are we measuring? *Neurosci Biobehav Rev*, *68*, 460-473. https://doi.org/10.1016/j.neubiorev.2016.05.009

Khalil, M., Teunissen, C. E., Otto, M., Piehl, F., Sormani, M. P., Gattringer, T., Barro, C., Kappos, L., Comabella, M., Fazekas, F., Petzold, A., Blennow, K., Zetterberg, H., & Kuhle, J. (2018). Neurofilaments as biomarkers in neurological disorders. *Nat Rev Neurol*, *14*(10), 577-589. https://doi.org/10.1038/s41582-018-0058-z

Kleindienst, A., Hesse, F., Bullock, M. R., & Buchfelder, M. (2007). The neurotrophic protein S100B: value as a marker of brain damage and possible therapeutic implications. *Prog Brain Res*, *161*, 317-325. https://doi.org/10.1016/s0079-6123(06)61022-4

Kourbeti, I. S., Vakis, A. F., Papadakis, J. A., Karabetsos, D. A., Bertsias, G., Filippou, M., Ioannou, A., Neophytou, C., Anastasaki, M., & Samonis, G. (2012). Infections in traumatic brain injury patients. *Clin Microbiol Infect*, *18*(4), 359-364. https://doi.org/10.1111/j.1469-0691.2011.03625.x

Kumar, A., Barrett, J. P., Alvarez-Croda, D. M., Stoica, B. A., Faden, A. I., & Loane, D. J. (2016). NOX2 drives M1-like microglial/macrophage activation and neurodegeneration following experimental traumatic brain injury. *Brain Behav Immun*, *58*, 291-309. https://doi.org/10.1016/j.bbi.2016.07.158

Kuwabara, W. M., Zhang, L., Schuiki, I., Curi, R., Volchuk, A., & Alba-Loureiro, T. C. (2015). NADPH oxidase-dependent production of reactive oxygen species induces endoplasmatic reticulum stress in neutrophil-like HL60 cells. *PLoS One*, *10*(2), e0116410. https://doi.org/10.1371/journal.pone.0116410

Lee, K., & Rincon, F. (2012). Pulmonary complications in patients with severe brain injury. *Crit Care Res Pract*, *2012*, 207247. https://doi.org/10.1155/2012/207247

Li, L., Liang, J., & Fu, H. (2021). An update on the association between traumatic brain injury and Alzheimer's disease: Focus on Tau pathology and synaptic dysfunction. *Neurosci Biobehav Rev*, *120*, 372-386. https://doi.org/10.1016/j.neubiorev.2020.10.020

Li, M., Li, F., Luo, C., Shan, Y., Zhang, L., Qian, Z., Zhu, G., Lin, J., & Feng, H. (2011). Immediate splenectomy decreases mortality and improves cognitive function of rats after severe traumatic brain injury. *J Trauma*, *71*(1), 141-147. https://doi.org/10.1097/TA.0b013e3181f30fc9

Liao, Y., Liu, P., Guo, F., Zhang, Z. Y., & Zhang, Z. (2013). Oxidative burst of circulating neutrophils following traumatic brain injury in human. *PLoS One*, *8*(7), e68963. https://doi.org/10.1371/journal.pone.0068963

Loane, D. J., Kumar, A., Stoica, B. A., Cabatbat, R., & Faden, A. I. (2014). Progressive neurodegeneration after experimental brain trauma: association with chronic microglial activation. *J Neuropathol Exp Neurol*, *73*(1), 14-29. https://doi.org/10.1097/nen.0000000000000021

Ma, M. W., Wang, J., Dhandapani, K. M., Wang, R., & Brann, D. W. (2018). NADPH oxidases in traumatic brain injury - Promising therapeutic targets? *Redox Biol*, *16*, 285-293. https://doi.org/10.1016/j.redox.2018.03.005

Maas, A. I. R., Menon, D. K., Adelson, P. D., Andelic, N., Bell, M. J., Belli, A., Bragge, P., Brazinova, A., Büki, A., Chesnut, R. M., Citerio, G., Coburn, M., Cooper, D. J., Crowder, A. T., Czeiter, E., Czosnyka, M., Diaz-Arrastia, R., Dreier, J. P., Duhaime, A. C., . . . Yaffe, K. (2017). Traumatic brain injury: integrated approaches to improve prevention, clinical care, and research. *Lancet Neurol*, *16*(12), 987-1048. https://doi.org/10.1016/s1474-4422(17)30371-x

Mao, X., Terpolilli, N. A., Wehn, A., Cheng, S., Hellal, F., Liu, B., Seker, B., & Plesnila, N. (2020). Progressive Histopathological Damage Occurring Up to One Year after Experimental Traumatic Brain Injury Is Associated with Cognitive Decline and Depression-Like Behavior. *J Neurotrauma*, *37*(11), 1331-1341. https://doi.org/10.1089/neu.2019.6510

Marks, W., Gołąbek-Dropiewska, K., Bryl, E., Dudek, R., Wieruszewski, J., Stasiak, M., Witkowski, Z., Lasek, J., Pawłowska, J., & Jóźwik, A. (2013). Immunomonitoring in patients with early moderate and severe head trauma [journal article]. *Central European Journal of Immunology*, *38*(4), 494-499. https://doi.org/10.5114/ceji.2013.39767

Marrali, G., Casale, F., Salamone, P., Fuda, G., Caorsi, C., Amoroso, A., Brunetti, M., Restagno, G., Barberis, M., Bertuzzo, D., Canosa, A., Moglia, C., Calvo, A., & Chiò, A. (2014). NADPH

oxidase (NOX2) activity is a modifier of survival in ALS. *J Neurol*, *261*(11), 2178-2183. https://doi.org/10.1007/s00415-014-7470-0

McDonald, S. J., Sharkey, J. M., Sun, M., Kaukas, L. M., Shultz, S. R., Turner, R. J., Leonard, A. V., Brady, R. D., & Corrigan, F. (2020). Beyond the Brain: Peripheral Interactions after Traumatic Brain Injury. *J Neurotrauma*, *37*(5), 770-781. https://doi.org/10.1089/neu.2019.6885

Millius, A., & Weiner, O. D. (2010). Manipulation of neutrophil-like HL-60 cells for the study of directed cell migration. *Methods Mol Biol*, *591*, 147-158. https://doi.org/10.1007/978-1-60761-404-3_9

Minkkinen, M., Iverson, G. L., Kotilainen, A. K., Pauniaho, S. L., Mattila, V. M., Lehtimäki, T., Berghem, K., Posti, J. P., & Luoto, T. M. (2019). Prospective Validation of the Scandinavian Guidelines for Initial Management of Minimal, Mild, and Moderate Head Injuries in Adults. *J Neurotrauma*, *36*(20), 2904-2912. https://doi.org/10.1089/neu.2018.6351

Mohamed, A. Z., Cumming, P., & Nasrallah, F. A. (2021). Traumatic brain injury augurs ill for prolonged deficits in the brain's structural and functional integrity following controlled cortical impact injury. *Sci Rep*, *11*(1), 21559. https://doi.org/10.1038/s41598-021-00660-5

Mondello, S., Papa, L., Buki, A., Bullock, M. R., Czeiter, E., Tortella, F. C., Wang, K. K., & Hayes, R. L. (2011). Neuronal and glial markers are differently associated with computed tomography findings and outcome in patients with severe traumatic brain injury: a case control study. *Crit Care*, *15*(3), R156. https://doi.org/10.1186/cc10286

Mondello, S., Sorinola, A., Czeiter, E., Vámos, Z., Amrein, K., Synnot, A., Donoghue, E., Sándor, J., Wang, K. K. W., Diaz-Arrastia, R., Steyerberg, E. W., Menon, D. K., Maas, A. I. R., & Buki, A. (2021). Blood-Based Protein Biomarkers for the Management of Traumatic Brain Injuries in Adults Presenting to Emergency Departments with Mild Brain Injury: A Living Systematic Review and Meta-Analysis. *J Neurotrauma*, *38*(8), 1086-1106. https://doi.org/10.1089/neu.2017.5182

Nauseef, W. M., Volpp, B. D., McCormick, S., Leidal, K. G., & Clark, R. A. (1991). Assembly of the neutrophil respiratory burst oxidase. Protein kinase C promotes cytoskeletal and membrane association of cytosolic oxidase components. *J Biol Chem*, *266*(9), 5911-5917.

Nguyen, G. T., Green, E. R., & Mecsas, J. (2017). Neutrophils to the ROScue: Mechanisms of NADPH Oxidase Activation and Bacterial Resistance. *Front Cell Infect Microbiol*, *7*, 373. https://doi.org/10.3389/fcimb.2017.00373

Pischiutta, F., Micotti, E., Hay, J. R., Marongiu, I., Sammali, E., Tolomeo, D., Vegliante, G., Stocchetti, N., Forloni, G., De Simoni, M. G., Stewart, W., & Zanier, E. R. (2018). Single severe traumatic brain injury produces progressive pathology with ongoing contralateral white matter damage one year after injury. *Exp Neurol*, *300*, 167-178. https://doi.org/10.1016/j.expneurol.2017.11.003

Quinn, M. T., DeLeo, F. R., & Bokoch, G. M. (2007). Neutrophil methods and protocols. Preface. *Methods Mol Biol*, *412*, vii-viii. https://doi.org/10.1007/978-1-59745-467-4

Ramos-Cejudo, J., Wisniewski, T., Marmar, C., Zetterberg, H., Blennow, K., de Leon, M. J., & Fossati, S. (2018). Traumatic Brain Injury and Alzheimer's Disease: The Cerebrovascular Link. *EBioMedicine*, *28*, 21-30. https://doi.org/10.1016/j.ebiom.2018.01.021

Rasouli, J., Lekhraj, R., Ozbalik, M., Lalezari, P., & Casper, D. (2011). Brain-Spleen Inflammatory Coupling: A Literature Review. *Einstein J Biol Med*, *27*(2), 74-77. https://doi.org/10.23861/ejbm20112768

Rastogi, R., Geng, X., Li, F., & Ding, Y. (2017). NOX Activation by Subunit Interaction and Underlying Mechanisms in Disease [Review]. *Frontiers in Cellular Neuroscience*, *10*. https://doi.org/10.3389/fncel.2016.00301

Reis, J., Massari, M., Marchese, S., Ceccon, M., Aalbers, F. S., Corana, F., Valente, S., Mai, A., Magnani, F., & Mattevi, A. (2020). A closer look into NADPH oxidase inhibitors: Validation and insight into their mechanism of action. *Redox Biol*, *32*, 101466. https://doi.org/10.1016/j.redox.2020.101466

Richardson, M. P., Ayliffe, M. J., Helbert, M., & Davies, E. G. (1998). A simple flow cytometry assay using dihydrorhodamine for the measurement of the neutrophil respiratory burst in whole blood: comparison with the quantitative nitrobluetetrazolium test. *J Immunol Methods*, *219*(1-2), 187-193. https://doi.org/10.1016/s0022-1759(98)00136-7

Ritzel, R. M., Doran, S. J., Barrett, J. P., Henry, R. J., Ma, E. L., Faden, A. I., & Loane, D. J. (2018). Chronic Alterations in Systemic Immune Function after Traumatic Brain Injury. *J Neurotrauma*, *35*(13), 1419-1436. https://doi.org/10.1089/neu.2017.5399

Saber, M., Giordano, K. R., Hur, Y., Ortiz, J. B., Morrison, H., Godbout, J. P., Murphy, S. M., Lifshitz, J., & Rowe, R. K. (2020). Acute peripheral inflammation and post-traumatic sleep differ between sexes after experimental diffuse brain injury. *Eur J Neurosci*, *52*(1), 2791-2814. https://doi.org/10.1111/ejn.14611

Sabet, N., Soltani, Z., & Khaksari, M. (2021). Multipotential and systemic effects of traumatic brain injury. *J Neuroimmunol*, *357*, 577619. https://doi.org/10.1016/j.jneuroim.2021.577619

Sacco, K. A., Smith, M. J., Bahna, S. L., Buchbinder, D., Burkhardt, J., Cooper, M. A., Hartog, N. L., Kobrynski, L., Patel, K. P., & Abraham, R. S. (2020). NAPDH Oxidase-Specific Flow Cytometry Allows for Rapid Genetic Triage and Classification of Novel Variants in Chronic Granulomatous Disease. *J Clin Immunol*, *40*(1), 191-202. https://doi.org/10.1007/s10875-019-00712-6

Schwulst, S. J., Trahanas, D. M., Saber, R., & Perlman, H. (2013). Traumatic brain injury-induced alterations in peripheral immunity. *J Trauma Acute Care Surg*, *75*(5), 780-788. https://doi.org/10.1097/TA.0b013e318299616a

Scott, B. N., Roberts, D. J., Robertson, H. L., Kramer, A. H., Laupland, K. B., Ousman, S. S., Kubes, P., & Zygun, D. A. (2013). Incidence, prevalence, and occurrence rate of infection among adults hospitalized after traumatic brain injury: study protocol for a systematic review and meta-analysis. *Syst Rev*, *2*, 68. https://doi.org/10.1186/2046-4053-2-68

Seifert, H. A., Hall, A. A., Chapman, C. B., Collier, L. A., Willing, A. E., & Pennypacker, K. R. (2012). A transient decrease in spleen size following stroke corresponds to splenocyte release into systemic circulation. *J Neuroimmune Pharmacol*, *7*(4), 1017-1024. https://doi.org/10.1007/s11481-012-9406-8

Shahim, P., Politis, A., van der Merwe, A., Moore, B., Chou, Y. Y., Pham, D. L., Butman, J. A., Diaz-Arrastia, R., Gill, J. M., Brody, D. L., Zetterberg, H., Blennow, K., & Chan, L. (2020). Neurofilament light as a biomarker in traumatic brain injury. *Neurology*, *95*(6), e610-e622. https://doi.org/10.1212/wnl.0000000000009983

Shahim, P., Politis, A., van der Merwe, A., Moore, B., Ekanayake, V., Lippa, S. M., Chou, Y. Y., Pham, D. L., Butman, J. A., Diaz-Arrastia, R., Zetterberg, H., Blennow, K., Gill, J. M., Brody, D. L., & Chan, L. (2020). Time course and diagnostic utility of NfL, tau, GFAP, and UCH-L1 in subacute and chronic TBI. *Neurology*, *95*(6), e623-e636. https://doi.org/10.1212/wnl.0000000000009985

Sharma, R., Shultz, S. R., Robinson, M. J., Belli, A., Hibbs, M. L., O'Brien, T. J., & Semple, B. D. (2019). Infections after a traumatic brain injury: The complex interplay between the immune and neurological systems. *Brain Behav Immun*, *79*, 63-74. https://doi.org/10.1016/j.bbi.2019.04.034

Simon, D. W., McGeachy, M. J., Bayir, H., Clark, R. S. B., Loane, D. J., & Kochanek, P. M. (2017). The far-reaching scope of neuroinflammation after traumatic brain injury. *Nat Rev Neurol*, *13*(9), 572. https://doi.org/10.1038/nrneurol.2017.116

Solt, K., Cotten, J. F., Cimenser, A., Wong, K. F., Chemali, J. J., & Brown, E. N. (2011). Methylphenidate actively induces emergence from general anesthesia. *Anesthesiology*, *115*(4), 791-803. https://doi.org/10.1097/ALN.0b013e31822e92e5

Sorce, S., Stocker, R., Seredenina, T., Holmdahl, R., Aguzzi, A., Chio, A., Depaulis, A., Heitz, F., Olofsson, P., Olsson, T., Duveau, V., Sanoudou, D., Skosgater, S., Vlahou, A., Wasquel, D., Krause, K. H., & Jaquet, V. (2017). NADPH oxidases as drug targets and biomarkers in neurodegenerative diseases: What is the evidence? *Free Radic Biol Med*, *112*, 387-396. https://doi.org/10.1016/j.freeradbiomed.2017.08.006

Stocchetti, N., & Zanier, E. R. (2016). Chronic impact of traumatic brain injury on outcome and quality of life: a narrative review. *Crit Care*, *20*(1), 148. https://doi.org/10.1186/s13054-016-1318-1

Sun, L., Wang, X., Saredy, J., Yuan, Z., Yang, X., & Wang, H. (2020). Innate-adaptive immunity interplay and redox regulation in immune response. *Redox Biol*, *37*, 101759. https://doi.org/10.1016/j.redox.2020.101759

Taylor, C. A., Bell, J. M., Breiding, M. J., & Xu, L. (2017). Traumatic Brain Injury-Related Emergency Department Visits, Hospitalizations, and Deaths - United States, 2007 and 2013. *MMWR Surveill Summ*, *66*(9), 1-16. https://doi.org/10.15585/mmwr.ss6609a1

Teasdale, G., & Jennett, B. (1974). Assessment of coma and impaired consciousness. A practical scale. *Lancet*, *2*(7872), 81-84. https://doi.org/10.1016/s0140-6736(74)91639-0

Teasdale, G., & Jennett, B. (1976). Assessment and prognosis of coma after head injury. *Acta Neurochir (Wien)*, *34*(1-4), 45-55. https://doi.org/10.1007/bf01405862

Thelin, E., Al Nimer, F., Frostell, A., Zetterberg, H., Blennow, K., Nyström, H., Svensson, M., Bellander, B. M., Piehl, F., & Nelson, D. W. (2019). A Serum Protein Biomarker Panel Improves Outcome Prediction in Human Traumatic Brain Injury. *J Neurotrauma*, *36*(20), 2850-2862. https://doi.org/10.1089/neu.2019.6375

Trivedi, A., Tercovich, K. G., Casbon, A. J., Raber, J., Lowell, C., & Noble-Haeusslein, L. J. (2021). Neutrophil-specific deletion of Syk results in recruitment-independent stabilization of the barrier and a long-term improvement in cognitive function after traumatic injury to the developing brain. *Neurobiol Dis*, *157*, 105430. https://doi.org/10.1016/j.nbd.2021.105430

Turtzo, L. C., Lescher, J., Janes, L., Dean, D. D., Budde, M. D., & Frank, J. A. (2014). Macrophagic and microglial responses after focal traumatic brain injury in the female rat. *J Neuroinflammation*, *11*, 82. https://doi.org/10.1186/1742-2094-11-82

Undén, J., Ingebrigtsen, T., & Romner, B. (2013). Scandinavian guidelines for initial management of minimal, mild and moderate head injuries in adults: an evidence and consensus-based update. *BMC Med*, *11*, 50. https://doi.org/10.1186/1741-7015-11-50

Vincent, K. F., Zhang, E. R., Kato, R., Cho, A., Moody, O. A., & Solt, K. (2021). Return of the Righting Reflex Does Not Portend Recovery of Cognitive Function in Anesthetized Rats. *Front Syst Neurosci*, *15*, 762096. https://doi.org/10.3389/fnsys.2021.762096

Wang, M., & Luo, L. (2020). An Effective NADPH Oxidase 2 Inhibitor Provides Neuroprotection and Improves Functional Outcomes in Animal Model of Traumatic Brain Injury. *Neurochem Res*, *45*(5), 1097-1106. https://doi.org/10.1007/s11064-020-02987-3

Wolf, H., Frantal, S., Pajenda, G. S., Salameh, O., Widhalm, H., Hajdu, S., & Sarahrudi, K. (2013). Predictive value of neuromarkers supported by a set of clinical criteria in patients with mild traumatic brain injury: S100B protein and neuron-specific enolase on trial: clinical article. *J Neurosurg*, *118*(6), 1298-1303. https://doi.org/10.3171/2013.1.Jns121181

Wu, D. C., Ré, D. B., Nagai, M., Ischiropoulos, H., & Przedborski, S. (2006). The inflammatory NADPH oxidase enzyme modulates motor neuron degeneration in amyotrophic lateral sclerosis mice. *Proc Natl Acad Sci U S A*, *103*(32), 12132-12137. https://doi.org/10.1073/pnas.0603670103

Yarnell, A. M., Barry, E. S., Mountney, A., Shear, D., Tortella, F., & Grunberg, N. E. (2016). The Revised Neurobehavioral Severity Scale (NSS-R) for Rodents. *Curr Protoc Neurosci*, *75*, 9.52.51-59.52.16. https://doi.org/10.1002/cpns.10

Zetterberg, H., & Blennow, K. (2016). Fluid biomarkers for mild traumatic brain injury and related conditions. *Nat Rev Neurol*, *12*(10), 563-574. https://doi.org/10.1038/nrneurol.2016.127

Zhao, S., Wang, X., Gao, X., & Chen, J. (2018). Delayed and progressive damages to juvenile mice after moderate traumatic brain injury. *Sci Rep*, *8*(1), 7339. https://doi.org/10.1038/s41598-018-25475-9

Zucker, R. M., Whittington, K., & Price, B. J. (1983). Differentiation of HL-60 cells: cell volume and cell cycle changes. *Cytometry*, *3*(6), 414-418. https://doi.org/10.1002/cyto.990030605

SUPPLEMENTARY MATERIAL

Supplemental Figure 1

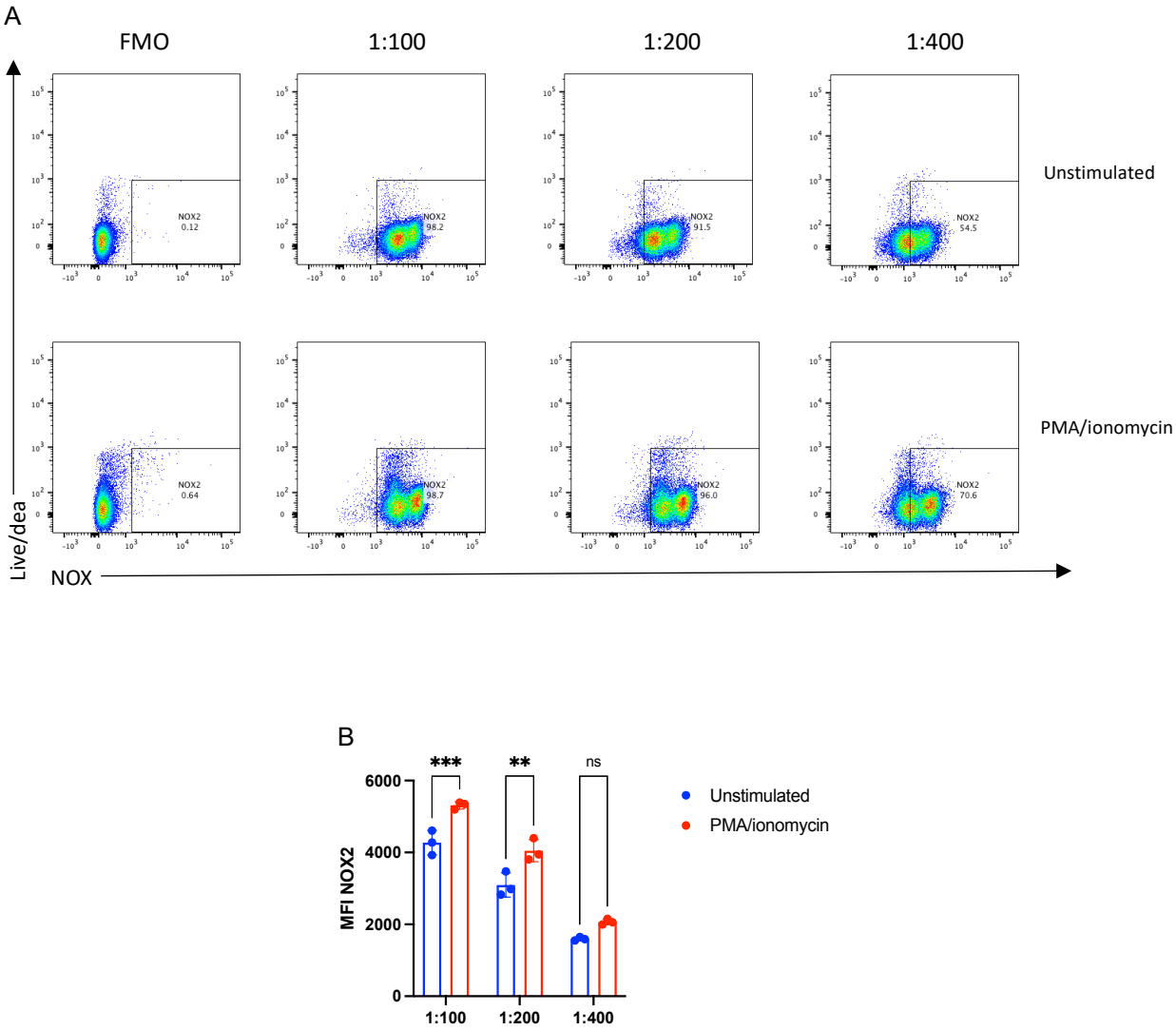

Supplemental Figure 1. Titration of NOX2 antibody

HL-60 cells were differentiated with 1.3% DMSO (v/v) for 5 days and then stimulated with PMA 81nM, ionomycin 1.34uM for 60 minutes. Cells were stained for DHR123, Live/Dead, intracellular gp91^{phox} and analysed by flow cytometry. (A)Representative FACS plots of dHL-60 cells already gated on live cells. Fluorescence Minus One (FMO) controls were used to determine the positivity of the NOX2 antibody. Different dilutions were tested 1:100, 1:200 and 1:400. (B) Results are expressed as Mean Fluorescence Index (MFI) of NOX2 (gp91^{phox}). Data are mean ±SEM (n=3 per group). *p<0.05; **p<0.01; ***p<0.001; ****p<0.0001 versus control by one-way ANOVA with post hoc Tukey's multiple comparisons test.

Supplemental Figure 2

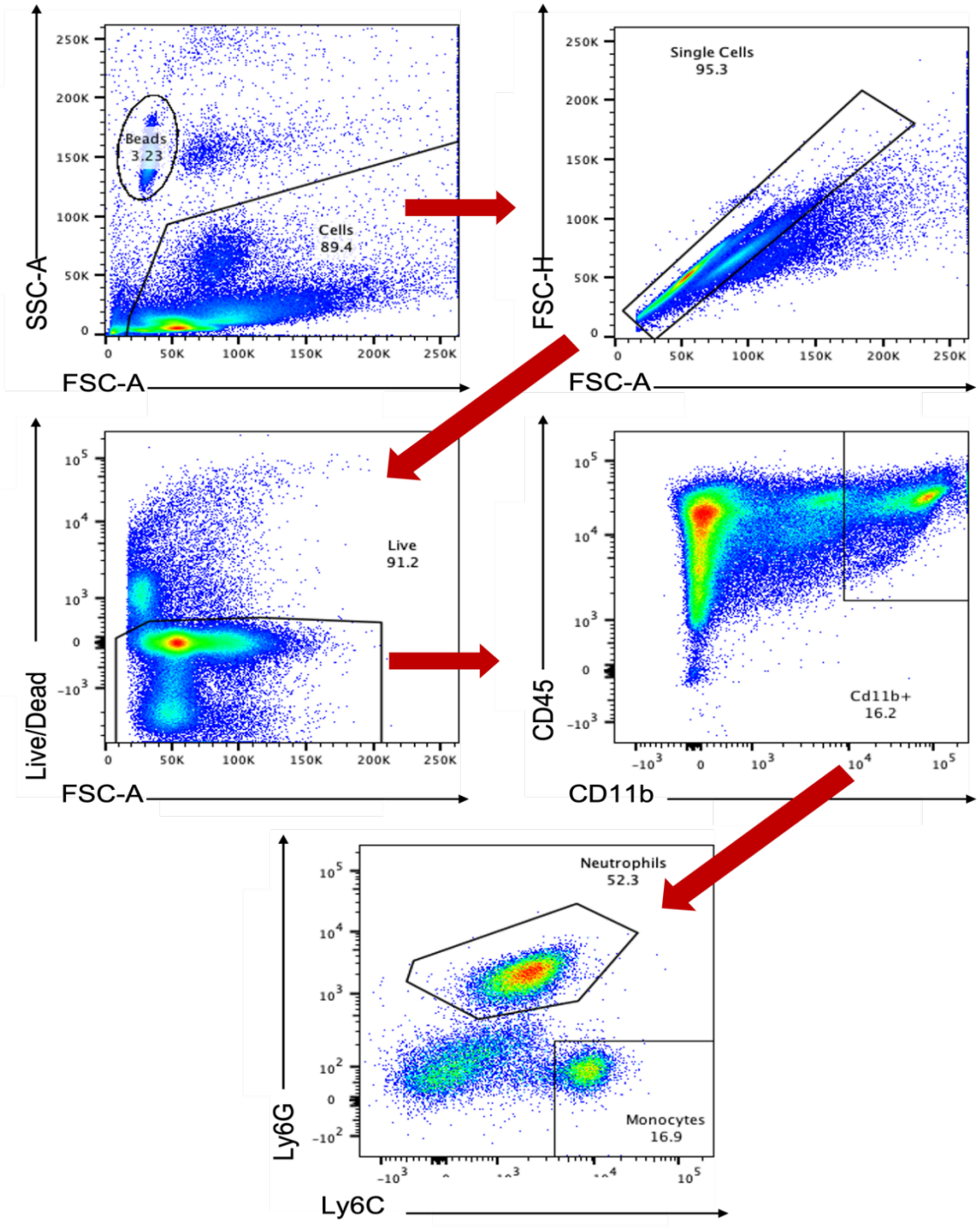

Supplemental Figure 2. Complete gating strategy
Blood was collected via cardiac puncture under anaesthesia and cells were processed for flow cytometry analysis. Cells were stained for surface CD45, CD11b, Ly6C, and Ly6G; and intracellular NOX2 ($gp91^{phox}$). Cells were first gated to isolate the single cells, then gated to identify the live cells. Myeloid cells were gated as $CD45^{+}CD11b^{+}$ followed by gating on $Ly6C^{-}Ly6G^{+}$ for neutrophils and $Ly6C^{+}Ly6G^{-}$ for monocytes. Cell-specific fluorescence minus one (FMO) controls were used to determine the positivity of each antibody. The same gating strategy was used for spleen samples.

Supplemental Figure 3

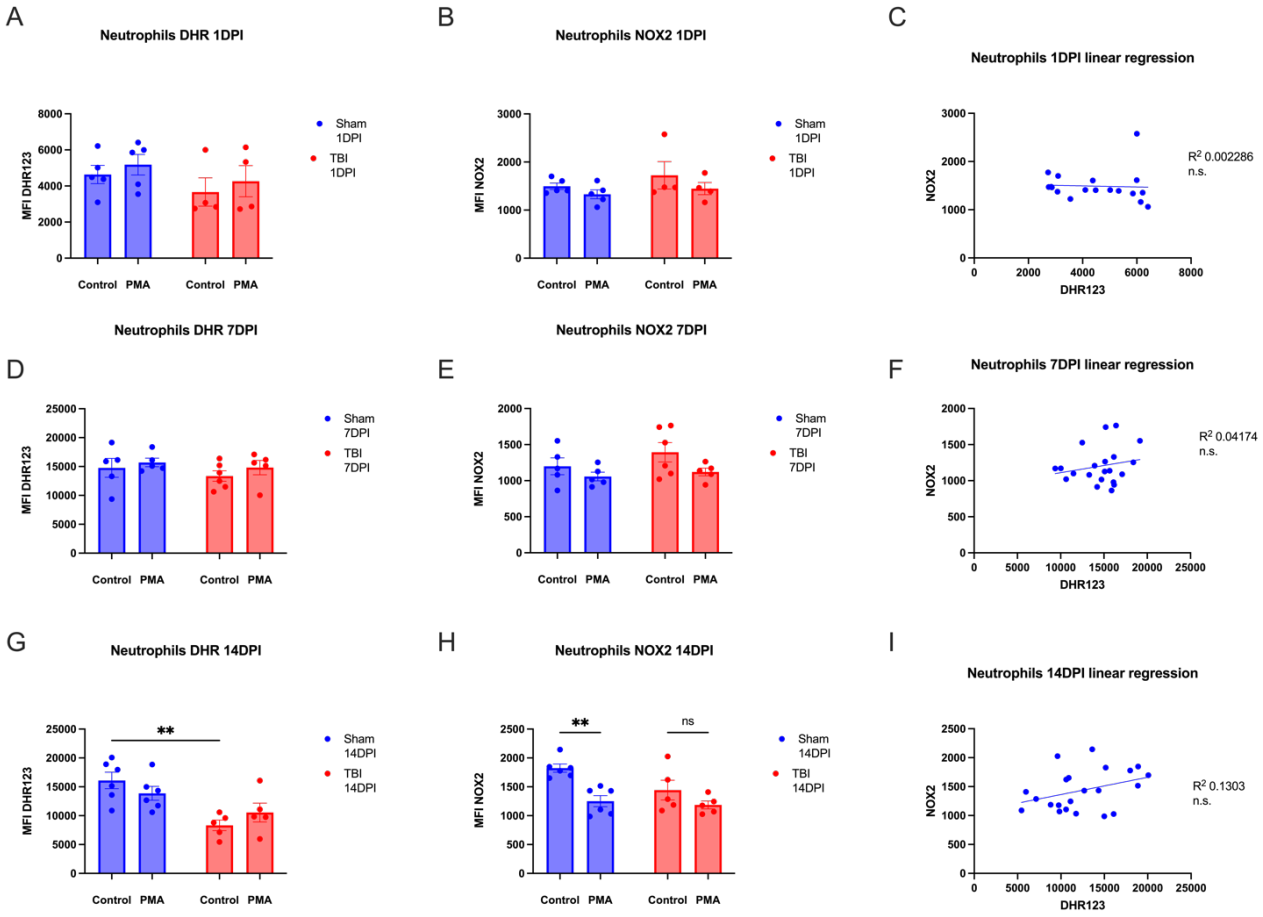

Supplemental Figure 3. Temporal assessment of NOX2/ROS activity in spleen neutrophils following experimental TBI

Spleens were removed immediately after blood collection, prior to transcardial perfusion and processed for flow cytometry analysis. Cells stained with DHR123 and with superficial makers (CD45, CD11b, Ly6C, Ly6G) and intracellular gp91phox (NOX2). Neutrophils were gated as $CD45^{+}CD11b^{+}Ly6C^{-}Ly6G^{+}$. Respiratory burst (A, D, G) and NOX2 activity (B, E, H) were measured following PMA/ionomycin stimulation for 30 minutes. No significant changes were observed in ROS generation or NOX2 activity at 1 or 7 DPI (A-B, D-E). At 14 DPI, ROS generation was significantly decreased in TBI at baseline (G) without affecting NOX2 activity (H); PMA/ionomycin stimulation significantly reduced NOX2 activity (H). Regression analyses were run to correlate ROS with NOX2 activity (C, F, I), but they found no significant correlation between ROS and NOX2 levels at any of the timepoints examined (C, F, I). For all experiments, n = 4–6/group. Data are mean ±SEM relative to control *p<0.05; **p<0.01; ***p<0.001; ****p<0.0001 by two-way ANOVA with post hoc Tukey's multiple comparisons test.

Supplemental Figure 4

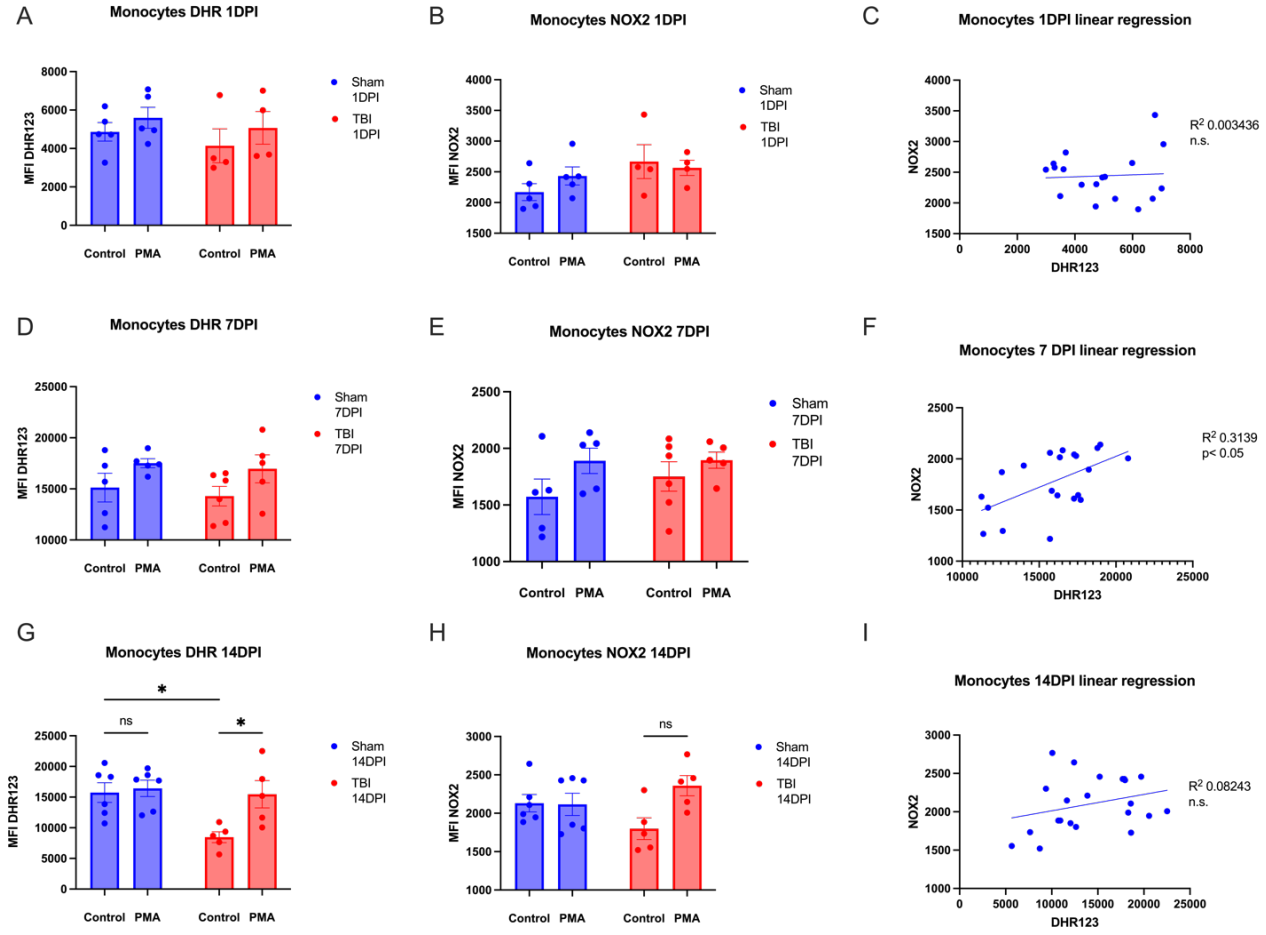

Supplemental Figure 4. Temporal assessment of NOX2/ROS activity in spleen monocytes following experimental TBI

Spleens were removed immediately after blood collection, prior to transcardial perfusion and processed for flow cytometry analysis. Cells were stained with DHR123 and with superficial makers (CD45, CD11b, Ly6C, Ly6G) and intracellular gp91phox (NOX2). Monocytes were gated as $CD45^{+}CD11b^{+}Ly6C^{+}Ly6G^{-}$. Respiratory burst (A, D, G) and NOX2 activity (B, E, H) were measured following PMA/ionomycin stimulation for 30 minutes. No significant changes were observed in ROS generation or NOX2 activity at 1 or 7 DPI (A-B, D-E). At 14 DPI, TBI significantly decreased ROS generation at baseline levels (G) without affecting NOX2 activity (H). Regression analyses were run to correlate ROS with NOX2 activity (C, F, I), but was only significant at 7 DPI (F). For all experiments, n = 4–6/group. Data are mean ±SEM relative to control *p<0.05; **p<0.01; ***p<0.001; ****p<0.0001 by two-way ANOVA with post hoc Tukey's multiple comparisons test.